



Imaging at High Spatial Resolution: Soft X-Ray Microscopy and EUV Lithography

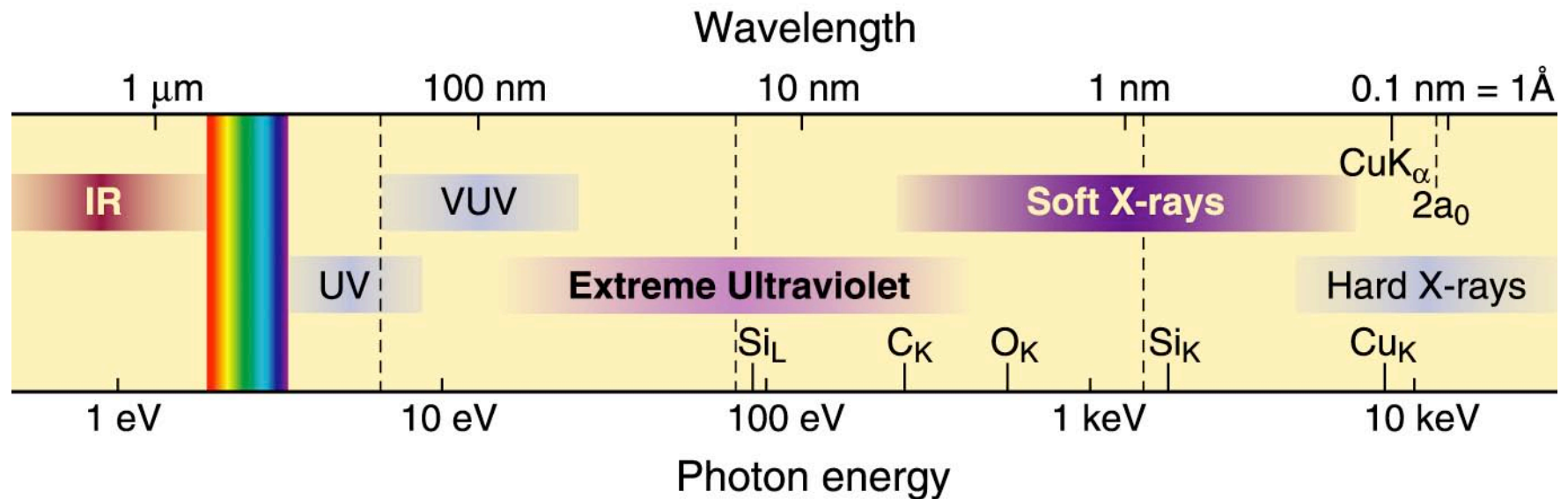
David Attwood

University of California, Berkeley
and
Center for X-Ray Optics, LBNL

W. Chao, E. Anderson, A. Liddle, P. Naulleau, C. Chang (Drexel), Y. Liu, E. Gullikson,
A. Sakdinawat, D. Olynick, B. Harteneck, G. Denbeaux (Albany), G. Schneider (BESSY),
C. Larabell (UCSF), M. LeGros, P. Fischer (Max Planck), T. Tyliczszak



The Short Wavelength Region of the Electromagnetic Spectrum



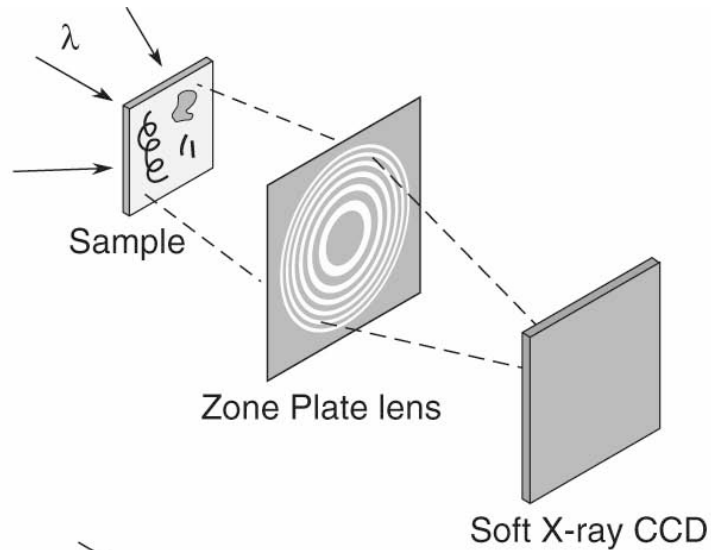
- See smaller features
- Write smaller patterns
- Elemental and chemical sensitivity



Two Common Soft X-Ray Microscopes

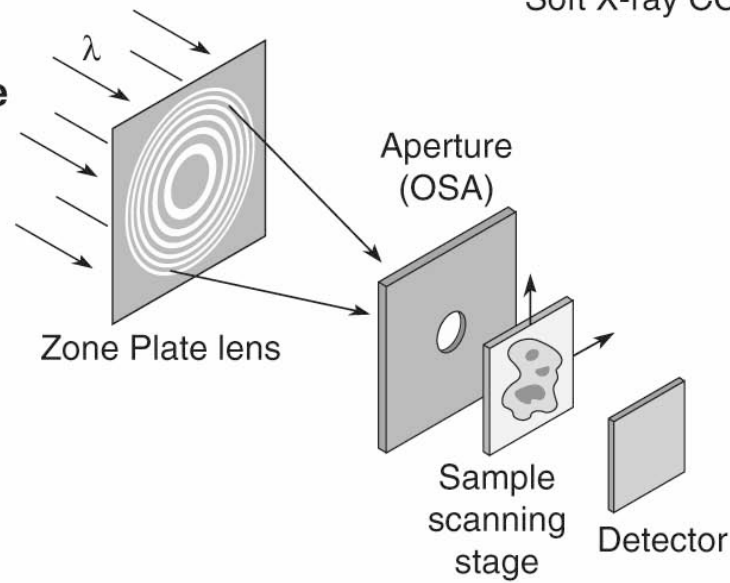


Full-Field Microscope



- Best spatial resolution
- Modest spectral resolution
- Shortest exposure time
- Bending magnet radiation
- Higher radiation dose
- Flexible sample environment (wet, cryo, labeled magnetic fields, electric fields, cement, ...)

Scanning Microscope



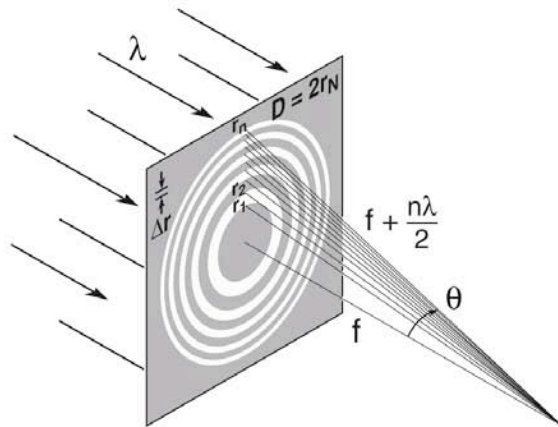
- Least radiation dose
- Good spatial resolution
- Best spectral resolution
- Requires spatially coherent radiation
- Long exposure time
- Flexible sample environment
- Photoemission (restricted magnetic fields), fluorescence imaging



Zone Plates for Soft X-Ray Image Formation



Zone Plate Lens



Zone Plate Formulae

$$r_n^2 = n\lambda f + \frac{n^2\lambda^2}{4} \quad (9.9)$$

$$\lambda = 2.5 \text{ nm},$$

$$\Delta r = 25 \text{ nm}$$

$$N = 618$$

$$D = 4N\Delta r \quad (9.13)$$

$$63 \mu\text{m}$$

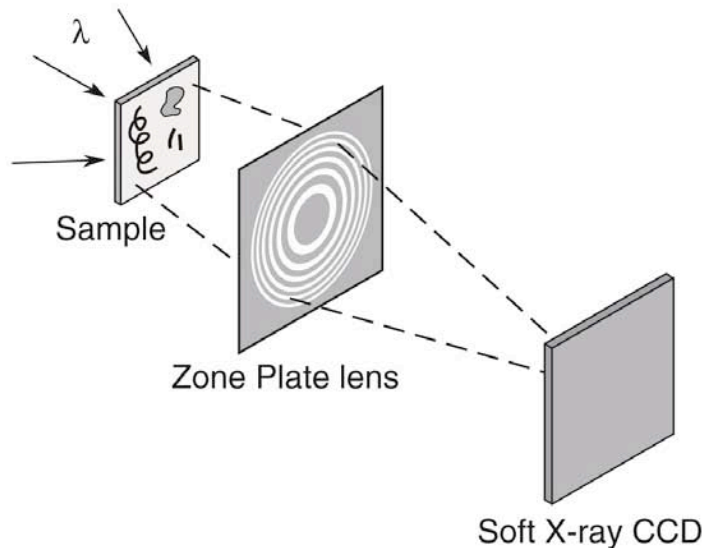
$$f = \frac{4N(\Delta r)^2}{\lambda} \quad (9.14)$$

$$0.63 \text{ mm}$$

$$NA = \frac{\lambda}{2\Delta r} \quad (9.15)$$

$$0.05$$

Soft X-Ray Microscope



$$\text{Res.} = k_1 \frac{\lambda}{NA} = 2k_1\Delta r \quad \begin{cases} k_1 = 0.61 \\ (\sigma = 0) \\ k_1 = 0.4 \\ (\sigma = 0.45) \end{cases}$$

$$1.22\Delta r = 30 \text{ nm}$$

$$0.8\Delta r = 19 \text{ nm}$$

$$\text{DOF} = \pm \frac{1}{2} \frac{\lambda}{(NA)^2} \quad (9.50)$$

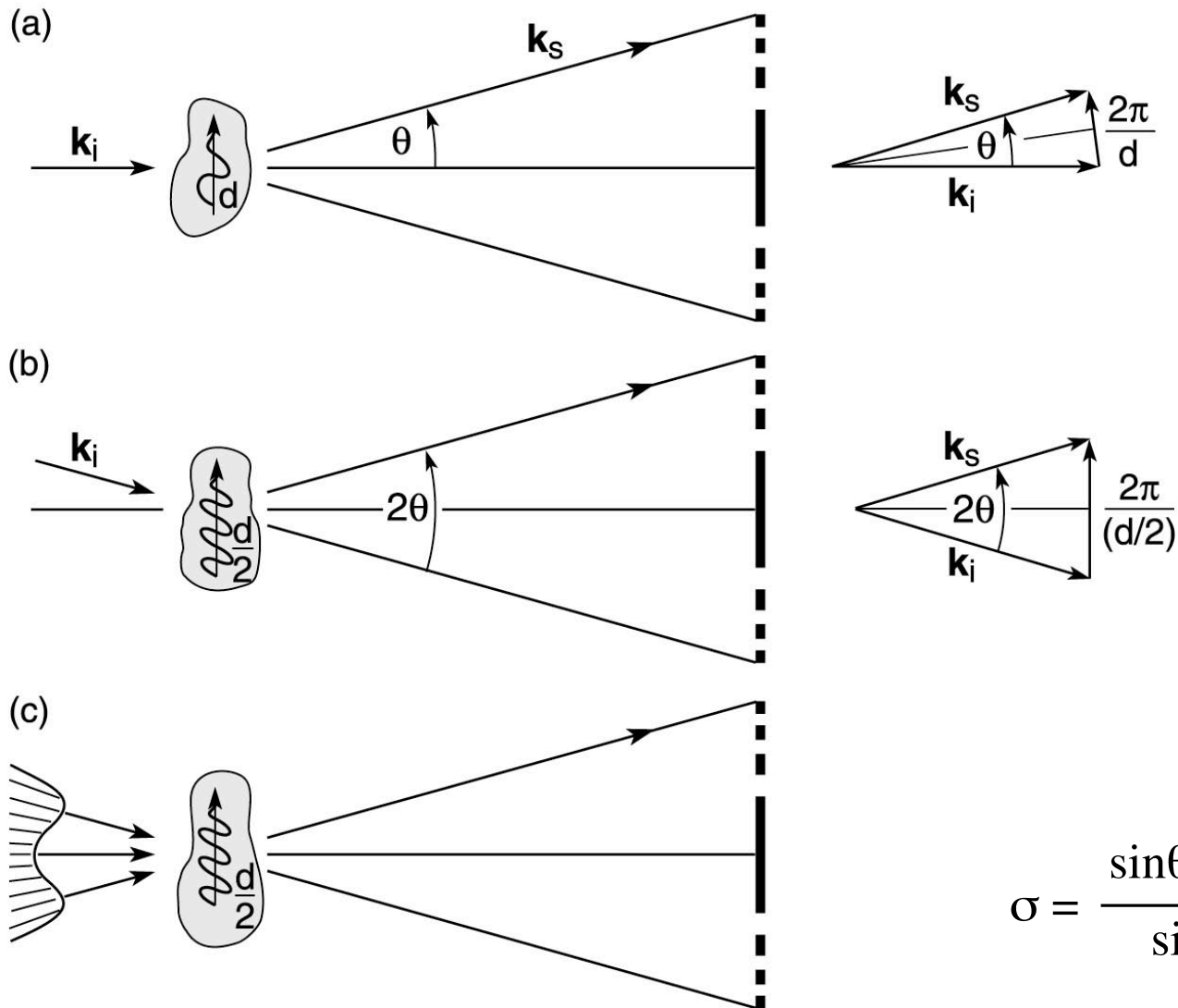
$$1 \mu\text{m}$$

$$\frac{\Delta\lambda}{\lambda} \leq \frac{1}{N} \quad (9.52)$$

$$1/700$$

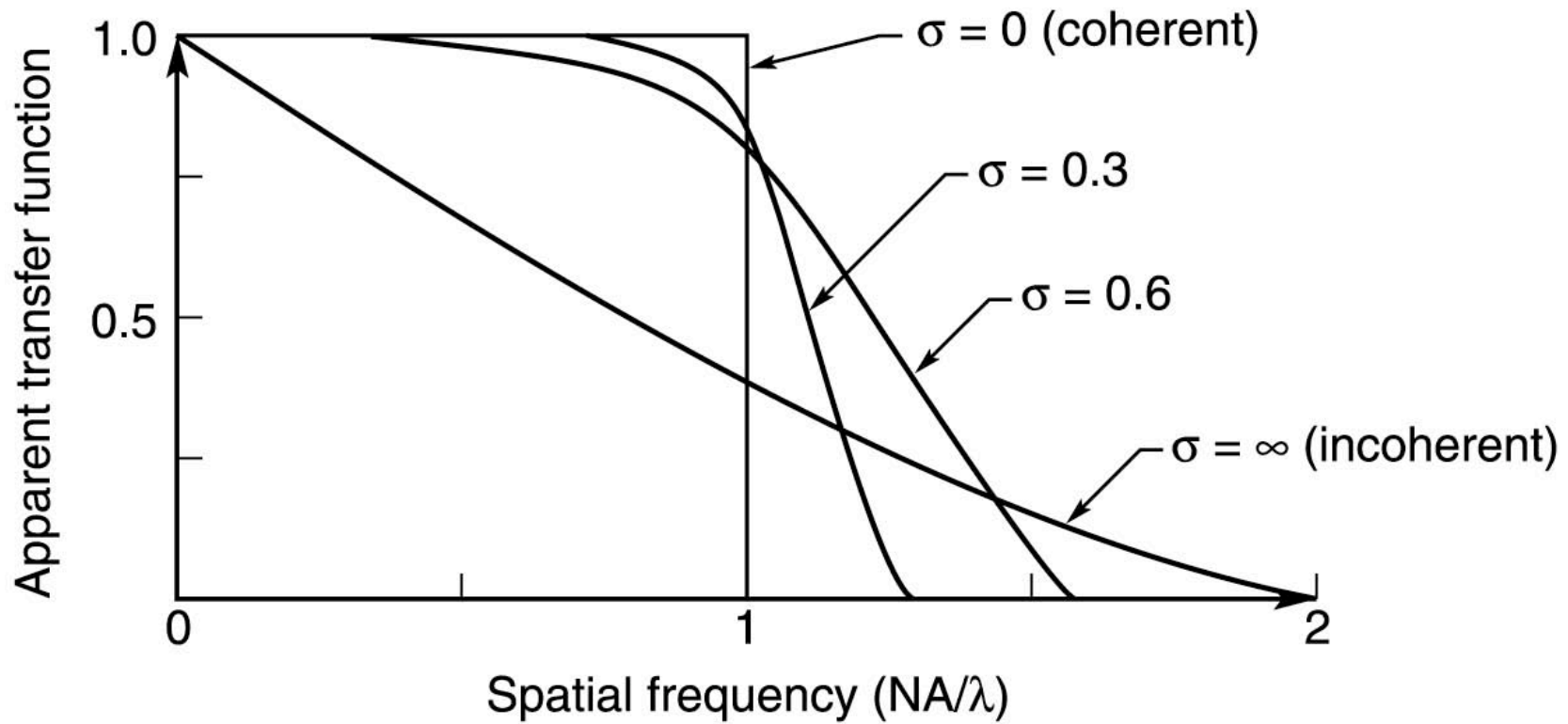


Partially Coherent Illumination Permits Improved Spatial Resolution by a Factor Approaching Two



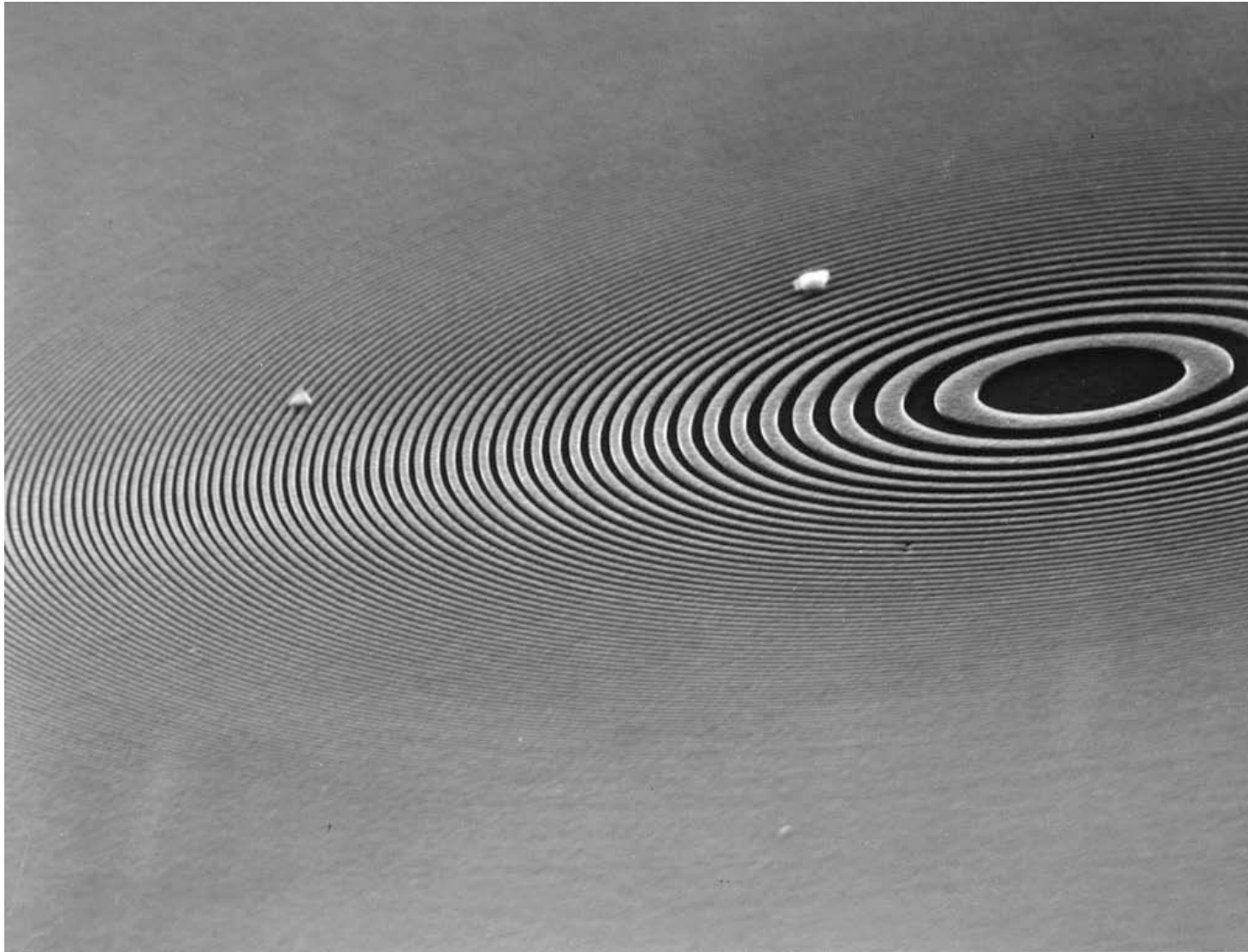


Optical Transfer Properties with Varying Degrees of Partially Coherent Illumination





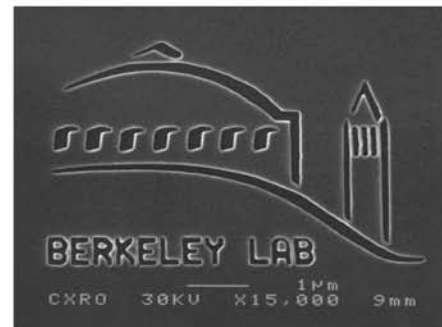
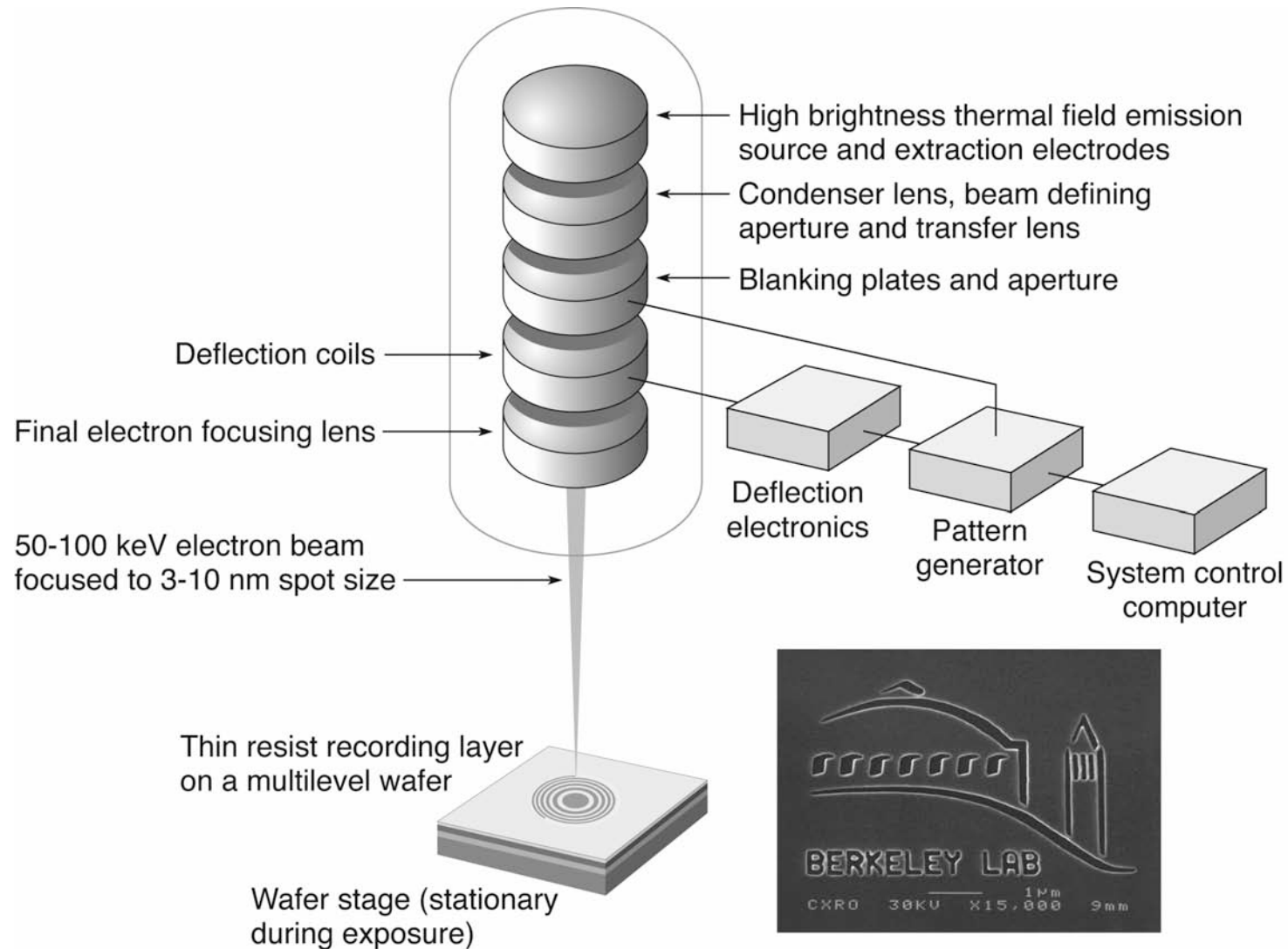
A Fresnel Zone Plate Lens Used for X-Ray Microscopy



Courtesy of E. Anderson (LBNL)



The Nanowriter: High Resolution Electron Beam Writing With High Placement Accuracy



Ch09_F43VG.ai

Courtesy of E. Anderson (LBNL)

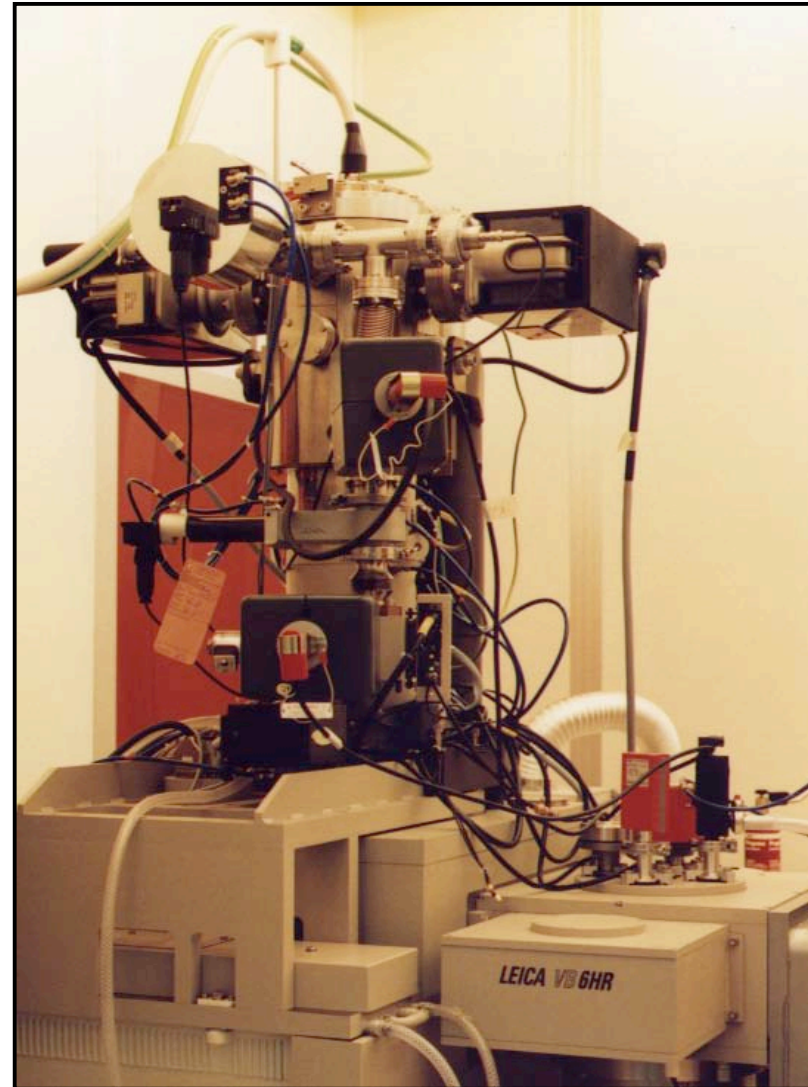


LBNL Nanowriter: Unique Ultra-High Resolution, High Accuracy Electron Beam Lithography Tool



Key Specifications

Parameter	Nanowriter
Beam size	5.0 nm 2.5 nm (New C3 lens)
Beam placement	2.5 nm (65 μm field) 20 nm (512 μm field)
Stitching	20 nm (1 cm field)
Beam voltage	20-100 kV
Beam current	1 nA at 10 nm 1.0-0.2 nA at 2.5 nm (new C3 lens)
Speed	25 MHz
Deflection field	16 bit
Interferometer	$\lambda/1024$
Wafer size	8"
Real time detection and feedback	Backscattered, transmitted and secondary electrons; digital image processing



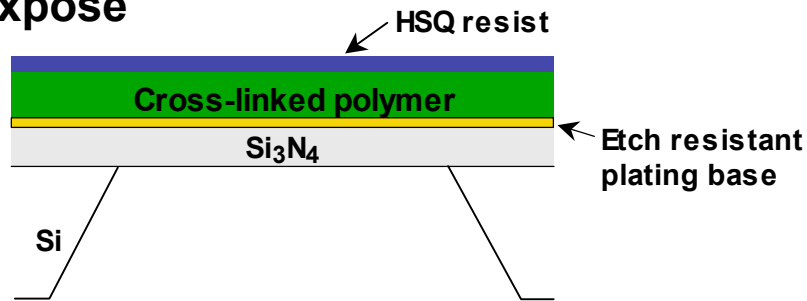
Courtesy of E. Anderson (LBNL)



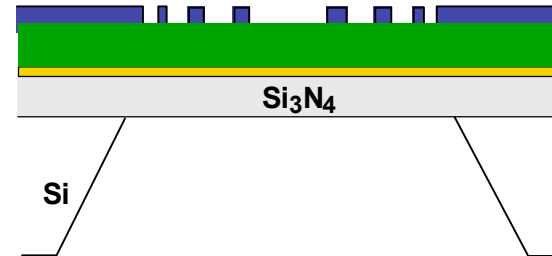
Nanofabrication is Critical for High Fidelity, High Aspect Ratio Zone Plates



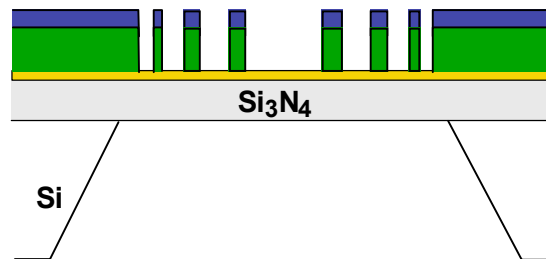
1. Expose



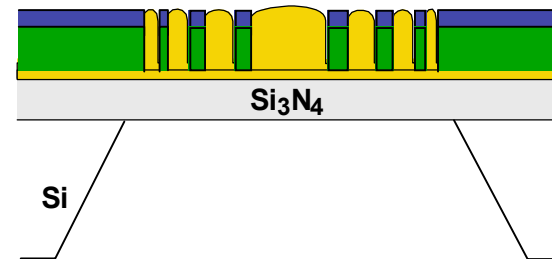
2. Develop



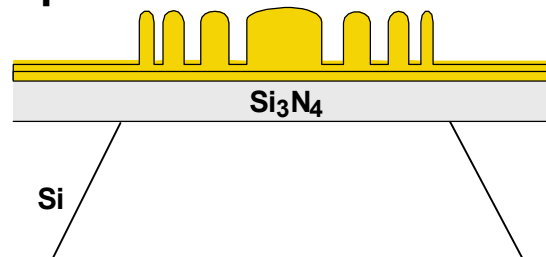
3. Cryogenic ICP Etch



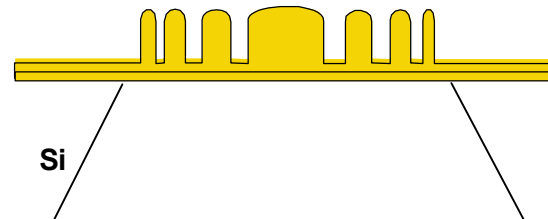
4. Plate



5. Strip Resist



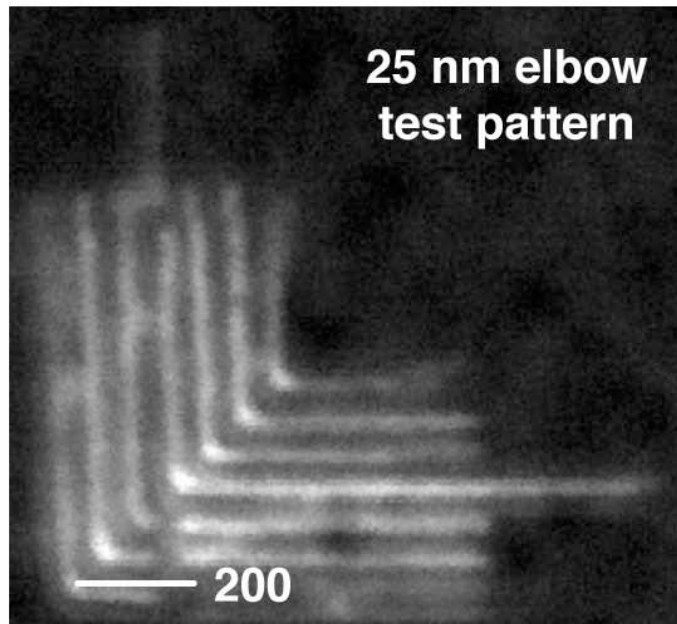
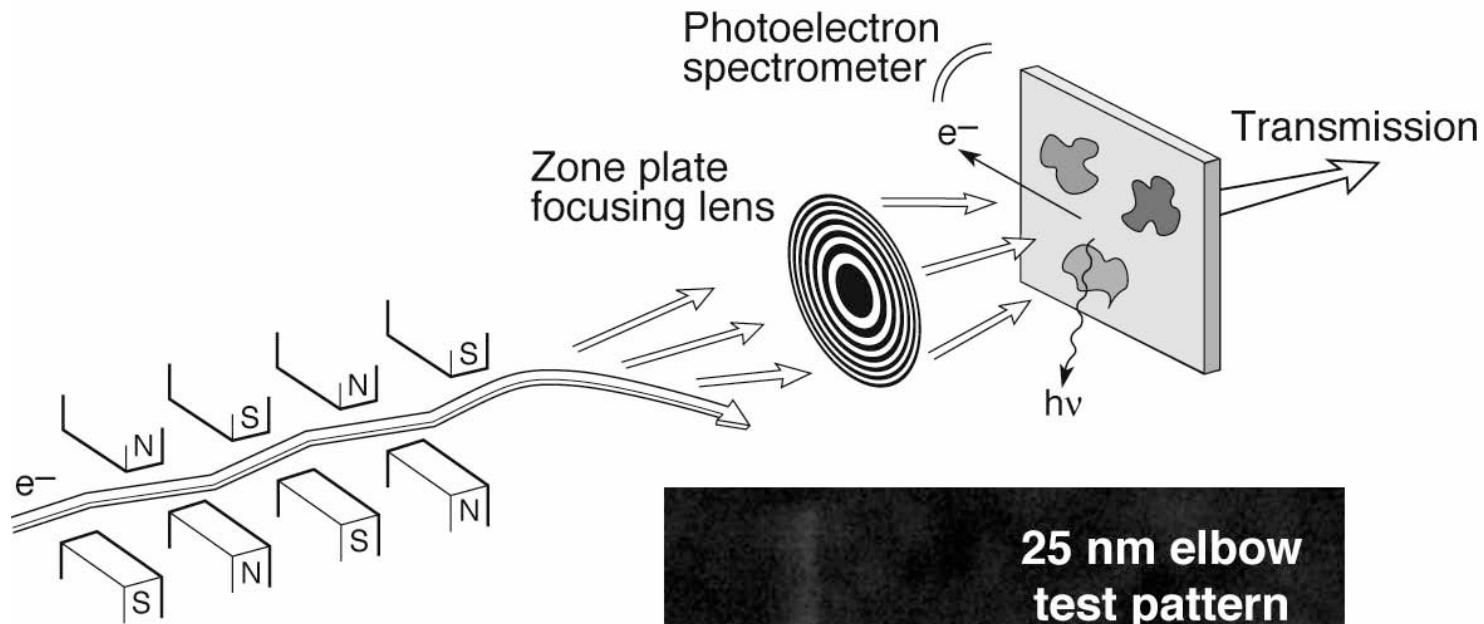
6. Strip Si₃N₄ and Cr/Au Plating Base



Courtesy of E. Anderson, A. Liddle, W. Chao, D. Olynick, and B. Harteneck (LBNL)



Spectromicroscopy: High Spatial and High Spectral Resolution Studies of Surface and Thin Films



25 nm elbow test pattern

Scanning Soft X-Ray Microscope

ALS beamline 11.0.2

395 eV; $\lambda/\Delta\lambda \approx 6000$

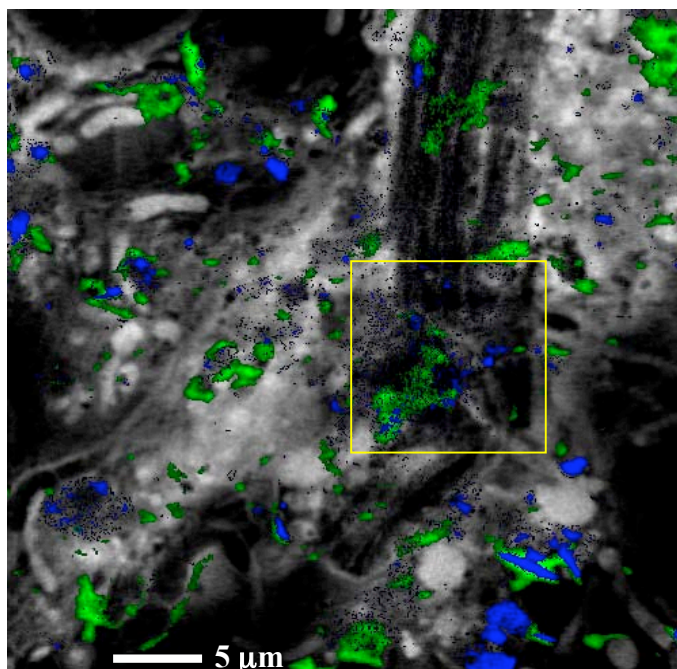
240 × 240 pixels

1.2 μm × 1.2 μm

2 ms dwell time

Courtesy of Tolek Tyliczszak (Dec. 2003)

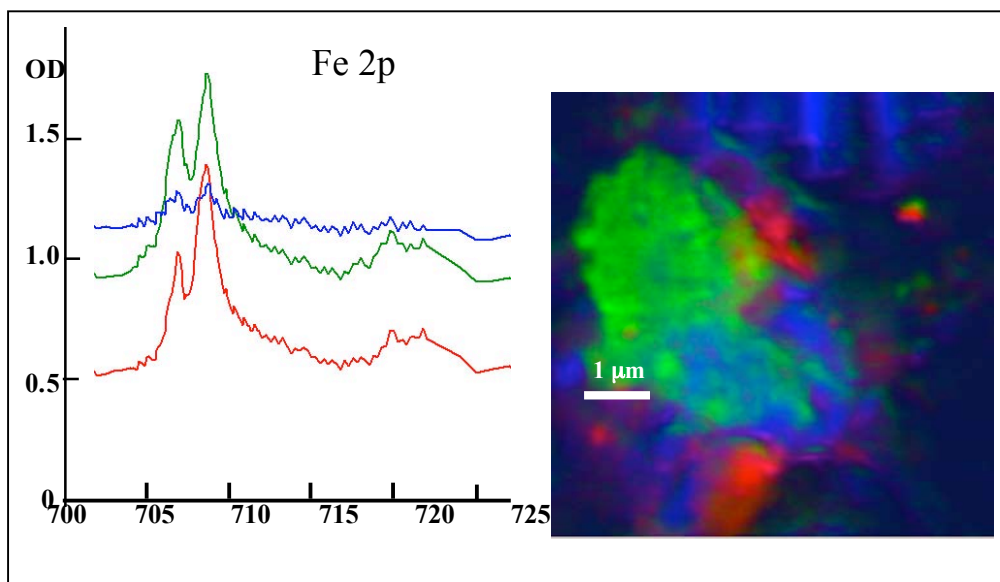
Biofilm from Saskatoon River



Protein (gray), Ca, K

RESULTS

- Ni, Fe, Mn, Ca, K, O, C elemental map, (there was no sign of Cr.)
- Different oxidation states for Fe and Ni



Different oxidation states (minerals) found for Fe & Ni

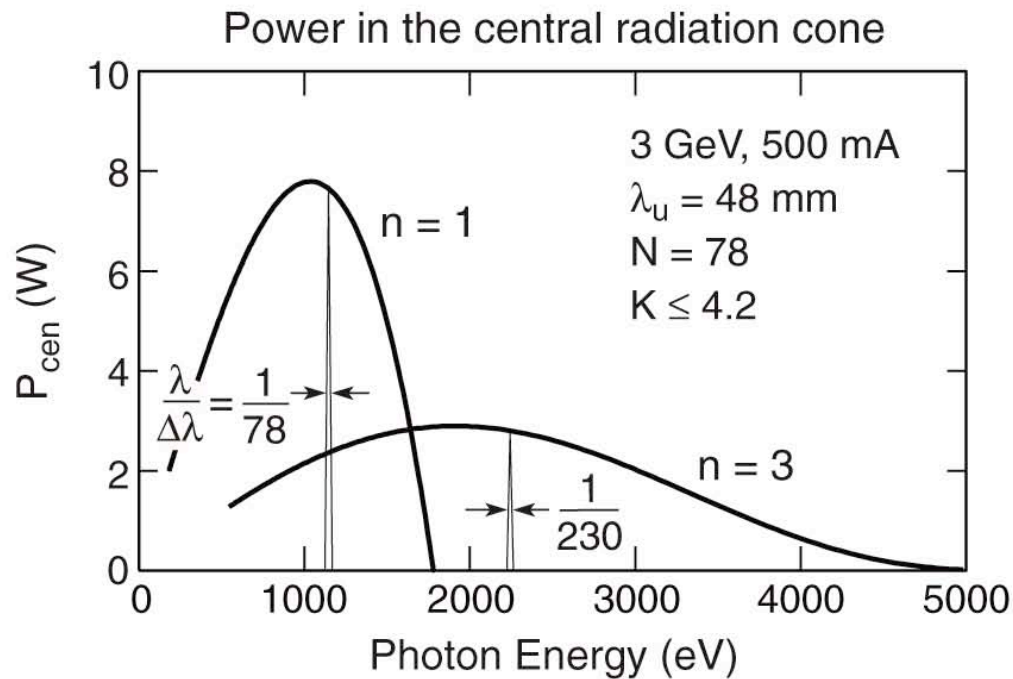
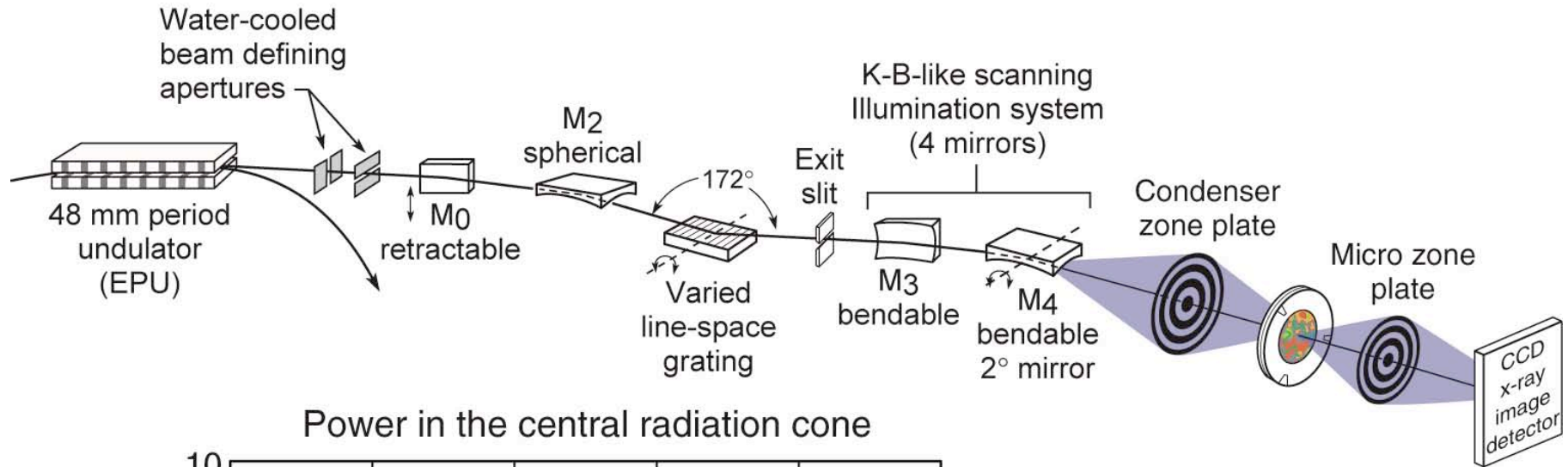
Tohru Araki, Adam Hitchcock (McMaster University)

Tolek Tyliszczak, LBNL

Sample from: John Lawrence, George Swerhone (NWRI-Saskatoon), Gary Leppard (NWRI-CCIW)

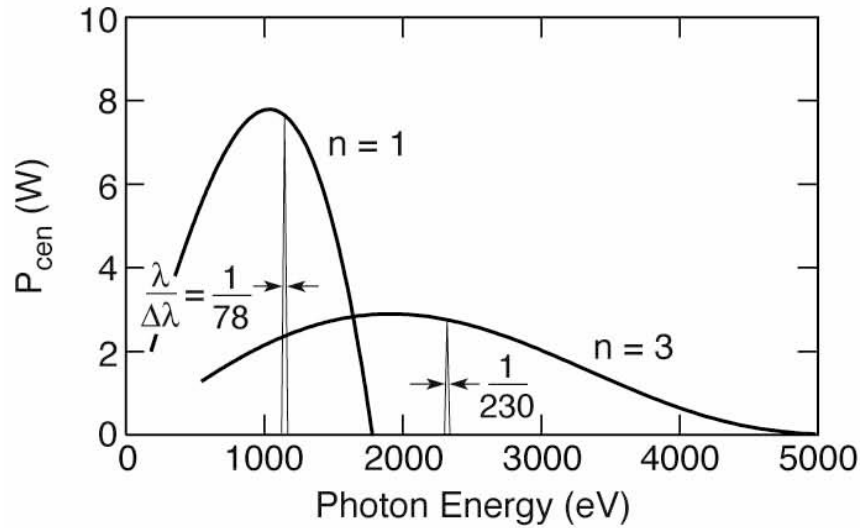


Beamline Layout for a High Spatial Resolution, High Spectral Resolution, Full Field Microscope

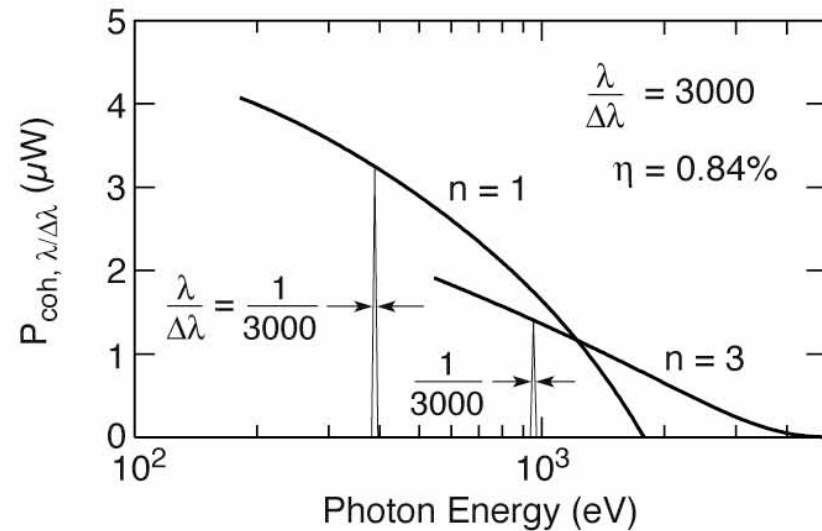
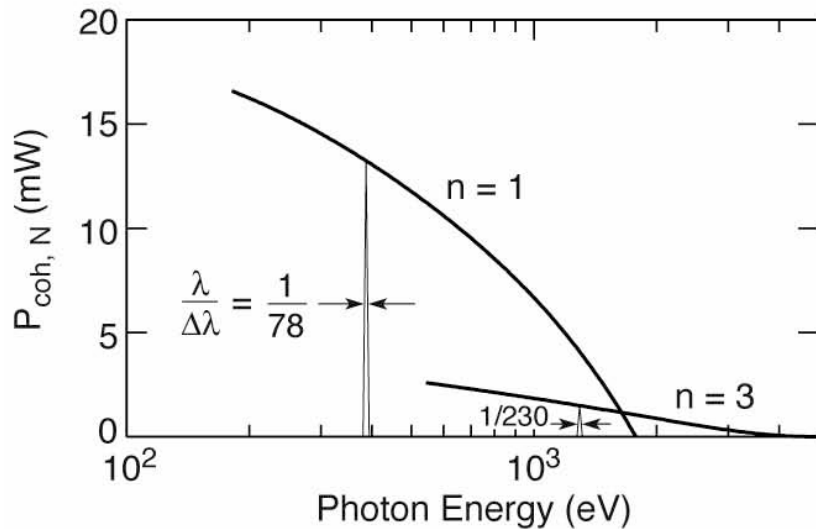




Power Curves for the Stanford EPU

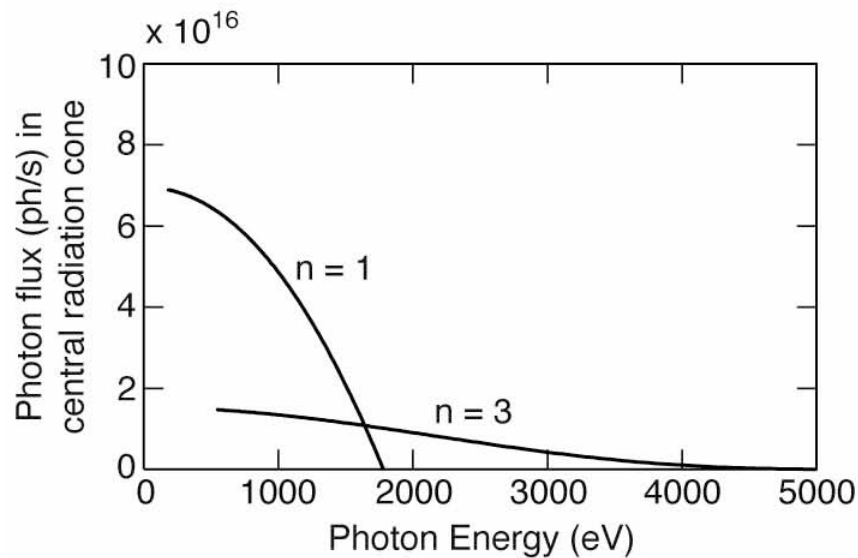


3 GeV, 500 mA
 $\lambda_u = 48$ mm
 $N = 78$
 $K \leq 4.2$
 $\sigma_h = 420 \mu\text{m}$
 $\sigma_v = 42 \mu\text{m}$
 $\sigma_h' = 42 \mu\text{r}$
 $\sigma_v' = 6 \mu\text{r}$
 $\theta_{cen} = 30 \mu\text{r}$

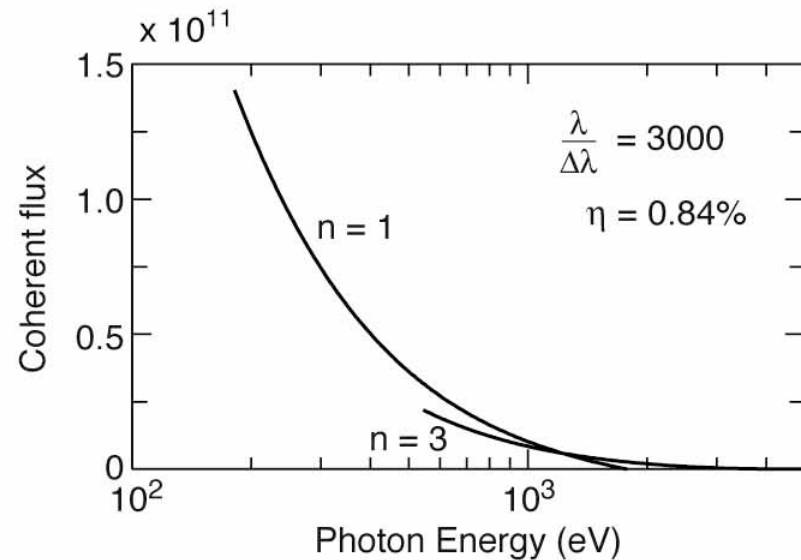
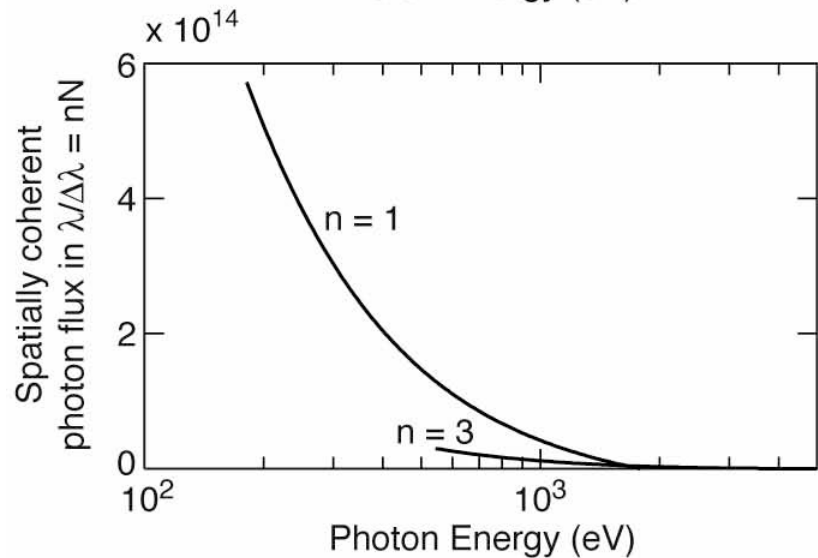




Photon Flux Curves for the Stanford EPU



3 GeV, 500 mA
 $\lambda_u = 48$ mm
 $N = 78$
 $K \leq 4.2$
 $\sigma_h = 420 \mu\text{m}$
 $\sigma_v = 42 \mu\text{m}$
 $\sigma_h' = 42 \mu\text{r}$
 $\sigma_v' = 6 \mu\text{r}$
 $\theta_{\text{cen}} = 30 \mu\text{r}$

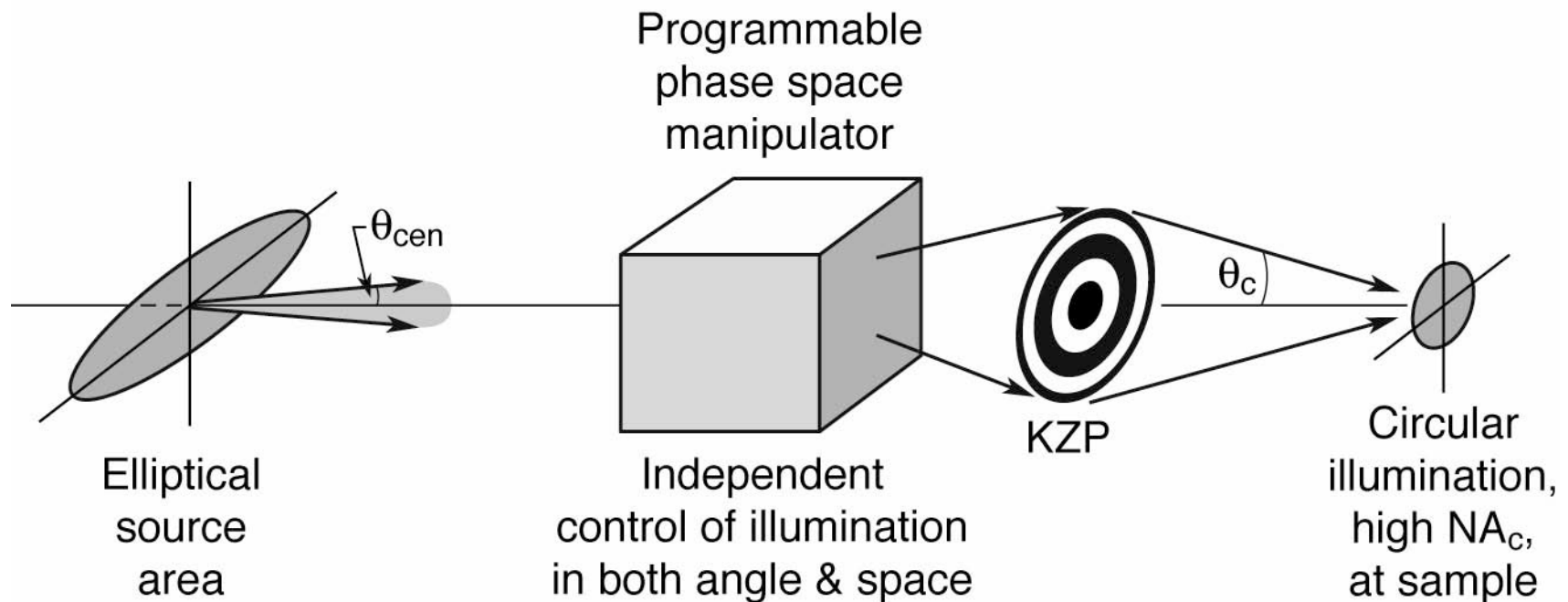




A Novel Illuminator is Required



Scanning optics modify phase space, transforming elliptical spatial distribution to circular, and increasing the angular illumination to provide the desired degree of partial coherence. Based on experience with EUV lithographic imaging at ALS Beamline 12.0, P. Naulleau and P. Denham (CXRO), SRI-2003, p. 792.



P. Naulleau et al., *Optics Commun.* 234, 53 (2004)

P. Naulleau et al., *Appl. Optics* 42, 820 (2004)



Exposure Time for a Full Field, High Spatial and High Spatial Resolution, Soft X-Ray Microscope on an EPU at Stanford



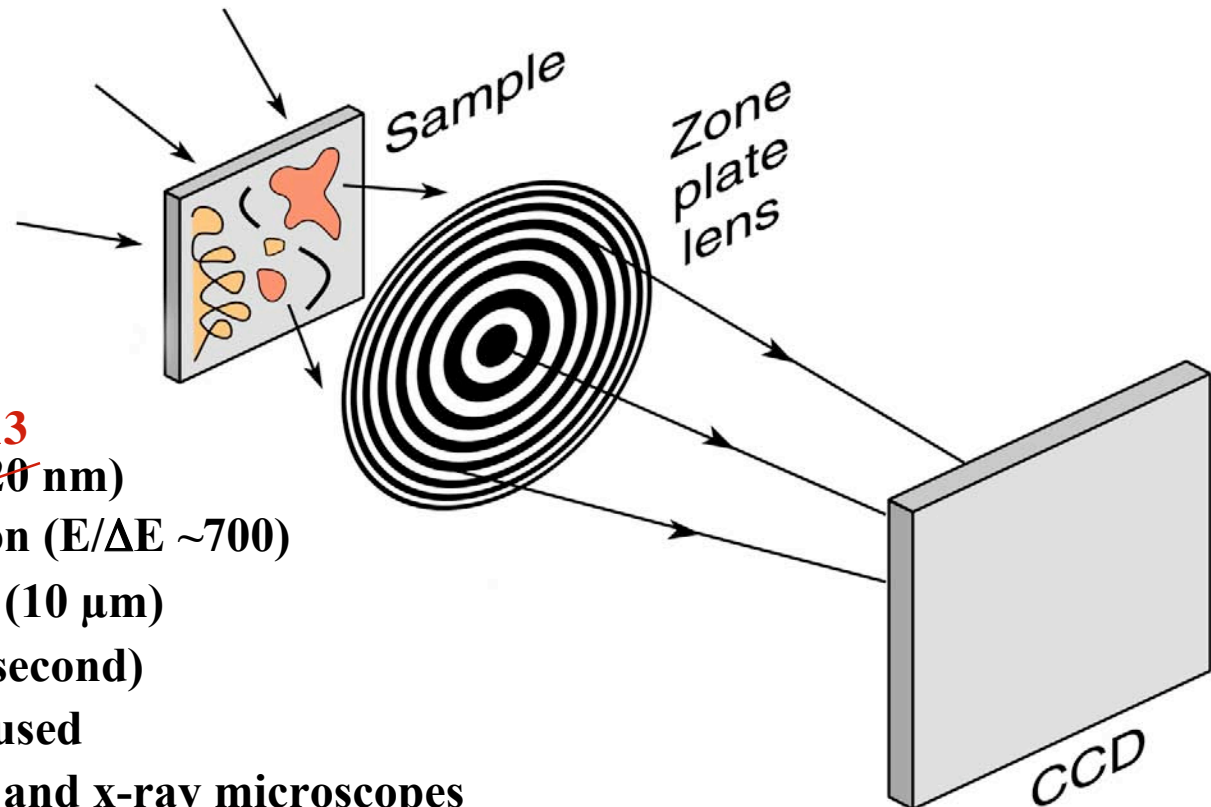
Photon flux in central radiation cone / $6.43E+16$ #/sec at 500 eV
 $(\lambda = 2.5 \text{ nm}, \lambda/\Delta\lambda = 78)$
 Spectral filter to $\lambda/\Delta\lambda = 3,000$
 / $1.7.76E+15$
 Beamline efficiency (0.84%)
 (7 mirrors plus 1 grating @ 10%) / $1.45E+13$

CONDENSER		
type	ZP	D=10mm, $\Delta r=30\text{nm}$)
collection NA		rad
collection solid angle	8.26E-03	sr
magnification	5	
illumination NA	0.0413	rad
illumination solid angle		sr
sigma	6.70E-01	
KZP collection percetage	100%	
collected flux	1.45E+13	#/sec at 2.5nm
efficiency	10%	
post-condenser flux	1.45E+12	#/sec at 2.5nm
SAMPLE		
illumination area (ellipse)	20 x 20	μm^2
sample size	10 x 10	μm^2
illumination efficiency	0.25	
efficiency	50%	
flux after sample	1.81E+11	#/sec at 2.5nm
MZP		
MZP D	63	μm
MZP Δr	20	nm
MZP f	525	μm
MZP NA	0.06	
MZP efficiency	8%	
flux after MZP	1.45E+10	
CCD		
CCD pixel size	12.5 μm x 12.5 μm	
CCD pixels	(2048) ²	
CCD dimension	1" x 1"	
CCD efficiency	80%	
total flux onto CCD	1.16E+10	#/sec at 2.5nm
CCD counts per pixel per sec	2.77E+03	#/sec at 2.5nm
exposure time (for 10³ counts per pixel)	0.36	sec

0.36 sec exposure time for full field microscope
 $\lambda = 2.5 \text{ nm}, \lambda/\Delta\lambda = 3000$
 Spatial resolution $\sim 20 \text{ nm}$



The XM-1 Soft X-Ray Microscope at the Advanced Light Source (ALS)



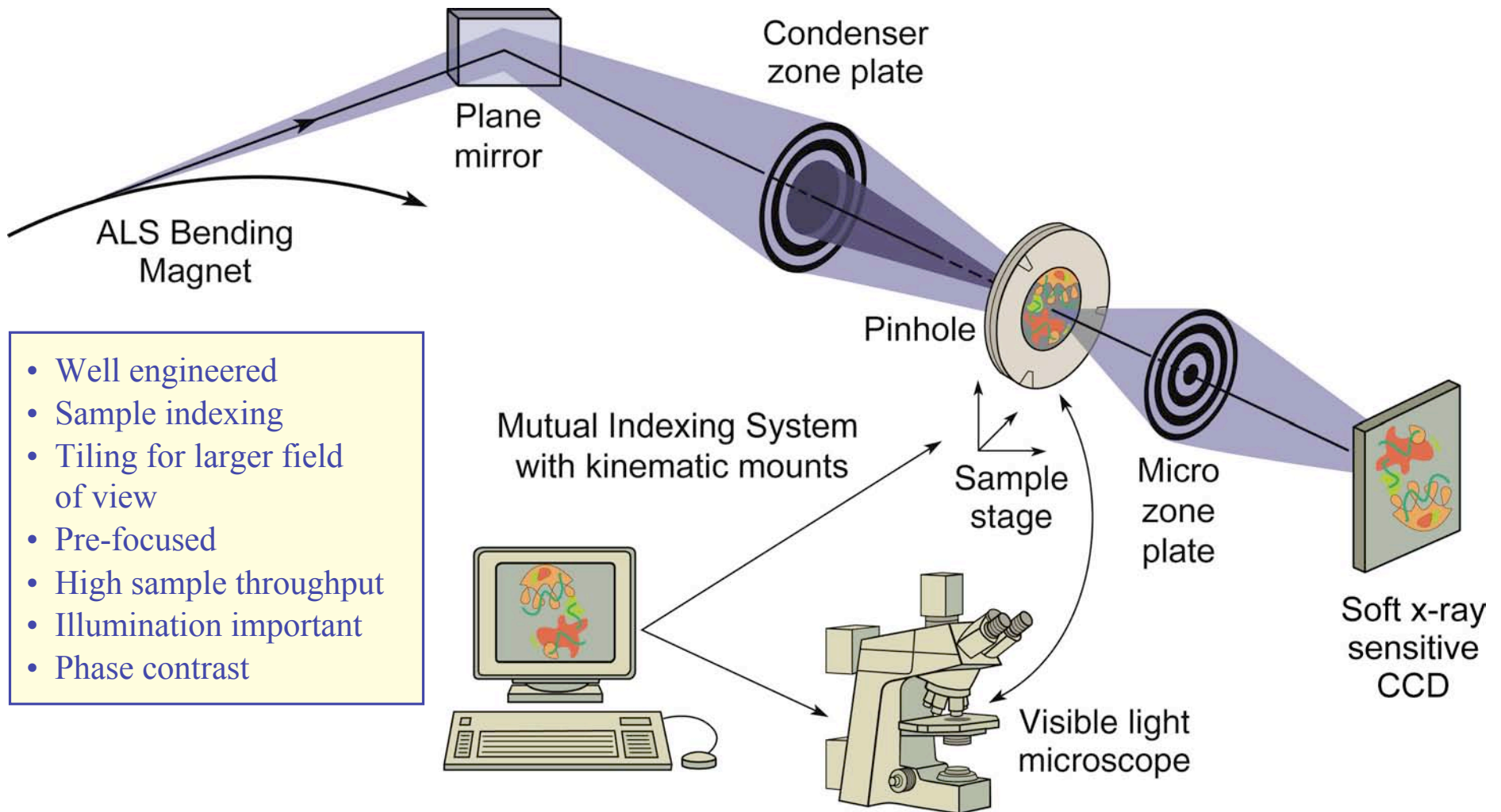
13

- High spatial resolution (~~20~~ nm)
- Modest spectral resolution ($E/\Delta E \sim 700$)
- Thick, hydrated samples (10 μm)
- Short exposure time (~ 1 second)
- Well engineered, pre-focused
- Mutually indexed visible and x-ray microscopes
- High throughput (hundreds of samples per day)
- Large image fields by tiling
- Easy access, user friendly
- Cryotomography

$E = 250 - 1.8 \text{ keV}$
 $\lambda = 0.7 \text{ nm} - 5 \text{ nm}$

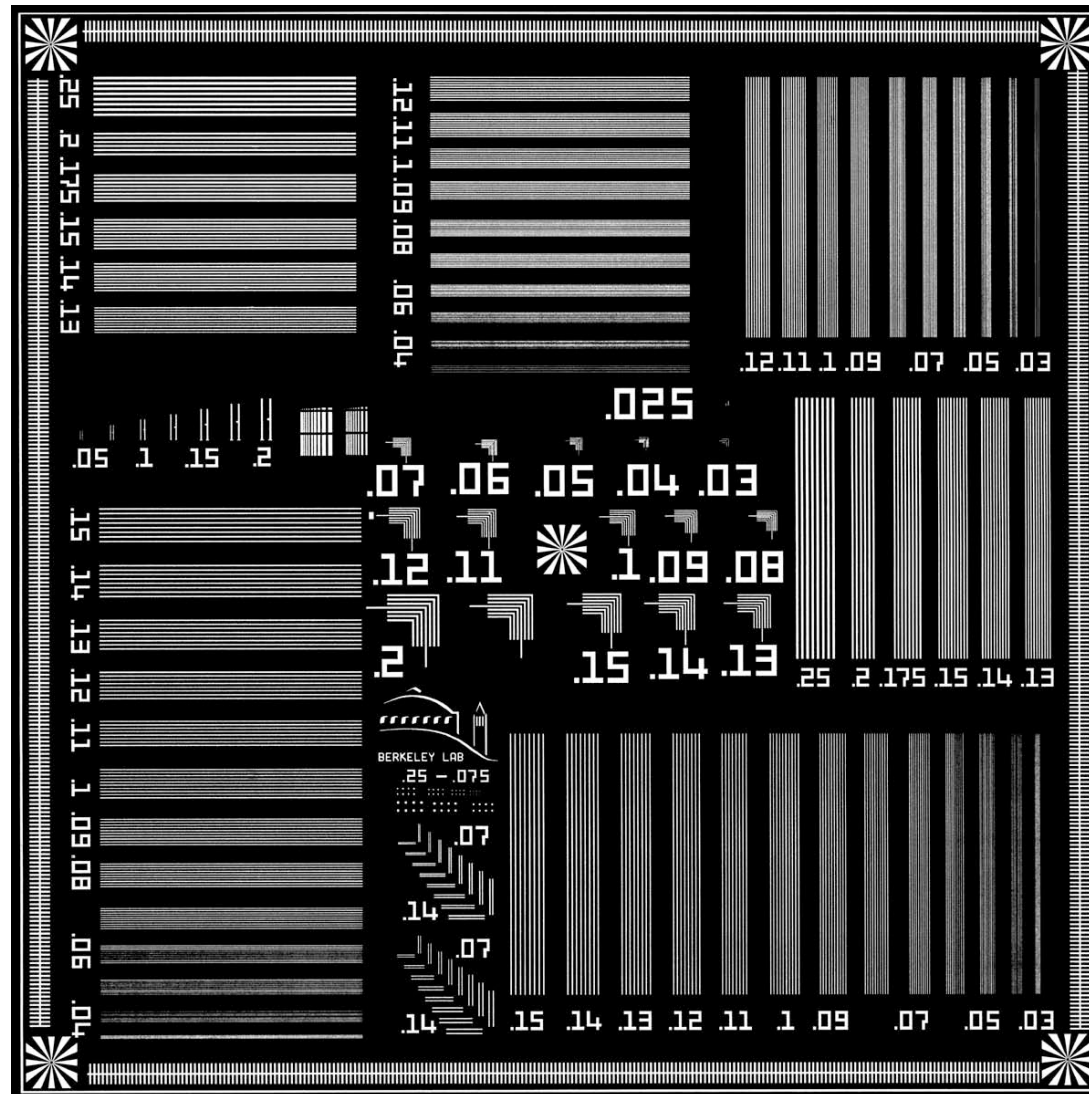


High Resolution Zone-Plate Microscope XM-1 at the ALS





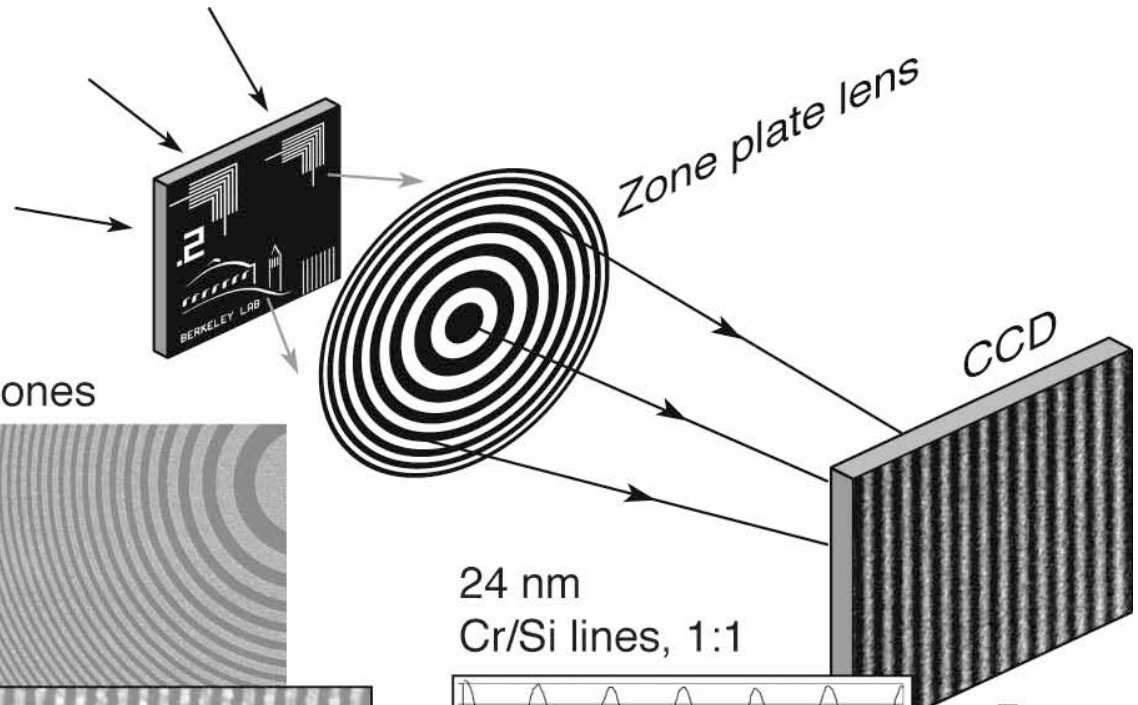
Test Pattern for Nanometer Soft X-Ray Imaging



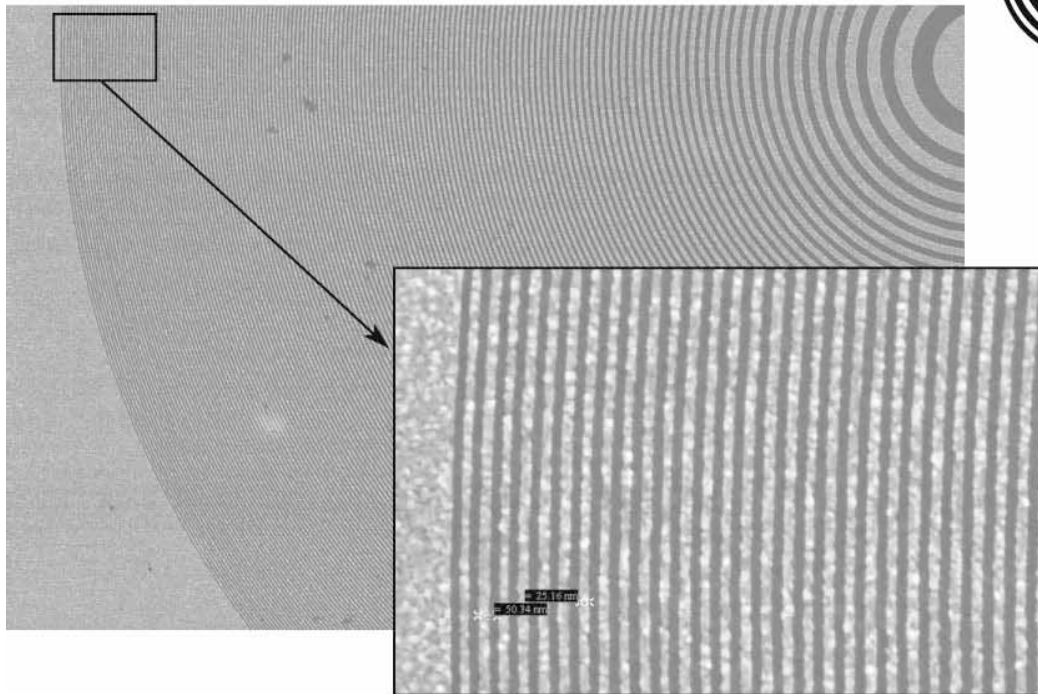
Courtesy of E. Anderson, D. Olynick, B. Harteneck, E. Veklerov



Soft X-Ray Microscopy at the ALS: 20 nm Spatial Resolution

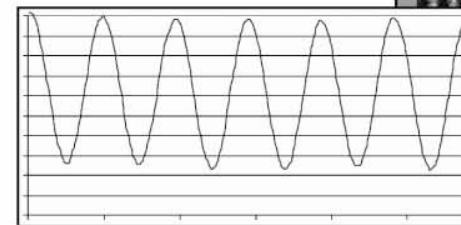


$\Delta r = 25 \text{ nm}$, $D = 63 \mu\text{m}$, $N = 618 \text{ zones}$



E. Anderson (LBNL)

24 nm
Cr/Si lines, 1:1

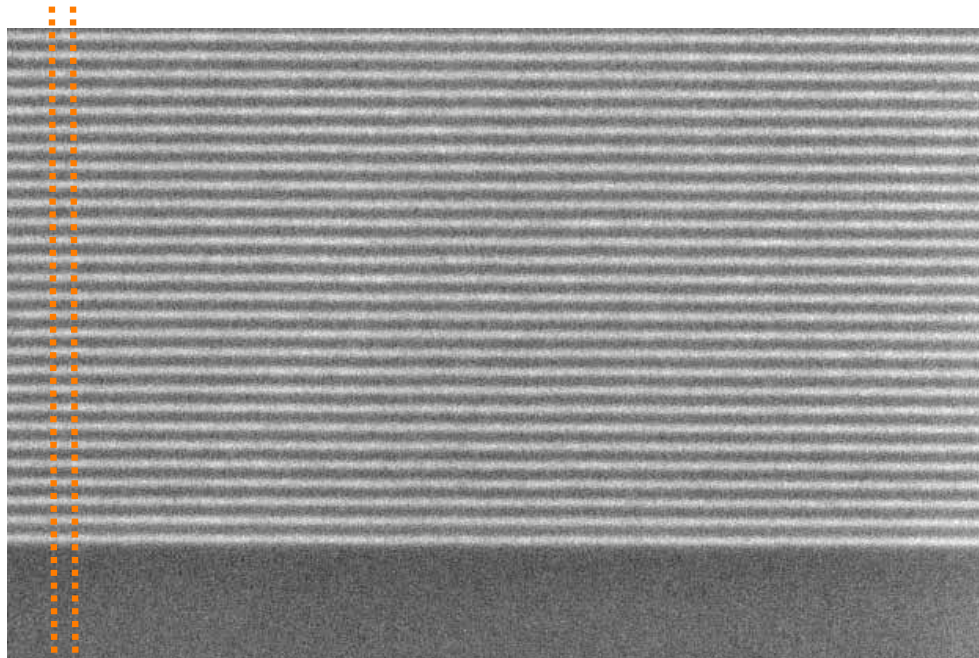


W. Chao (UCB & LBNL)

W. Chao et al.,
Opt. Lett. 28, 2019 (Nov 2003)



Multilayer Mirror Coatings Can Be Thinned and Used As Sub-20 nm Test Patterns



SEM Micrograph of Cr/Si test pattern

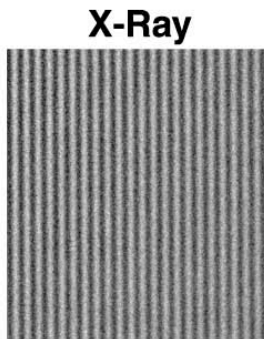


Courtesy of W. Chao (UCB & CXRO/LBNL)

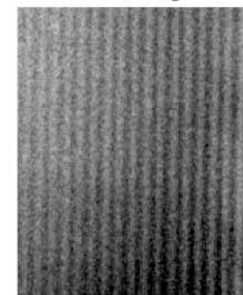
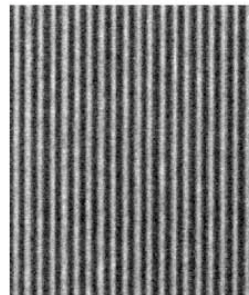
High quality test patterns can be fabricated with sections as thin as 5 nm.



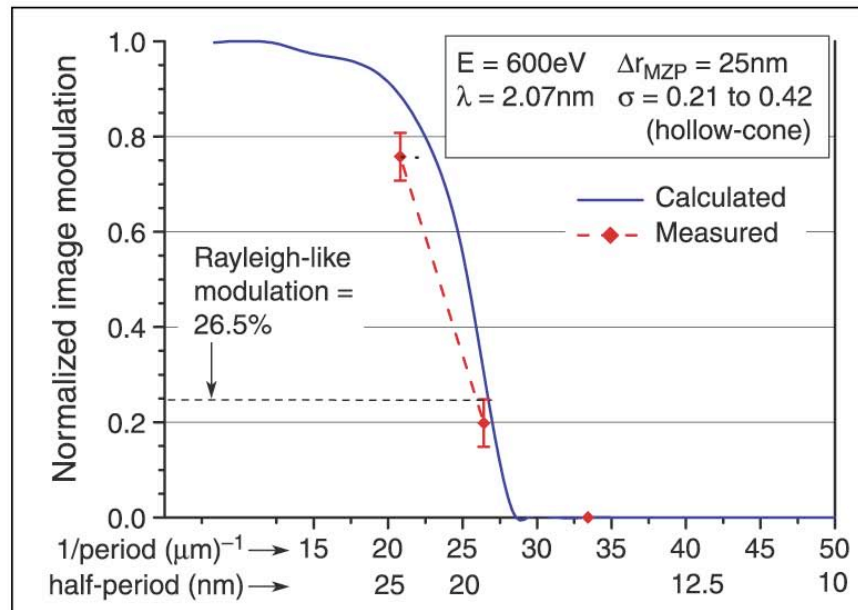
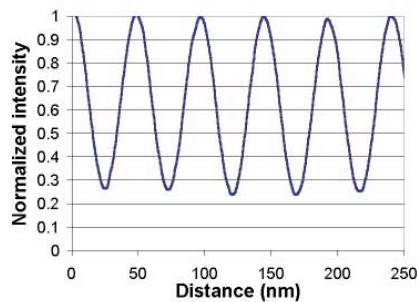
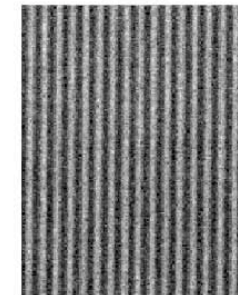
Near Diffraction Limited Soft X-Ray Microscopy: 20 nm Spatial Resolution at 2.07 nm Wavelength



24 nm lines and spaces (Cr/Si)
75% modulation
600 eV (2.07 nm)



19 nm lines and spaces (Cr/Si)
20% modulation

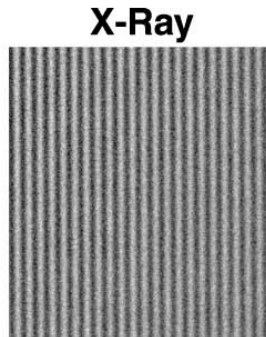


(Courtesy of Weilun Chao, UC Berkeley and CXRO/LBNL)

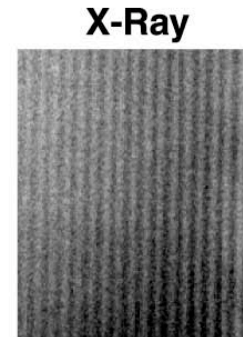
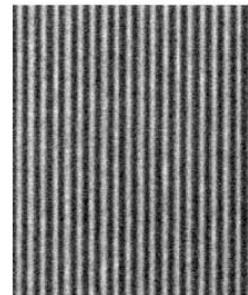
W. Chao et al.,
Opt. Lett. 28, 2019 (Nov 2003)



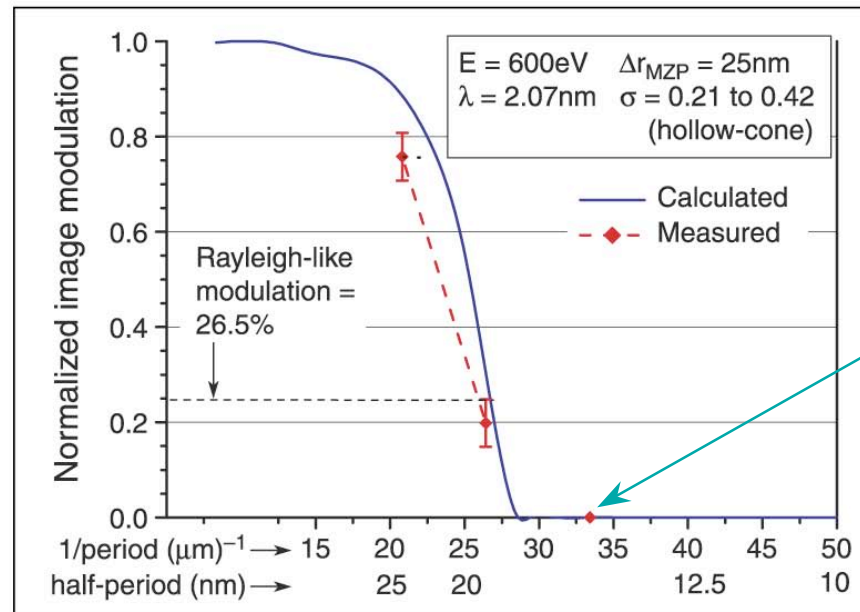
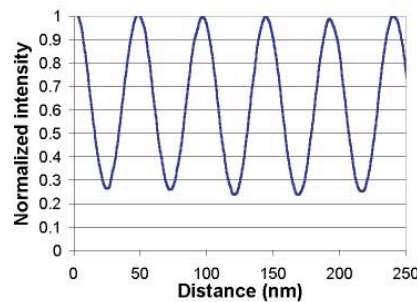
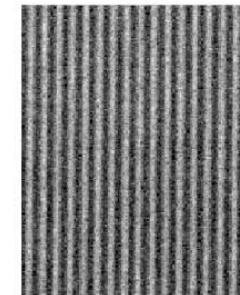
Near Diffraction Limited Soft X-Ray Microscopy: 20 nm Spatial Resolution at 2.07 nm Wavelength



X-Ray
24 nm lines and spaces (Cr/Si)
75% modulation
600 eV (2.07 nm)



X-Ray
19 nm lines and spaces (Cr/Si)
20% modulation (barely "resolved")



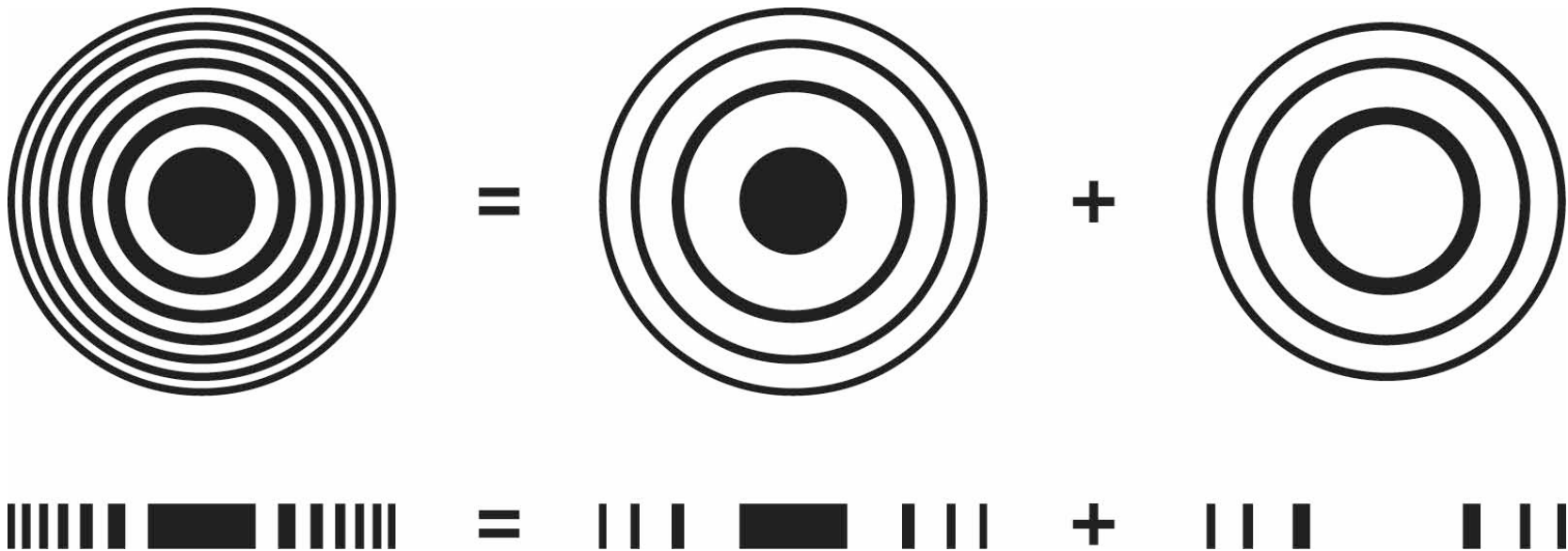
15 nm lines
not resolved,
no modulation

W. Chao et al.,
Opt. Lett. 28, 2019 (Nov 2003)

(Courtesy of Weilun Chao, UC Berkeley and CXRO/LBNL)



New Overlay Nanofabrication Technique for Narrower Outer Zones



$\Delta r = 15 \text{ nm}$

$\Delta t = 90 \text{ nm}$

Overlay $\simeq 2 \text{ nm}$ accuracy

Courtesy of J.A. Liddle, E.H. Anderson, B. Harteneck and W. Chao, LBNL

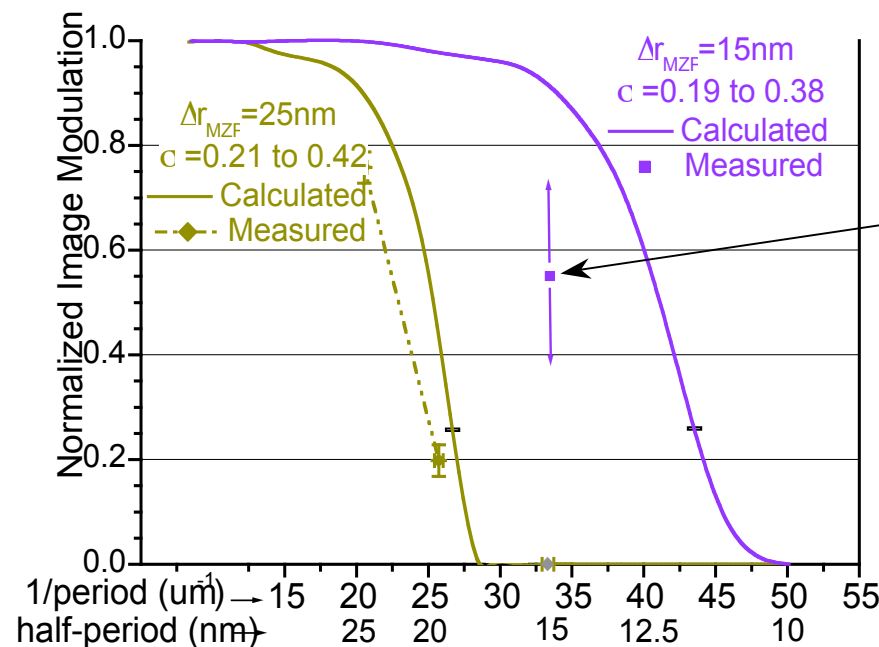
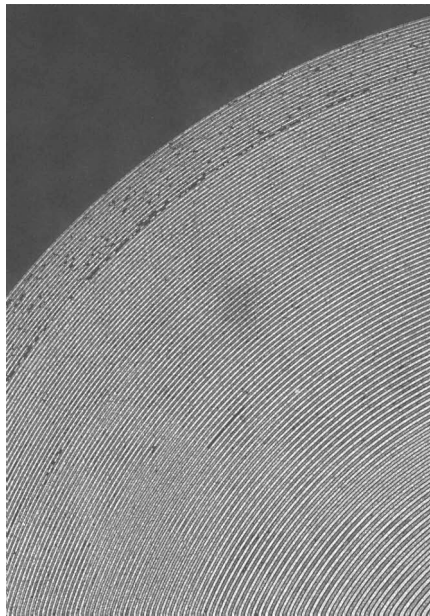


New Results Using Overlay Nanofabrication: Outer Zone Width of 15 nm



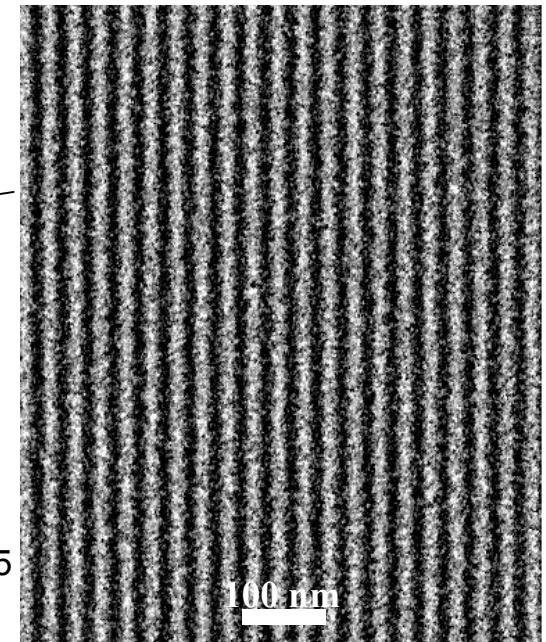
- Zone plate lenses made using a new, e-beam based nanofabrication technique have extended outer zones from 25 nm to 15 nm.
- The new lenses work as expected, resolving fine patterns not seen previously
- Shorter depth of focus (λ/NA^2) opens the opportunity for soft x-ray “optical sectioning” of biological material.

New zone plate lens with
15 nm outer zone width



Courtesy of W. Chao, A. Liddle, E. Anderson,
and B. Harteneck (CXRO/LBNL)

Soft x-ray image of
15 nm Cr/Si lines & spaces



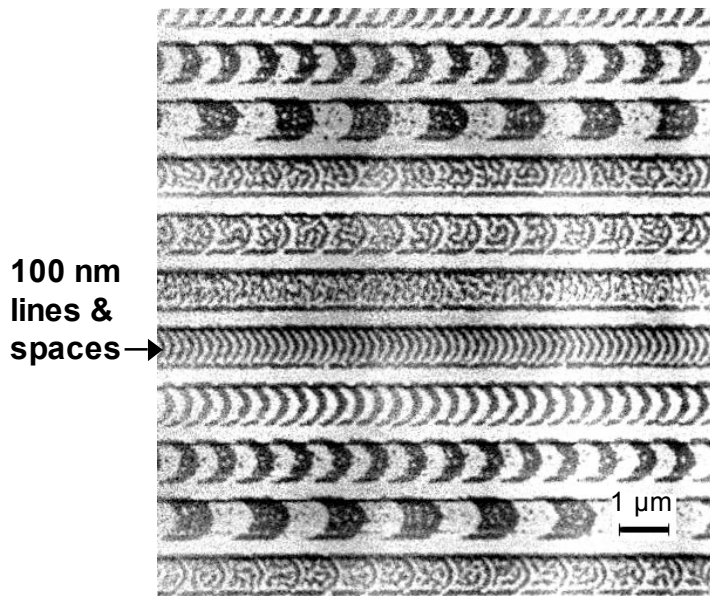
(Nature, in press)



Applications of Soft X-Ray Microscopy



Magnetic Recording Materials

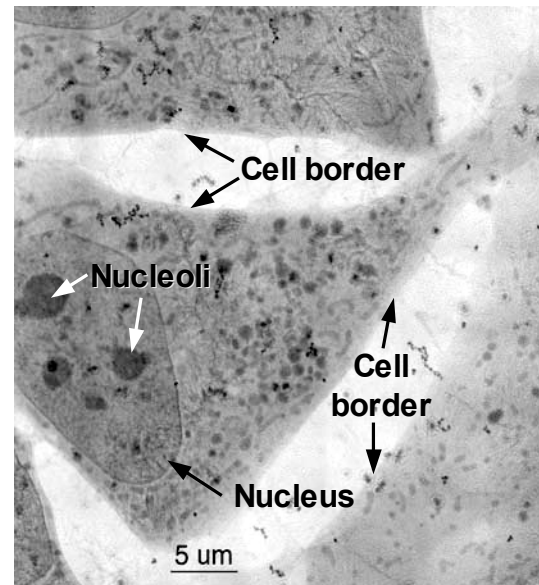


Fe L₃ @ 707.5 eV

FeTbCo Multilayer
with AL Capping Layer

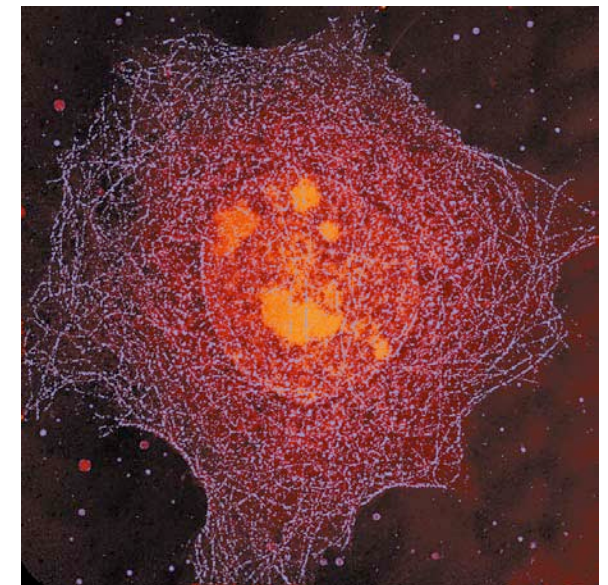
Courtesy of P. Fischer (Max Planck)
and G. Denbeaux (CXRO/LBNL)

Cryo Microscopy for the Life Sciences



Cryo X-Ray Microscopy
of 3T3 Fibroblast Cells

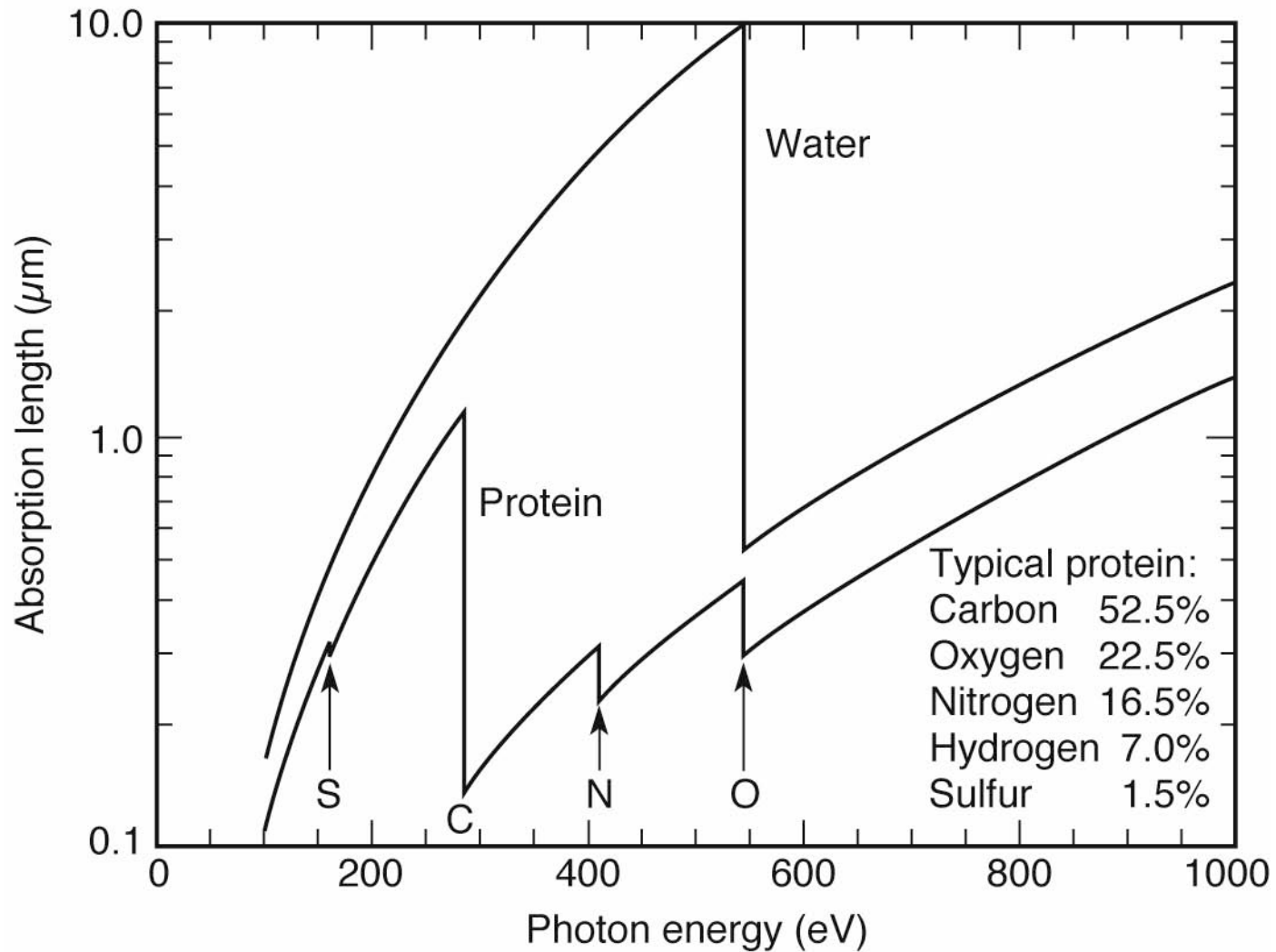
Courtesy of C. Larabell (UCSF)
and W. Meyer-Ilse (CXRO/LBNL)



Protein Labeled
Microtubule Network



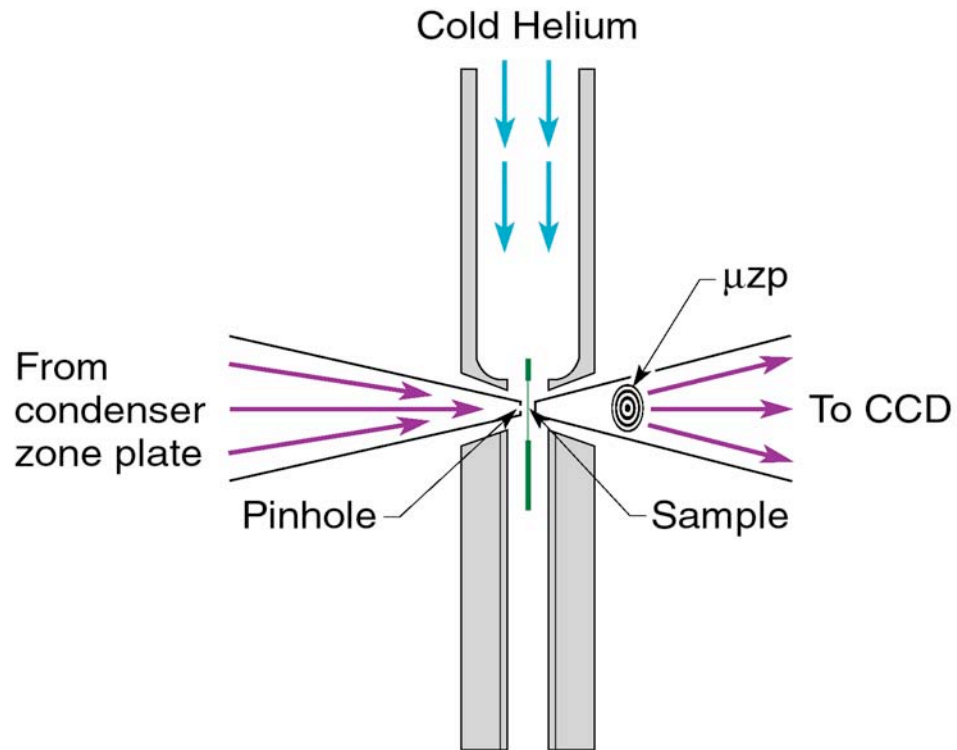
The Water Window for Biological X-Ray Microscopy



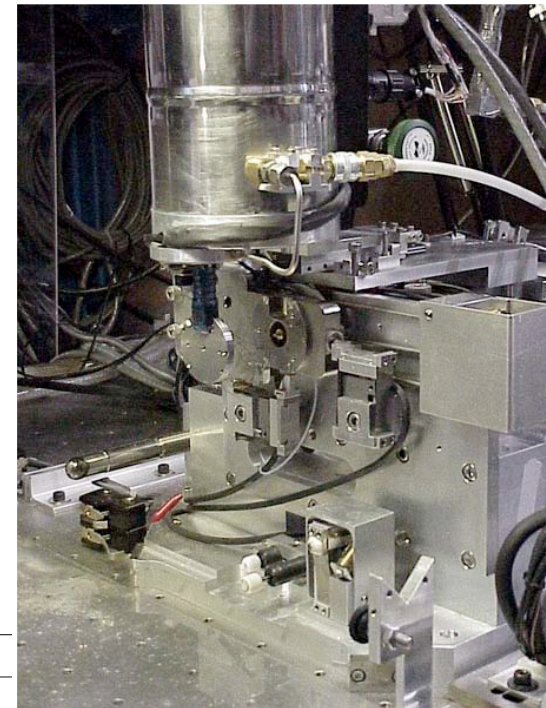
Ch09_F25VG.ai



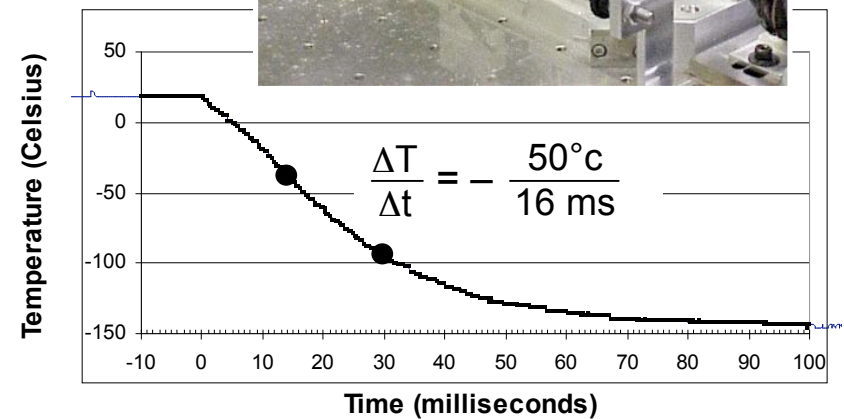
Fast Freeze Cryo Fixation Strongly Mitigates Radiation Dose Effects



Helium passes through LN, is cooled, and directed onto sample windows



Fast Freeze



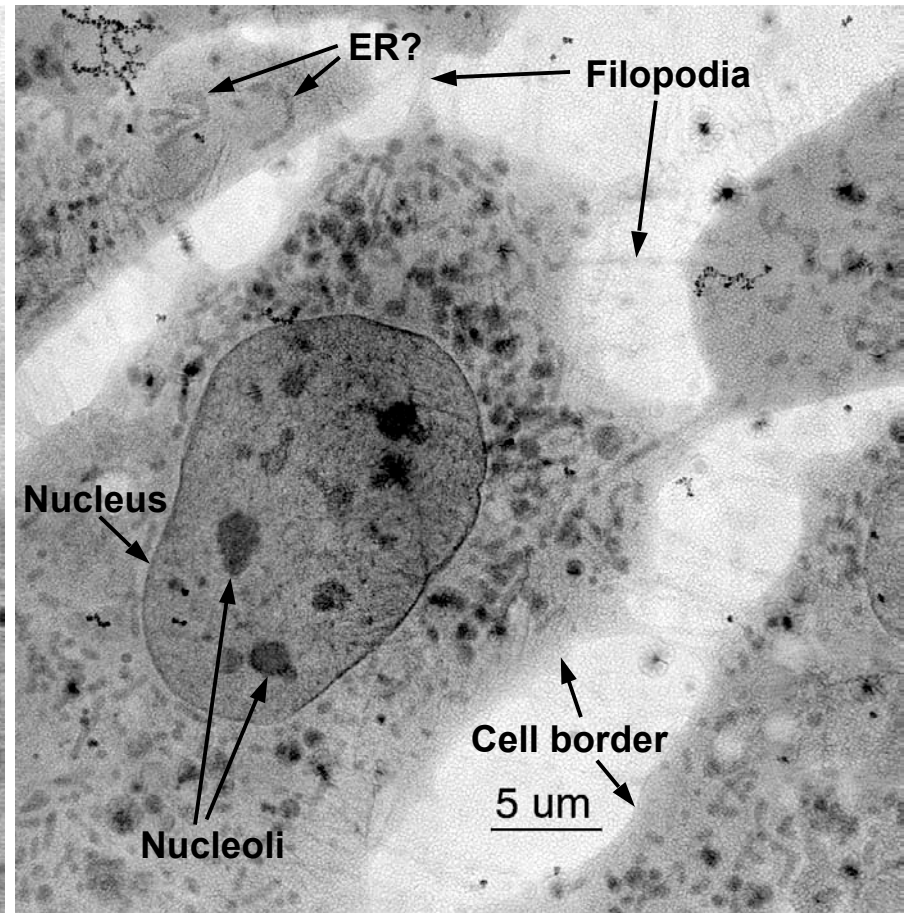
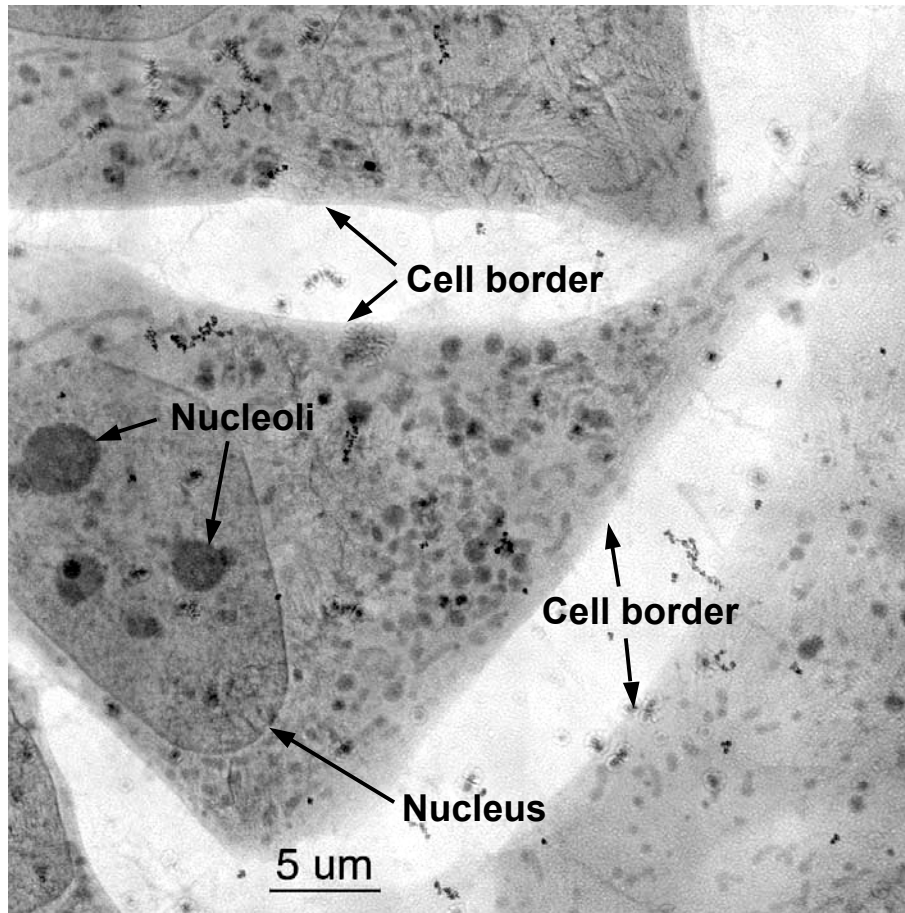
W. Meyer-Ilse, G. Denbeaux, L. Johnson, A. Pearson (CXRO-LBNL)



Organelle Details Imaged with Cryogenic Preservation and High Spatial Resolution



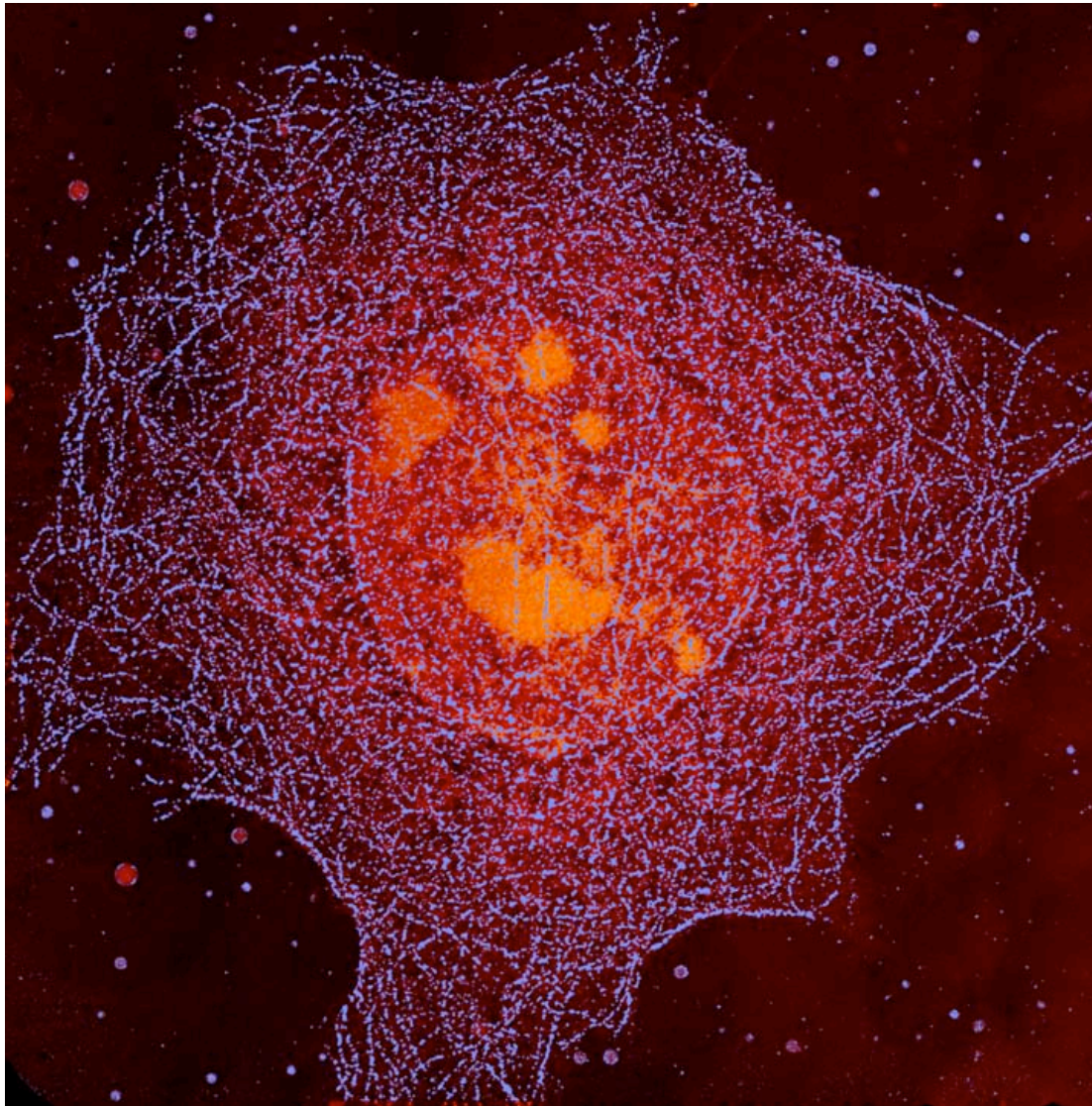
Cryo x-ray microscopy of 3T3 fibroblast cells



C. Larabell, D. Yager, D. Hamamoto, M. Bissell, T. Shin (LBNL Life Sciences Division)
W. Meyer-Ilse, G. Denbeaux, L. Johnson, A. Pearson (CXRO-LBNL)



Bending Magnet Radiation Used With a Soft X-Ray Microscope to Form a High Resolution Image of a Whole, Hydrated Mouse Epithelial Cell



$\hbar\omega = 520 \text{ eV}$

$32 \mu\text{m} \times 32 \mu\text{m}$

Ag enhanced Au labeling of the microtubule network, color coded blue.

Cell nucleus and nucleoli, moderately absorbing, coded orange.

Less absorbing aqueous regions coded black.

W. Meyer-Ilse et al.

J. Microsc. 201, 395 (2001)

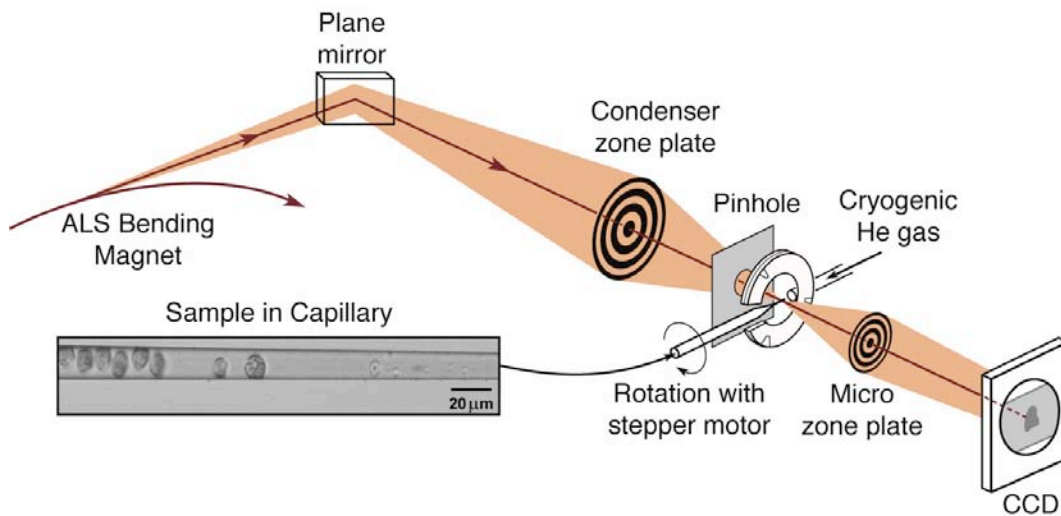
Courtesy of C. Larabell and W. Meyer-Ilse (LBNL)



Bio-Nanotomography for 3D Imaging of Cells

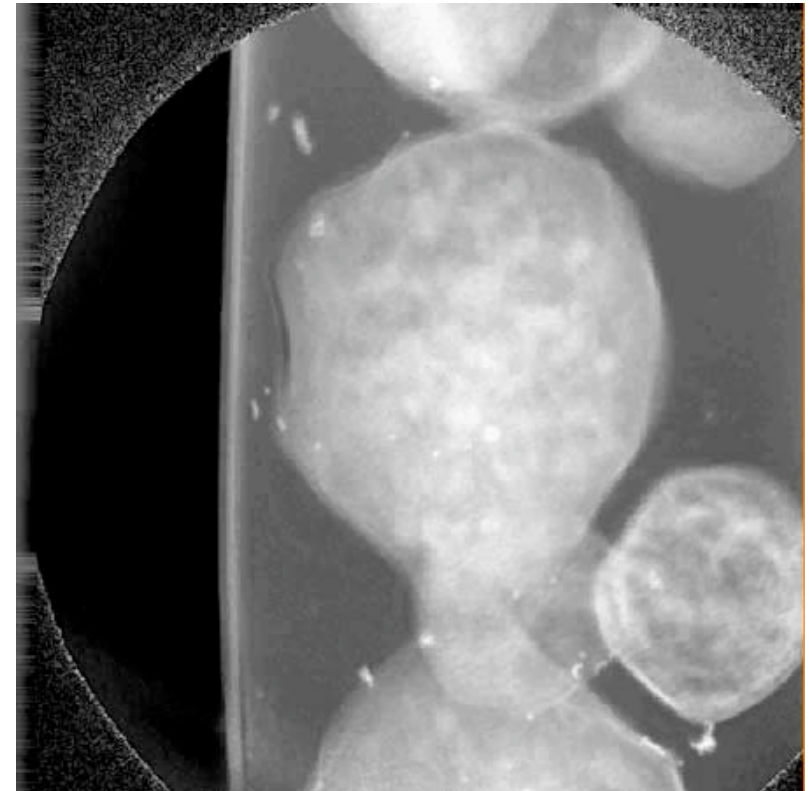


Nanotomography of Cryogenic Fixed Cells



Courtesy of G. Schneider (BESSY)
Surf. Rev. Lett. **9**, 177 (2002)

Soft X-Ray Nanotomography of a Yeast Cell



$\lambda = 2.5 \text{ nm}$

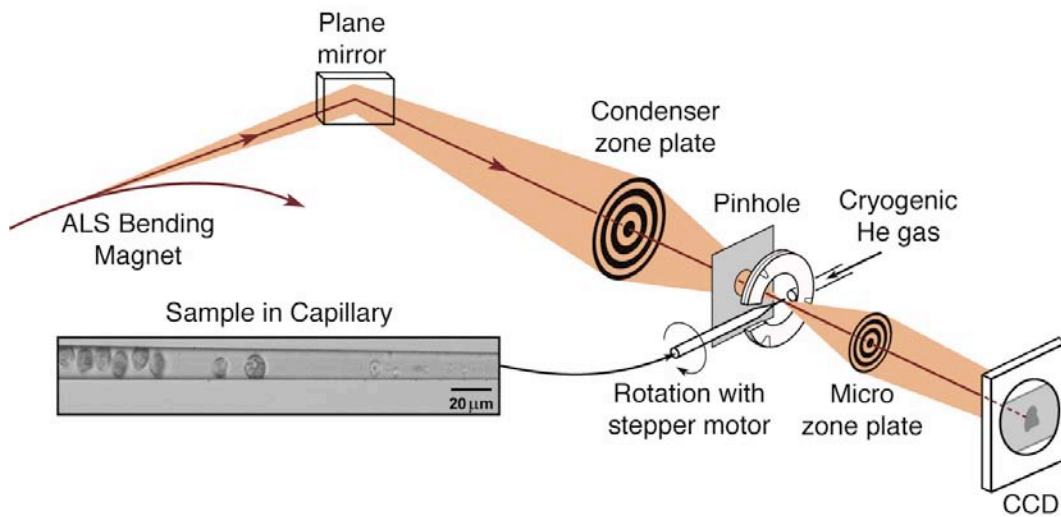
Courtesy of C. Larabell (UCSF & LBNL)
and M. LeGros (LBNL)



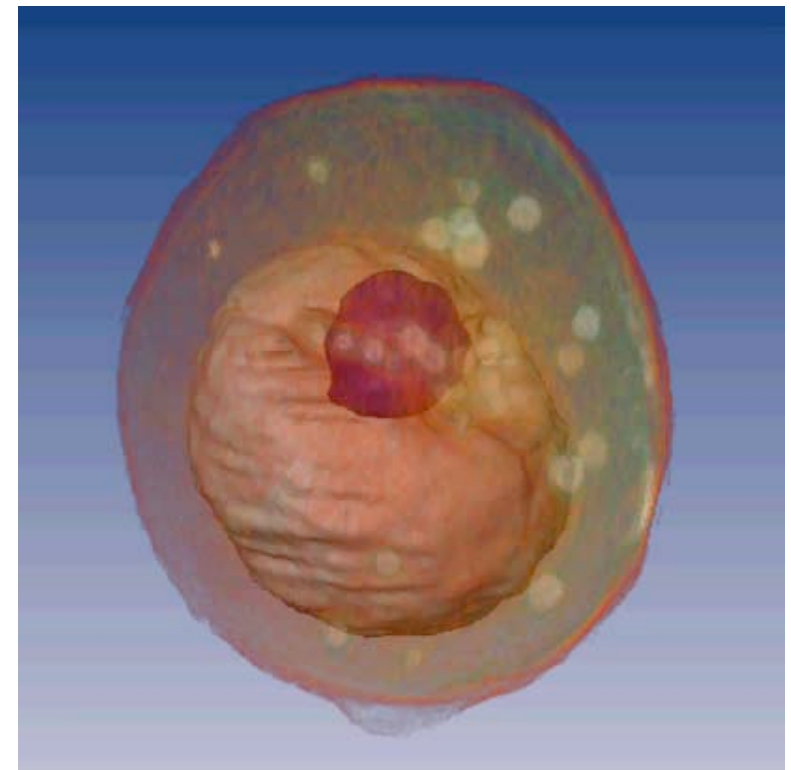
Bio-Nanotomography for 3D Imaging of Cells



Nanotomography of Cryogenic Fixed Cells



Soft X-Ray Nanotomography of a Yeast Cell



$\lambda = 2.5 \text{ nm}$

C. Larabell and M. LeGros,
Molec. Bio. Cell 15, 957 (2004)



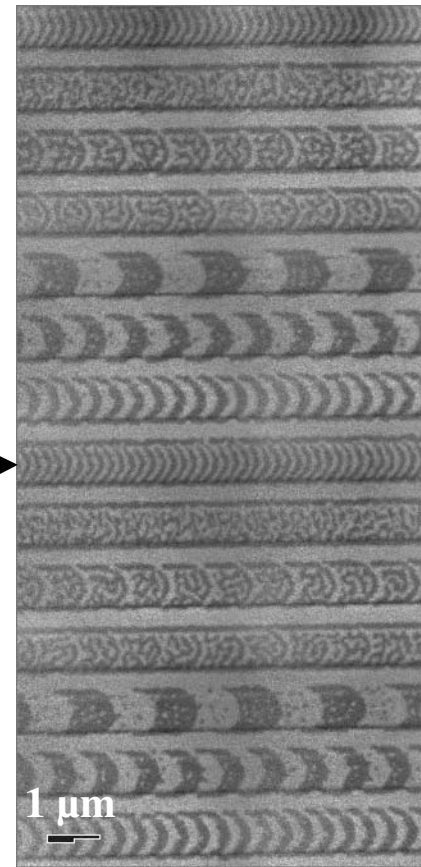
Magnetic X-Ray Microscopy Using X-Ray Magnetic Circular Dichroism (XMCD)



Magnetic X-Ray Microscopy

- High spatial resolution in transmission
- Bulk sensitive (thin films)
- Complements surface sensitive PEEM
- Good elemental sensitivity
- Good spin-orbit sensitivity
- Allows applied magnetic field
- Insensitive to capping layers
- In-plane and out-of-plane measurements

100 nm
lines & spaces



Courtesy of P. Fischer, (MPI, Stuttgart) and G. Denbeaux (CXRO/LBNL)

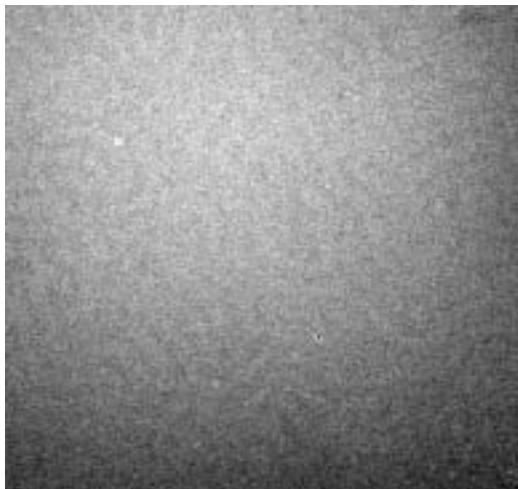


Magnetic Domains Imaged at Different Photons Energies

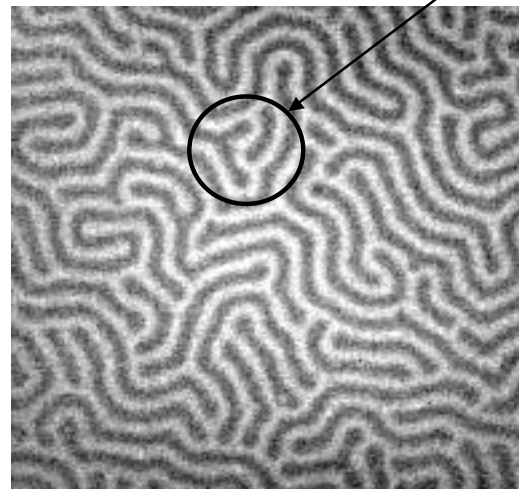


FeGd Multilayer

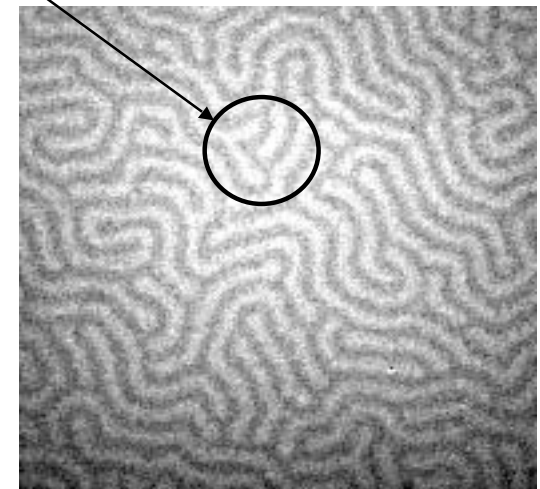
1 μm



$\hbar\omega = 704 \text{ eV}$
below Fe L-edges



$\hbar\omega = 707.5 \text{ eV}$
Fe L₃-edge



$\hbar\omega = 720.5 \text{ eV}$
Fe L₂-edge

Contrast reversal

P. Fischer, T. Eimuller, M. Koehler (U. Wuerzburg)
S. Tsunashima (U. Nagoya) and N. Tagaki (Sanyo)
G. Denbeaux, L. Johnson, A. Pearson (CXRO-LBNL)

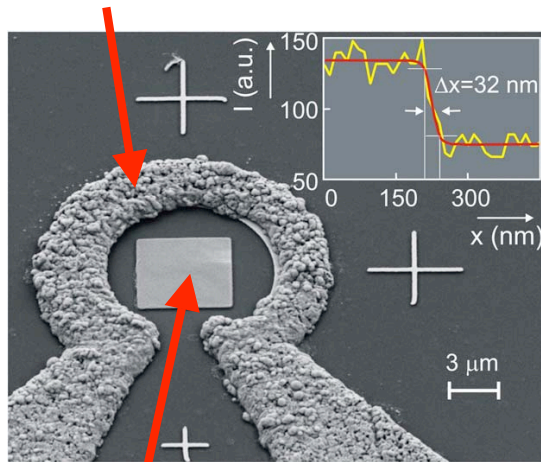


Imaging of Ultrafast Spin Dynamics with Magnetic Soft X-Ray Transmission Microscopy

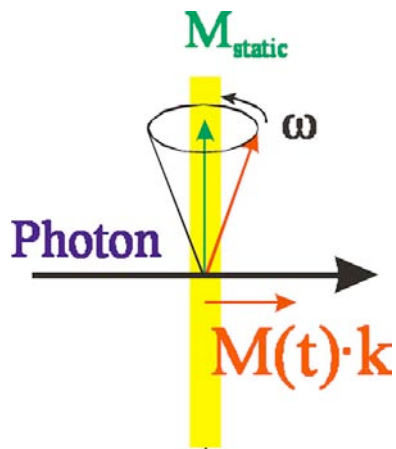


P. Fischer et al., MPI-MF, Stuttgart, Germany (now LBNL)

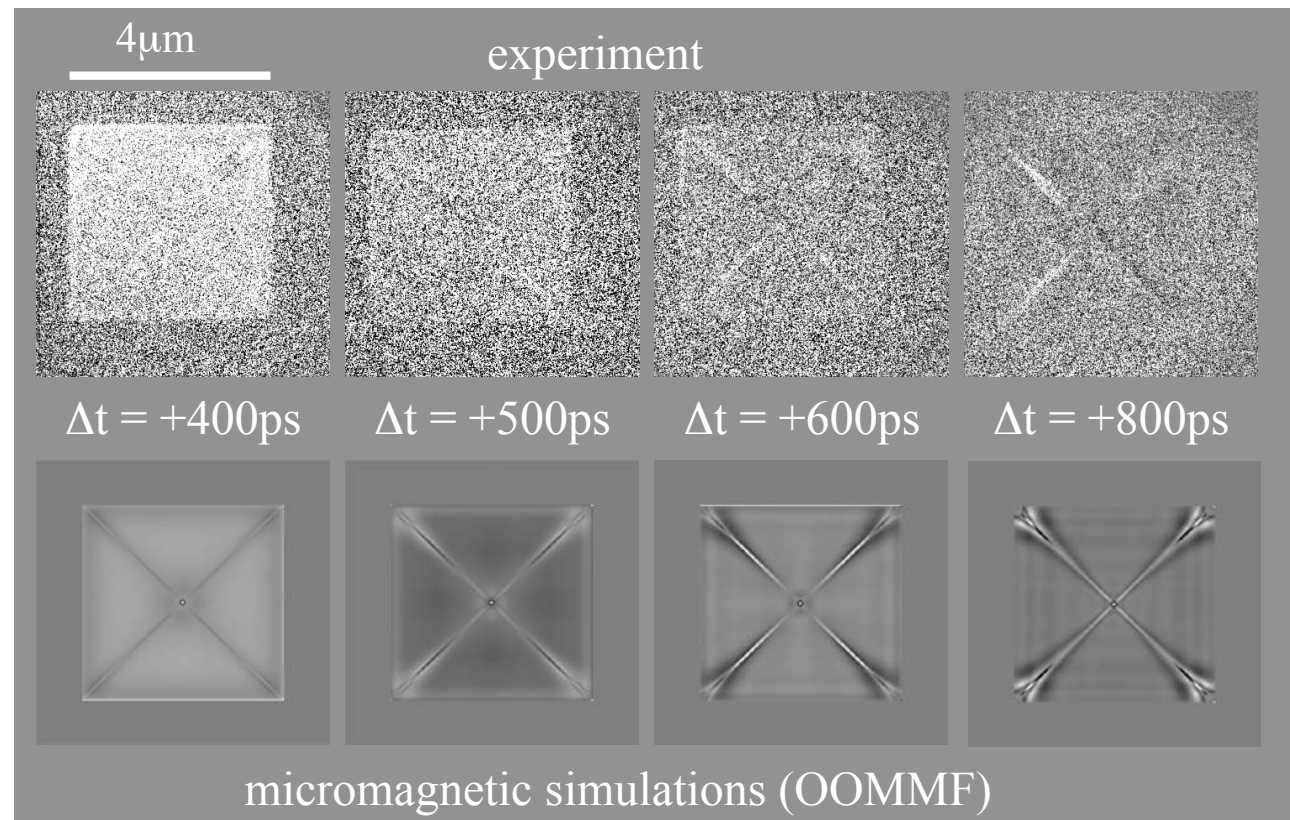
Microcoil



Sample: $4 \times 4 \mu\text{m}^2$ PY element

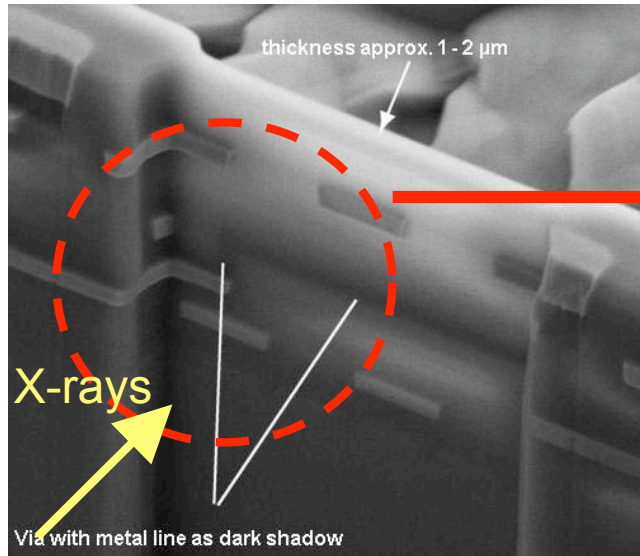


- stroboscopic **pump-and-probe** technique at variable delay times (Δt)
- high **lateral** resolution ($< 20 \text{ nm}$) provided by Fresnel zone plates
- high **temporal** resolution given by SR pulse width ($< 100 \text{ ps}$)
- inherent **chemical** sensitivity provided by XMCD magnetic contrast

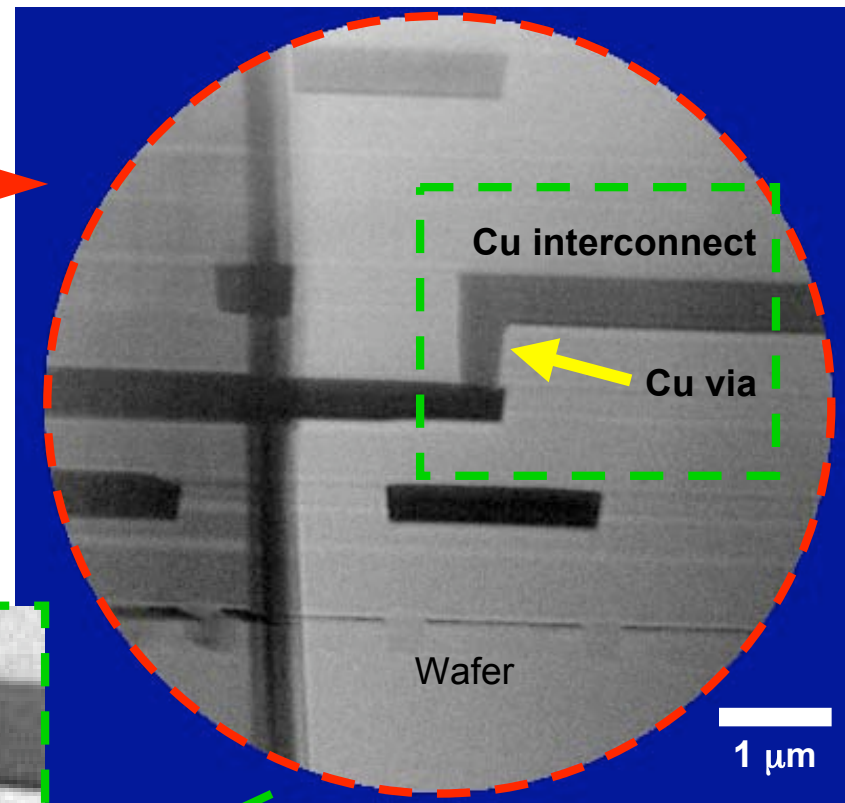


Electromigration in Latest Technology Computer Chips with Cu vias Connecting Multilevel Metallization Layers

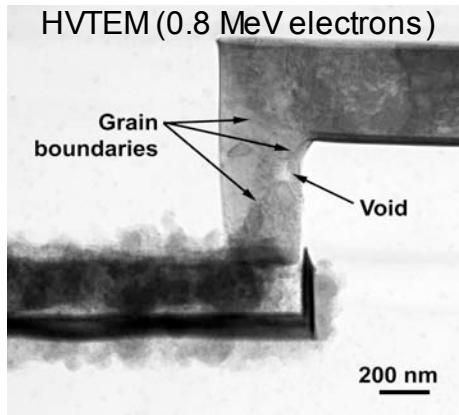
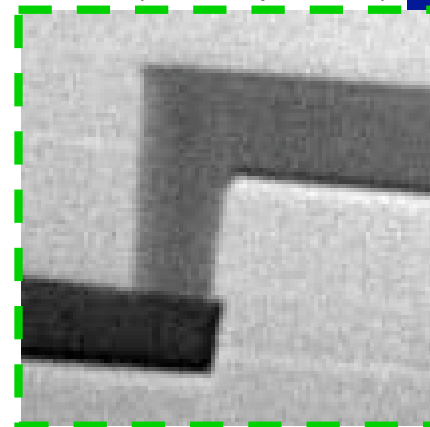
SEM micrograph



X-ray micrograph imaged at 1.8 keV



TXM (1.8 keV photons)



High current density

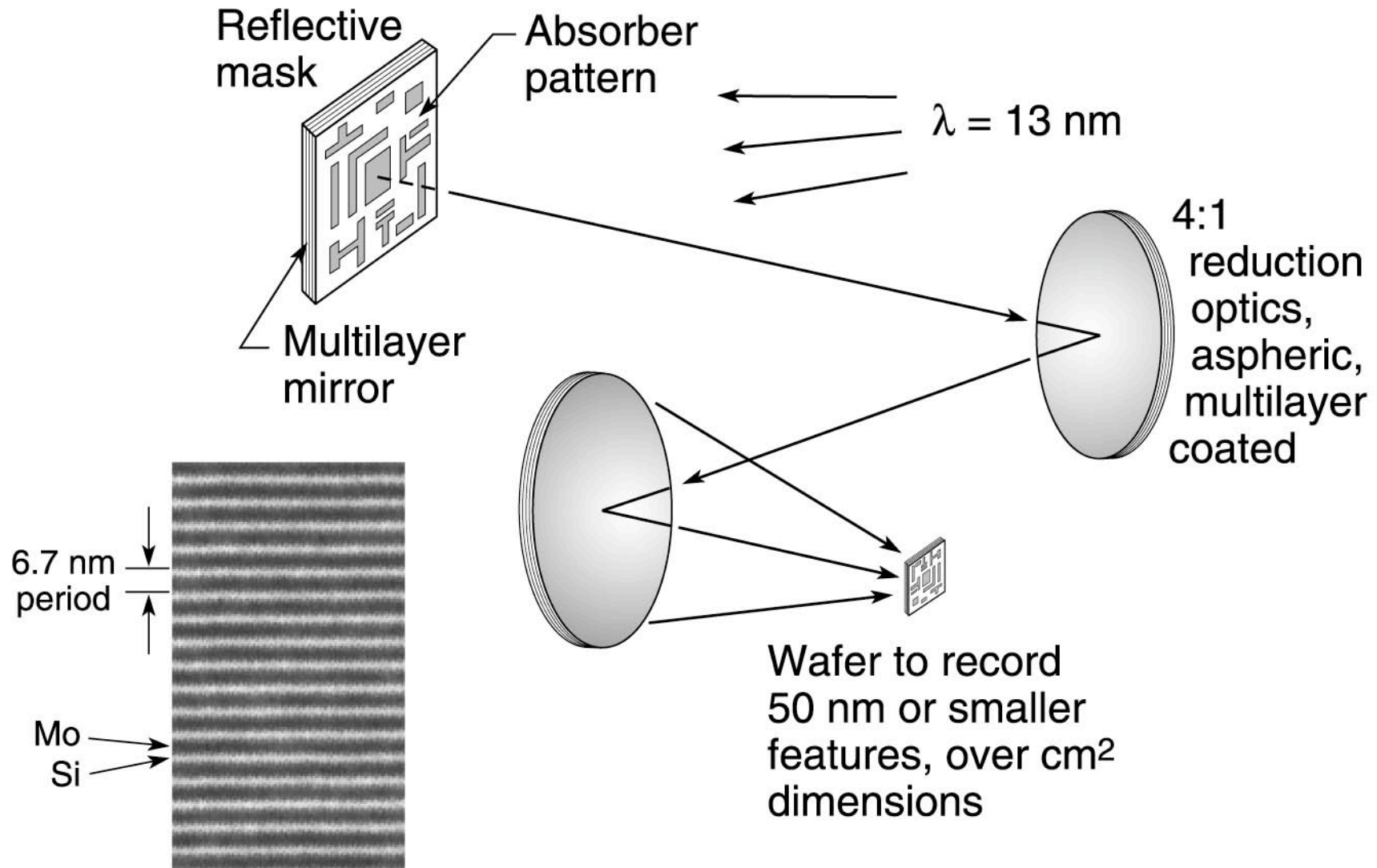
Courtesy of Gerd Schneider (BESSY)

G. Denbeaux, E. Anderson, A. Pearson and B. Bates (CXRO)

M. Meyer and E. Zschech (AMD Saxony Manufacturing GmbH) / E. Stach (NCEM / LBNL)

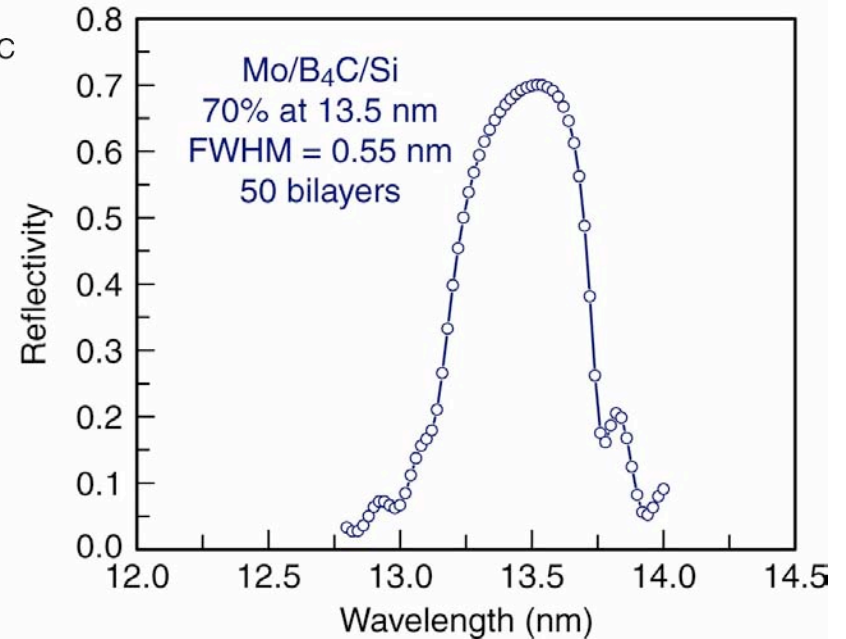
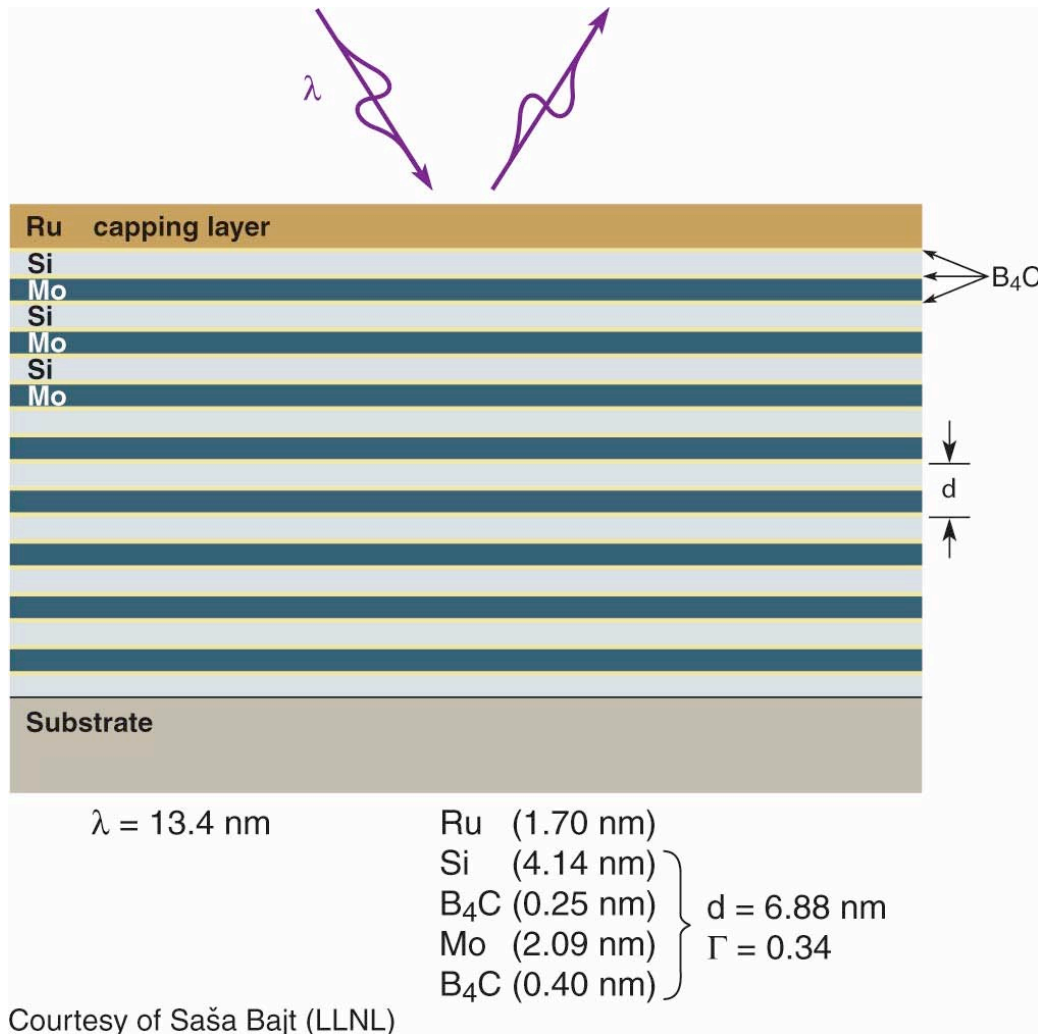


Extreme Ultraviolet (EUV) Lithography Based on Multilayer Coated Optics



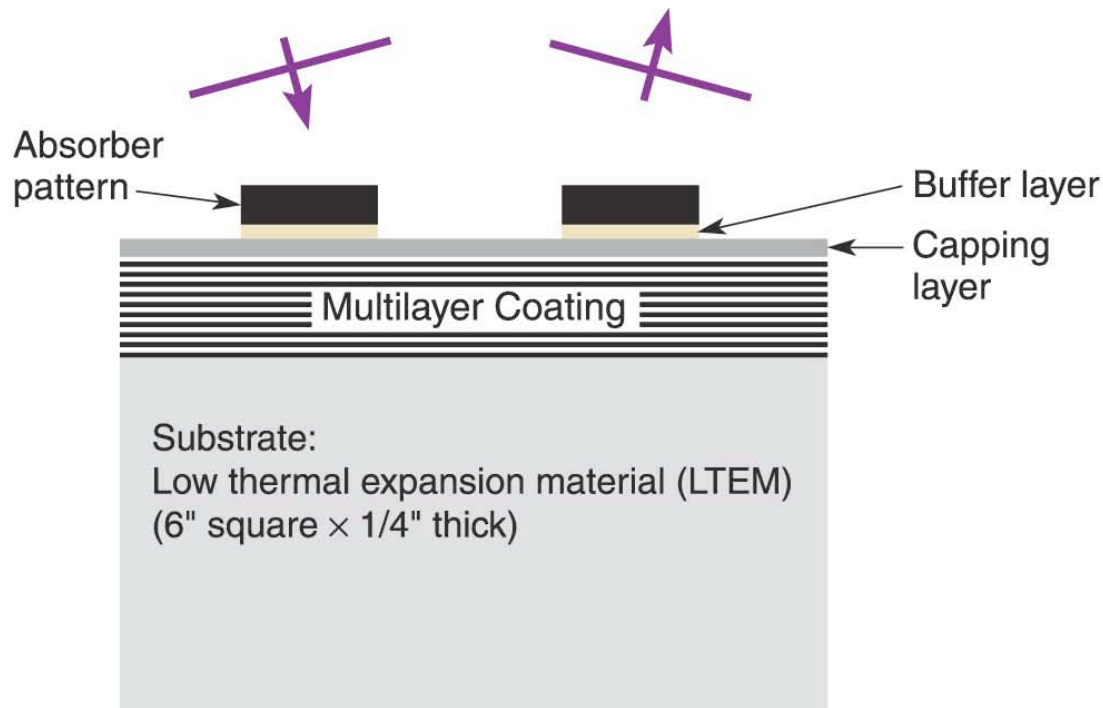


High Reflectivity, Thermally and Environmentally Robust Multilayers Coatings for High Throughput EUV Lithography



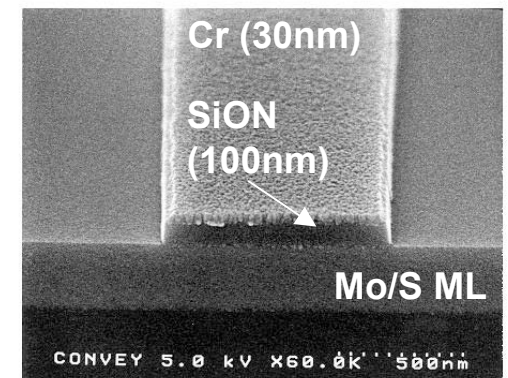


Reflective Mask for EUV Lithography



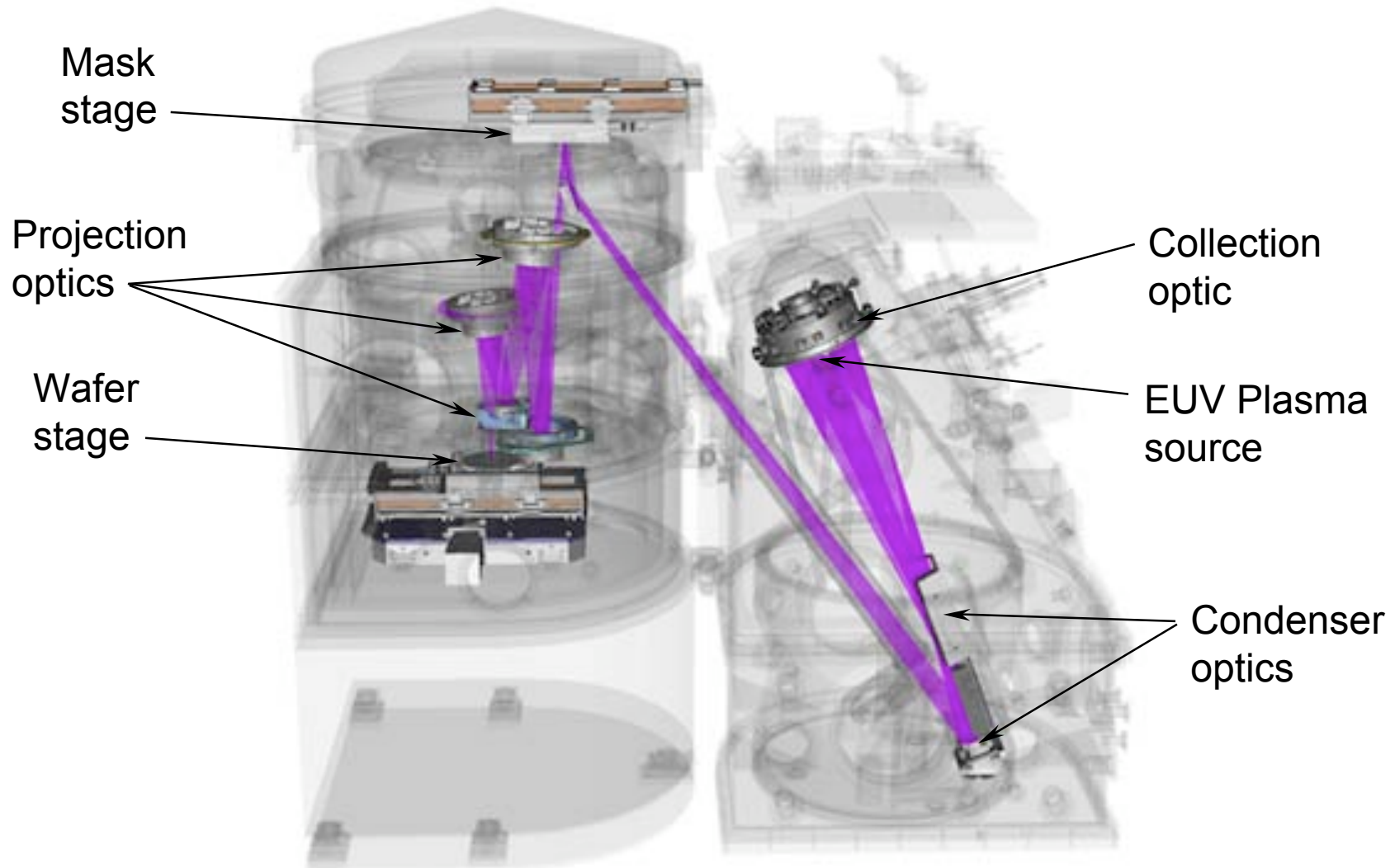
Typically
 Mo/Si multilayer ($d = 6.7 \text{ nm}$)
 with 30 nm SiO_2 capping layer
 Cr or TaN absorber ($\sim 70 \text{ nm}$)
 with 50 nm Ru Buffer layer
 LTEM substrate
 (Ti-doped fused silica)
 ULE (Corning), or
 Zerodur (Schott)

Attribute	TaN	Cr	Comments
CD control	✓		TaN has smaller RIE CD bias
Cleaning			Both resistant to standard cleans
Emissivity		✓	
Inspection contrast	✓		TaN has higher contrast
Repair selectivity			Both need small improvement
Aspect ratio	✓		TaN can be 8 nm thinner than Cr



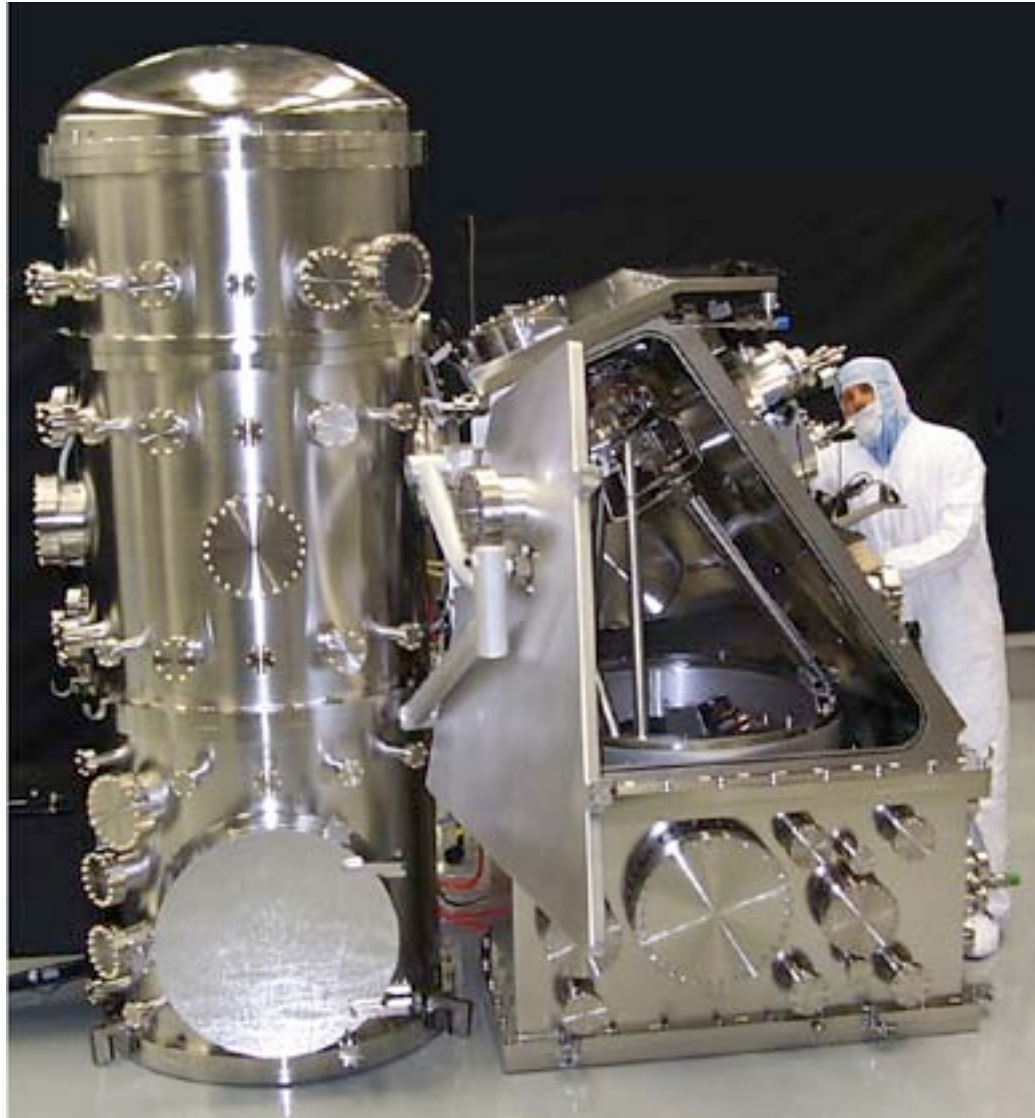


The Engineering Test Stand (ETS): A Pre-Manufacturing EUV Stepper





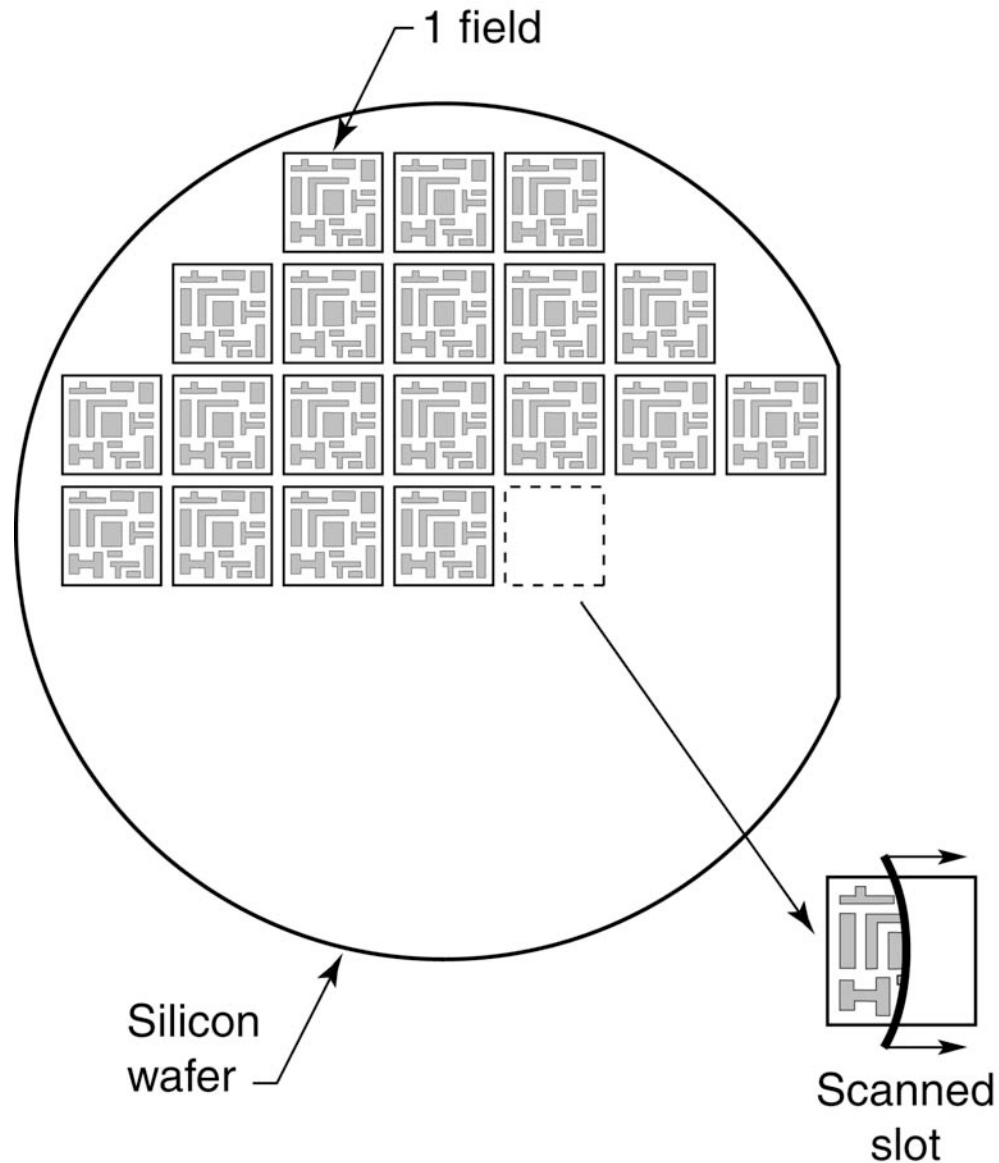
The Engineering Test Stand (ETS)



Courtesy of
Bill Replogle,
Sandia National
Laboratories

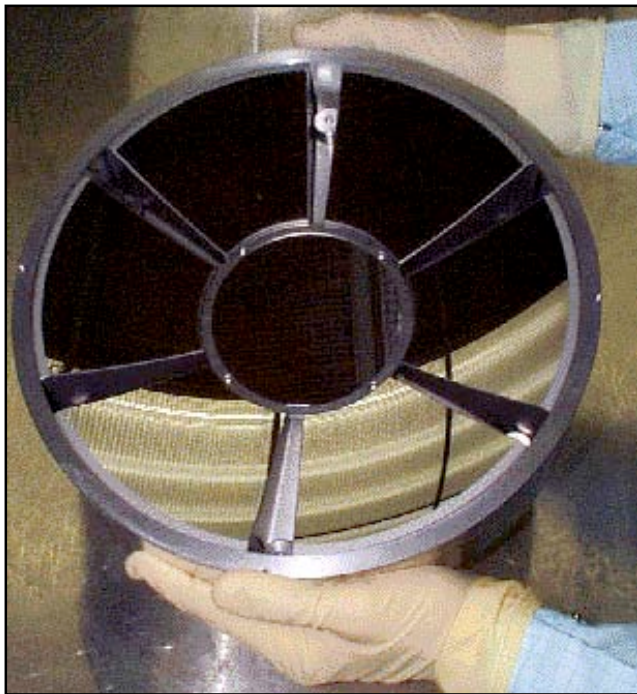


EUV Lithography Will Use a Step and Scan Ring Field System





ETS Optics Meet Tight Specifications



Condenser optic

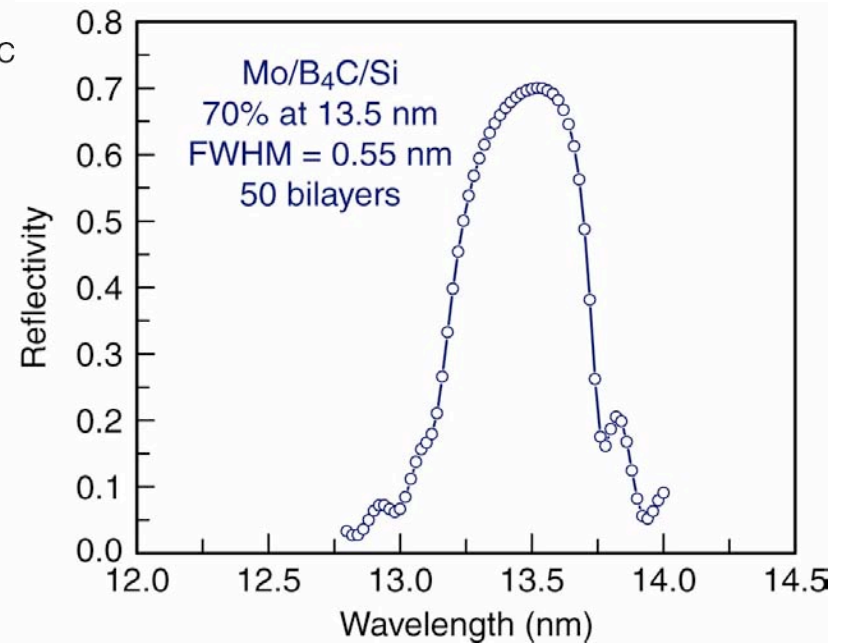
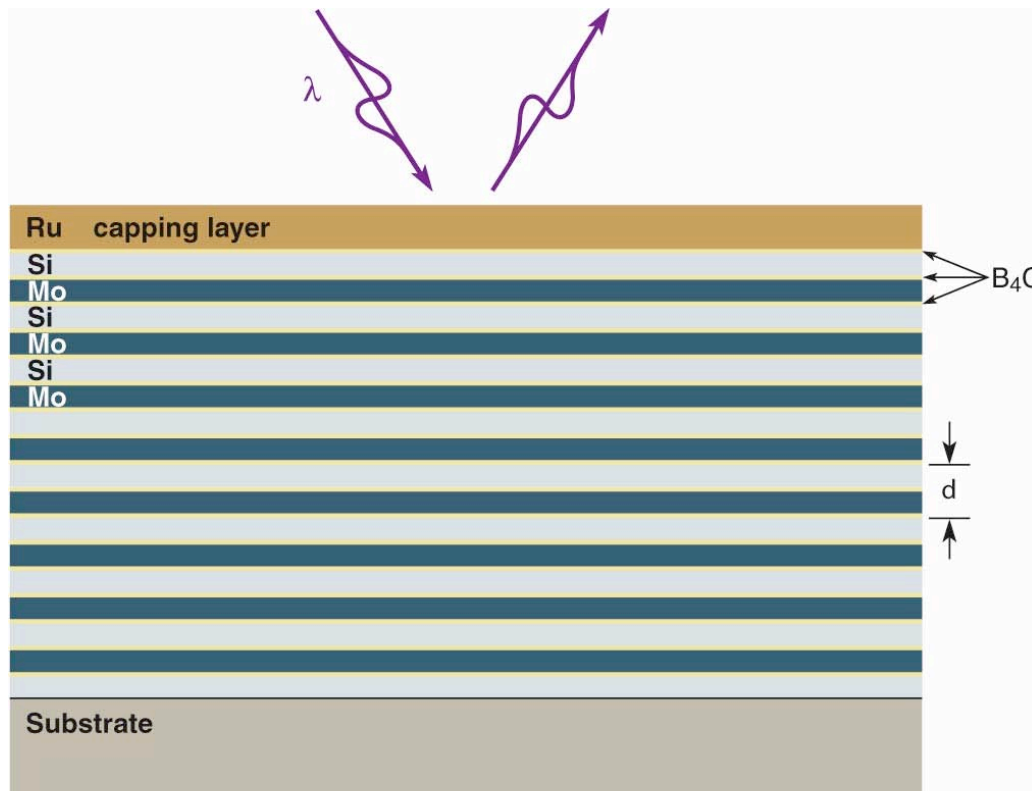


Projection optic

Courtesy of D. Sweeney (LLNL)



High Reflectivity, Thermally and Environmentally Robust Multilayer Coatings for High Throughput EUV Lithography



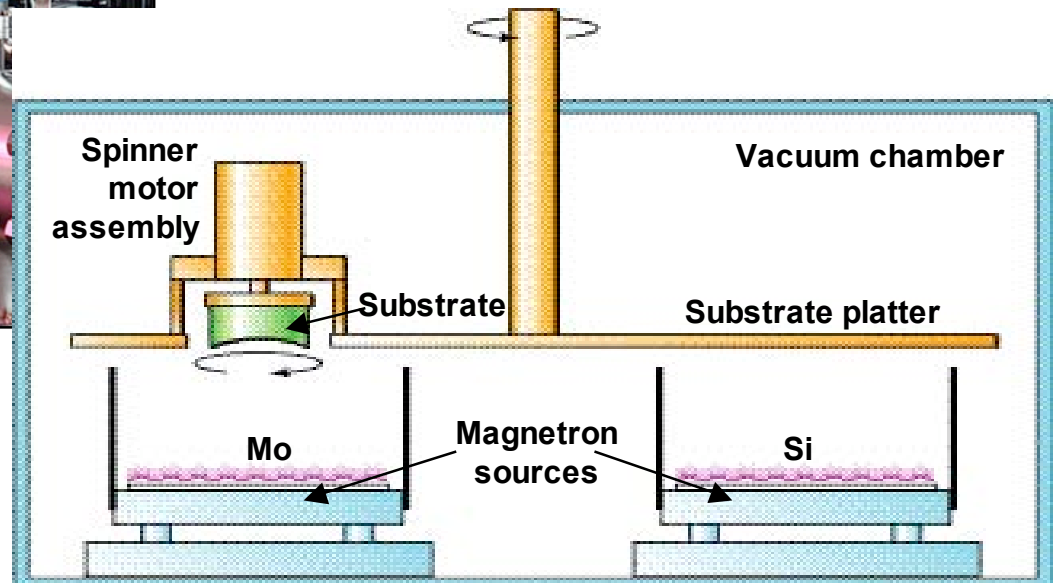
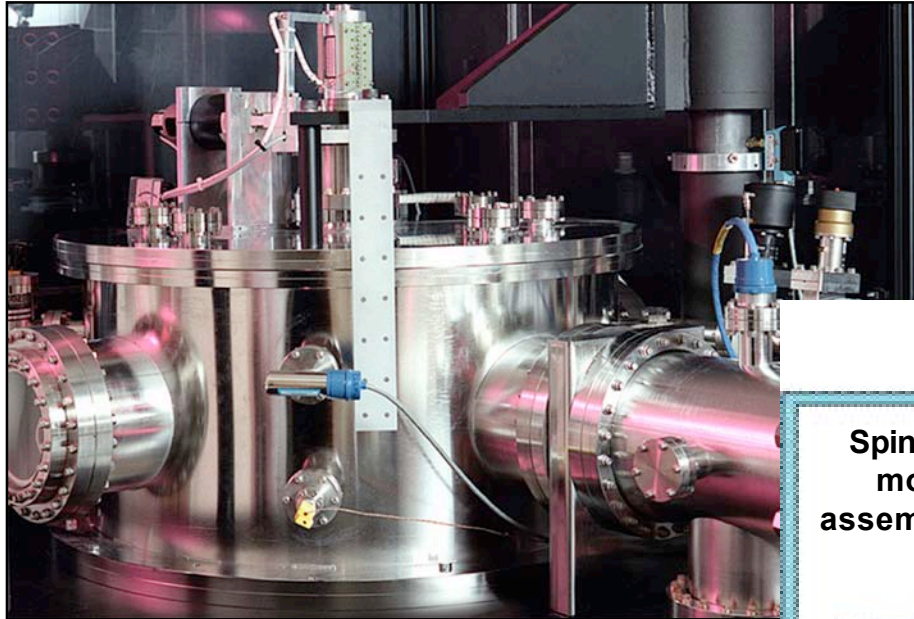
$\lambda = 13.4 \text{ nm}$

Ru (1.70 nm)	} $d = 6.88 \text{ nm}$ $\Gamma = 0.34$
Si (4.14 nm)	
B ₄ C (0.25 nm)	
Mo (2.09 nm)	
B ₄ C (0.40 nm)	

Courtesy of Saša Bajt (LLNL)



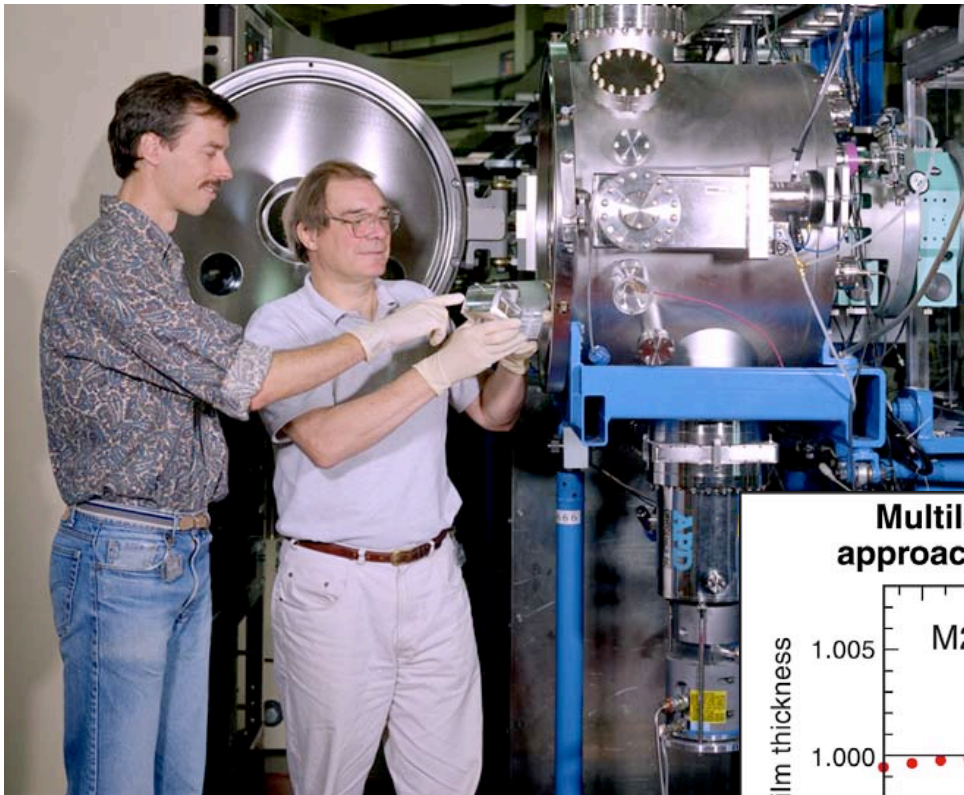
DC Magnetron Sputtering Is Used to Deposit Multilayer Coatings Onto Optical Substrates



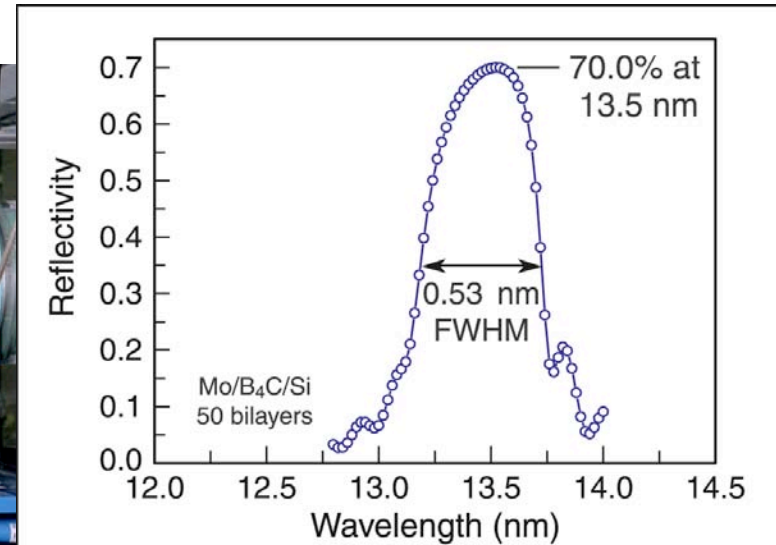
Substrates mounted on a rotating platter are swept across each sputter source sequentially to form the multilayer. Modulating the platter velocity provides precision control of radial thickness distribution and absolute film thickness. The substrate is also spun fast about its own axis for azimuthal uniformity.



Multilayer Reflectivity and Uniformity

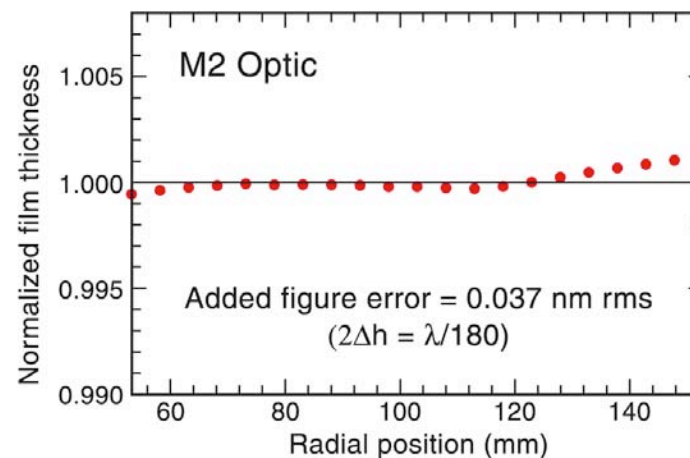


Courtesy of E. Gullikson and J. Underwood, Lawrence Berkeley National Laboratory.



Sasa Bajt, LLNL

Multilayer coatings for the ETS approach production specifications



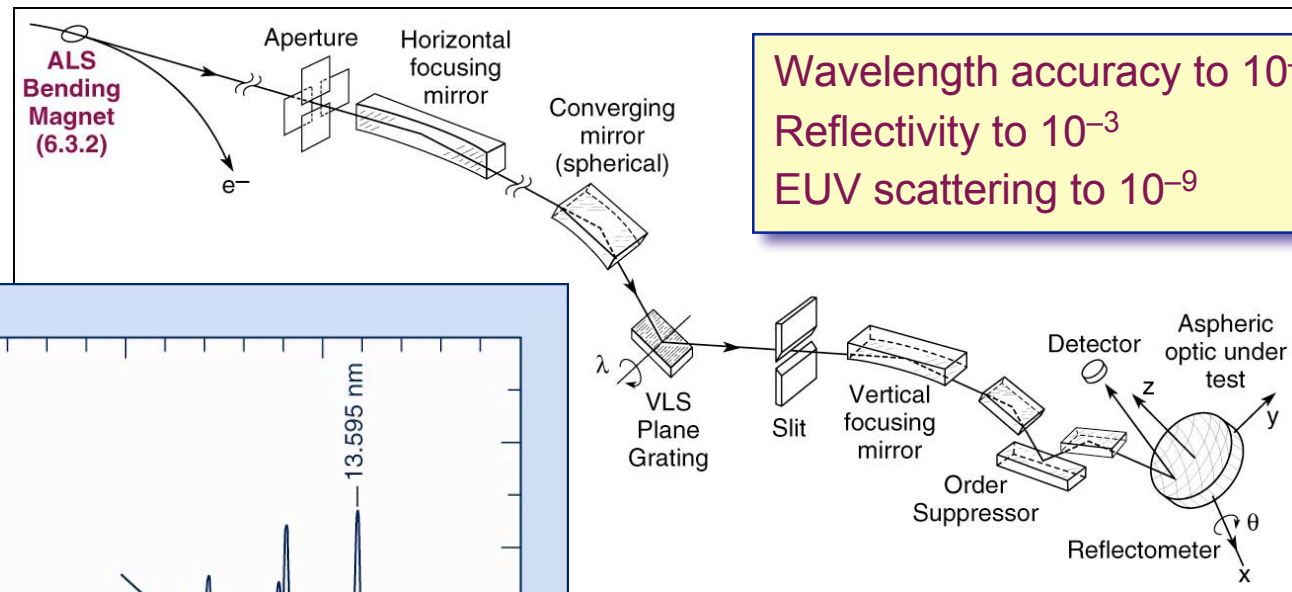
R. Soufli, and E. Spiller, LLNL



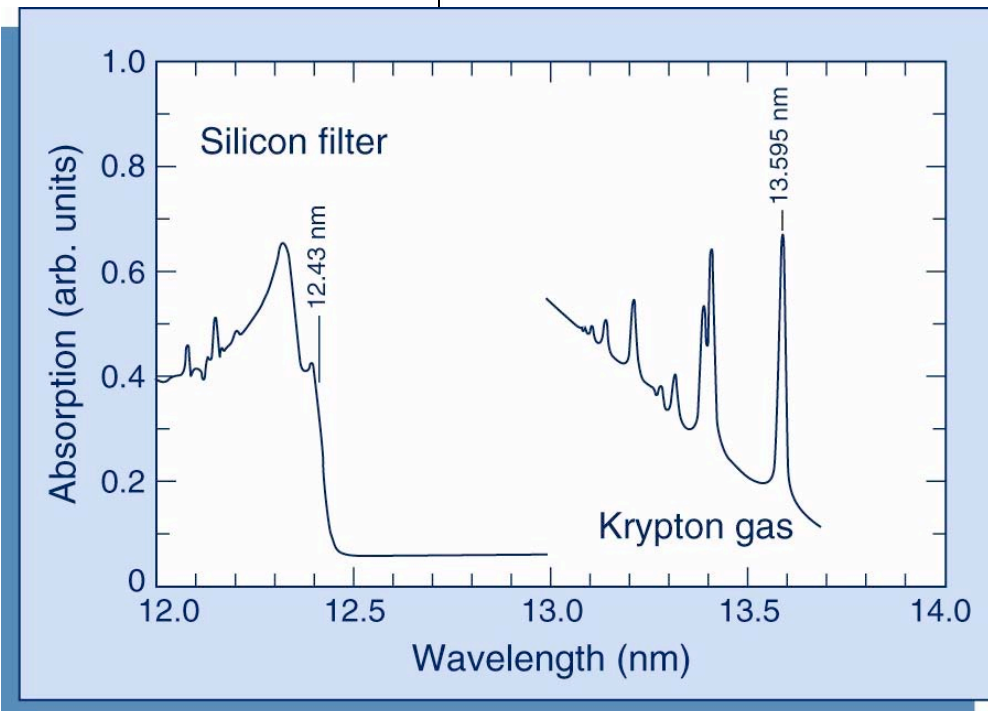
High Accuracy EUV Metrology for Multilayer Coated Optics



Multilayer Reflectivity and Uniformity



Wavelength accuracy to 10^{-4}
 Reflectivity to 10^{-3}
 EUV scattering to 10^{-9}



Calibration lines		
Xe	4d _{5/2} – 6p	19.0423 nm
Kr	3d _{5/2} – 5p	13.5948 nm
Ar	2p _{3/2} – 4s	5.0736 nm
CO	1s – π*	4.3140 nm
N ₂	1s – π*	3.0911 nm

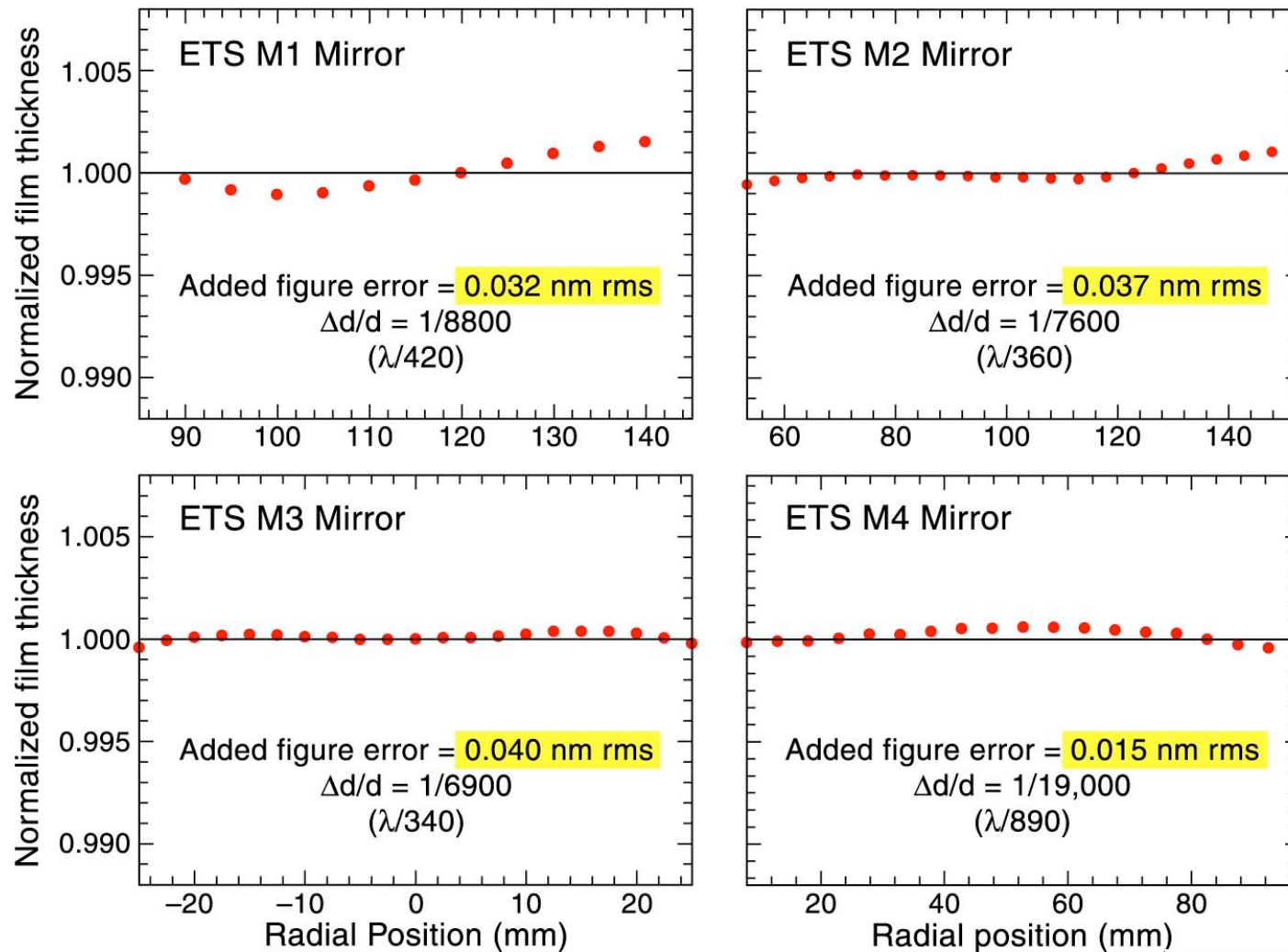
Courtesy of E. Gullikson and J. Underwood (LBNL)



Multilayer Coatings for the ETS Projection Optics Approach Production Specifications

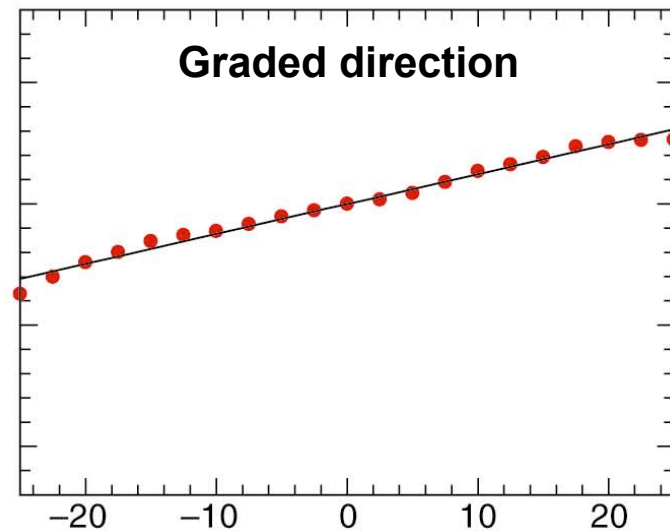
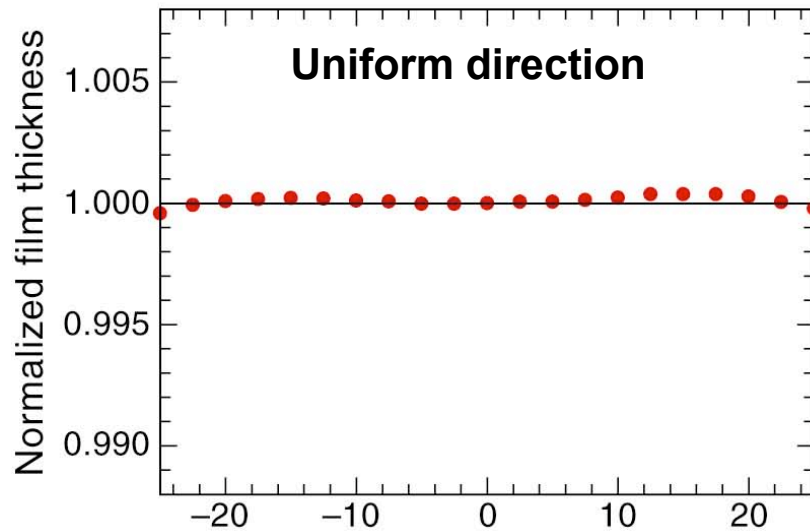
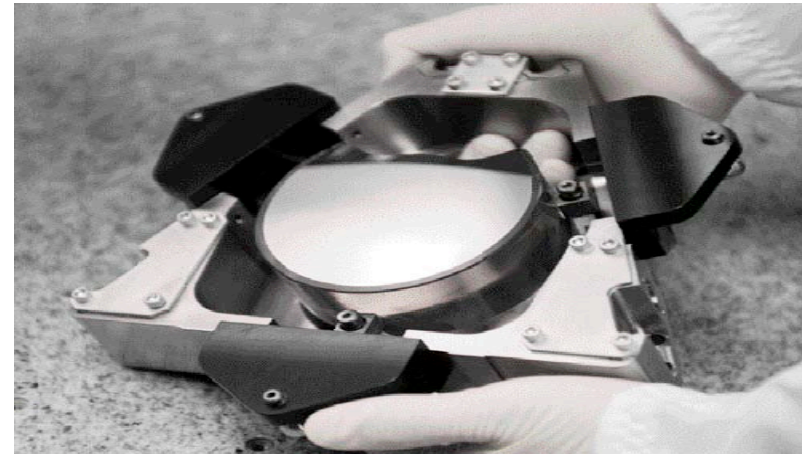
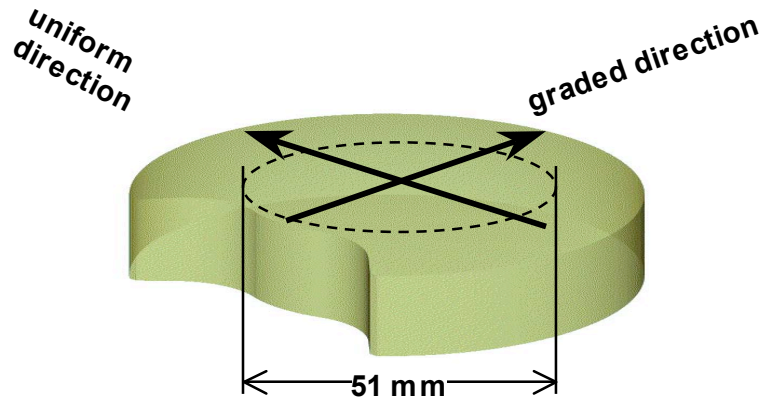


Systematic d-space variations suggest path to further improvements.





ETS Mirror M3 Was Successfully Coated While Preserving the Surface Figure



Radial Position (mm)



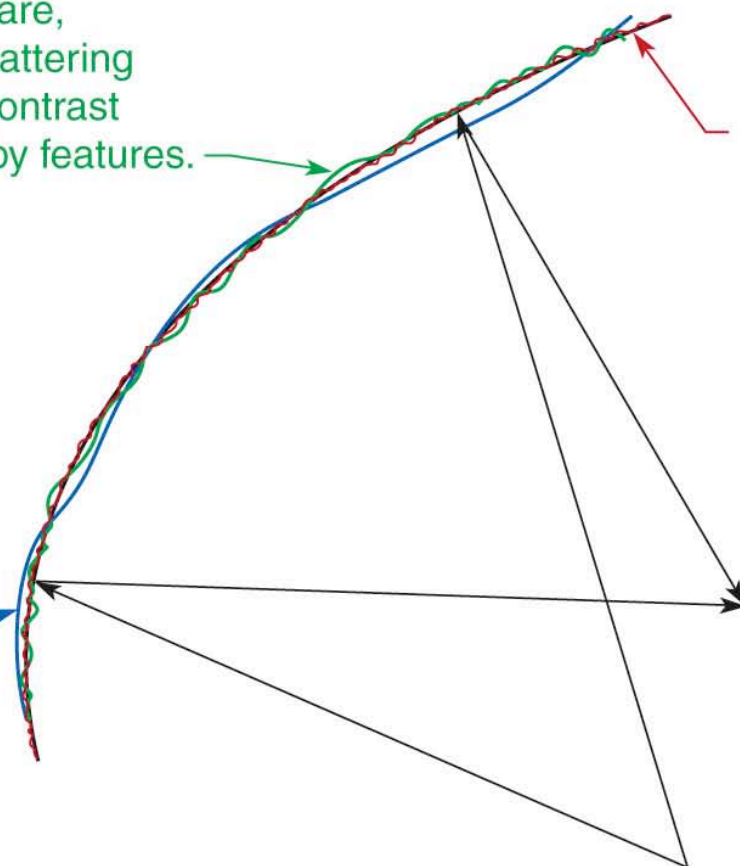
Figure and Finish Low, Mid, and High Spatial Frequency Variations from the Perfect Optical Surface



Mid spatial frequency surface variations contribute to flare, small angle scattering that reduces contrast between nearby features.

Low spatial frequency substrate errors are associated with aberrations, blurred features.

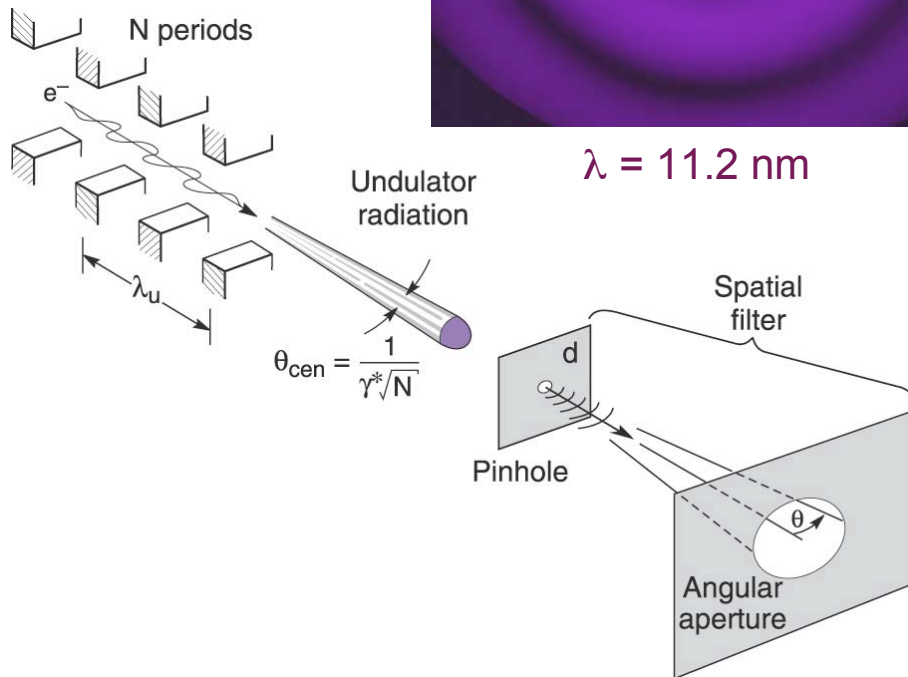
High spatial frequency roughness scatters radiation to large angles, reducing power throughput to the image (wafer).



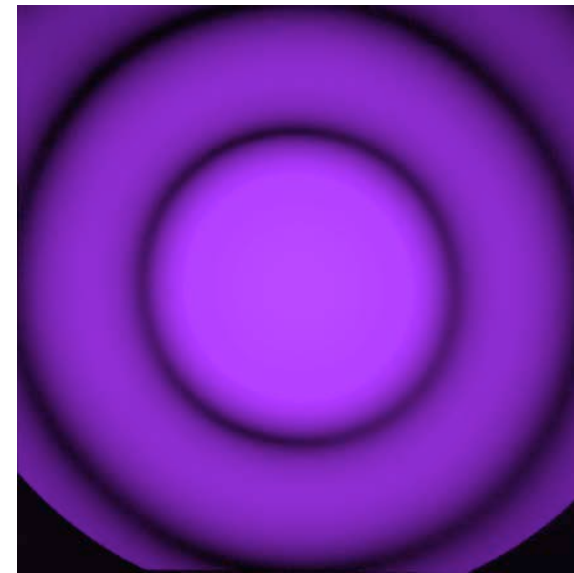
Note: Multilayer coatings must be sufficiently uniform that they do not contribute significantly to the top surface error budget. For an rms d-space variation Δd , the coating thickness variation $\Delta h = N \Delta d < \lambda_{\text{euv}}/500$.



Spatially Coherent Radiation for At-Wavelength EUV Interferometry



$\lambda = 11.2 \text{ nm}$



$\lambda = 13.4 \text{ nm}$

1 μm^D pinhole

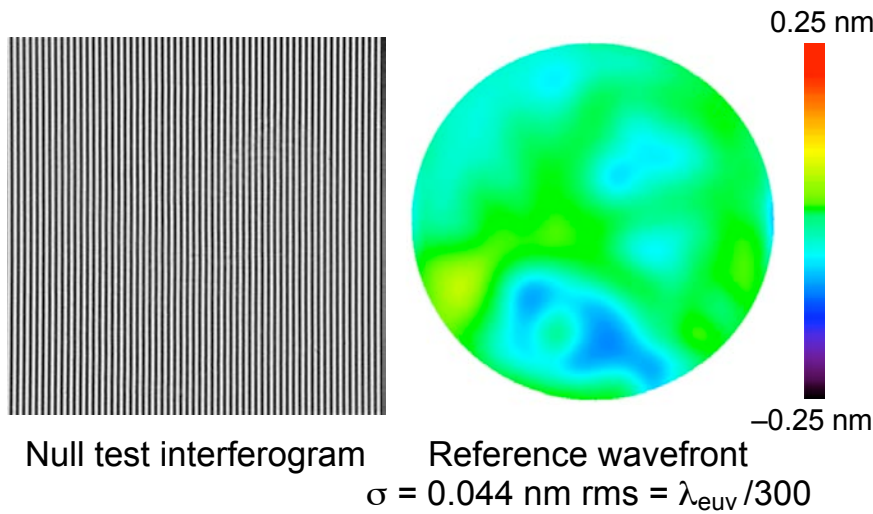
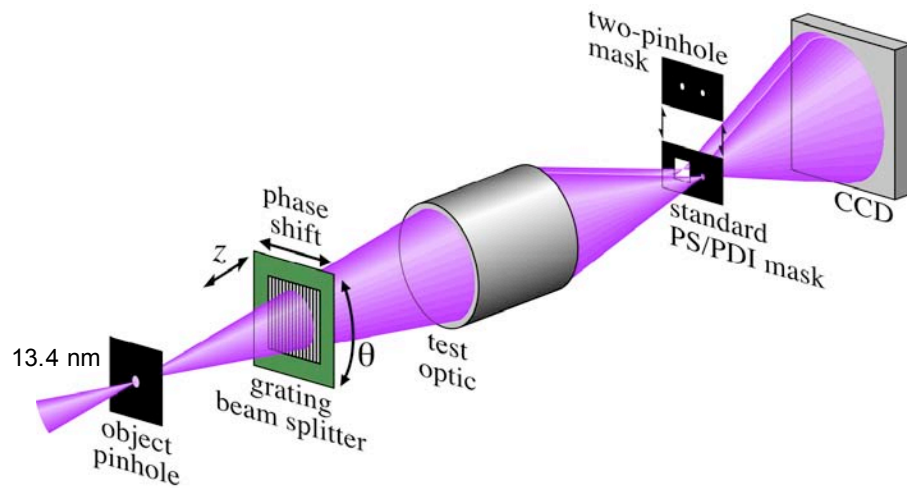
**25 mm wide CCD
at 410 mm**



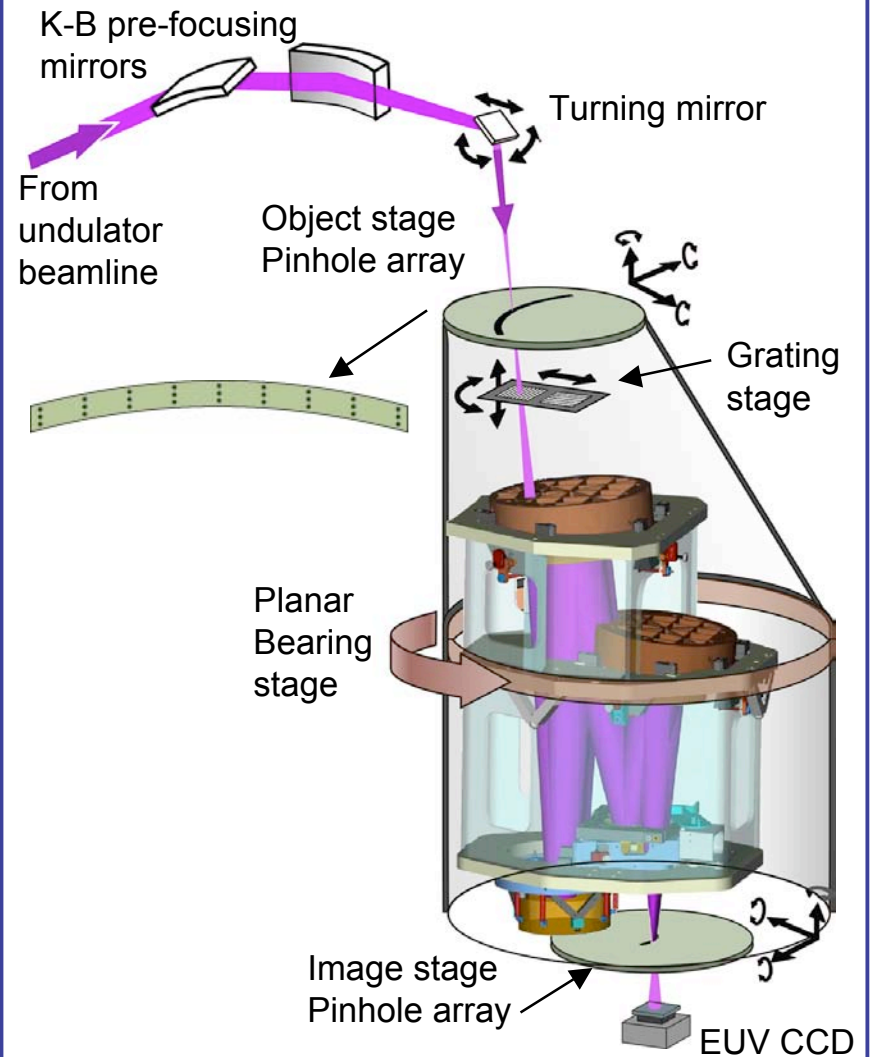
At-Wavelength EUV Interferometry



Wavefront Accuracy to $\lambda_{\text{EUV}}/300$

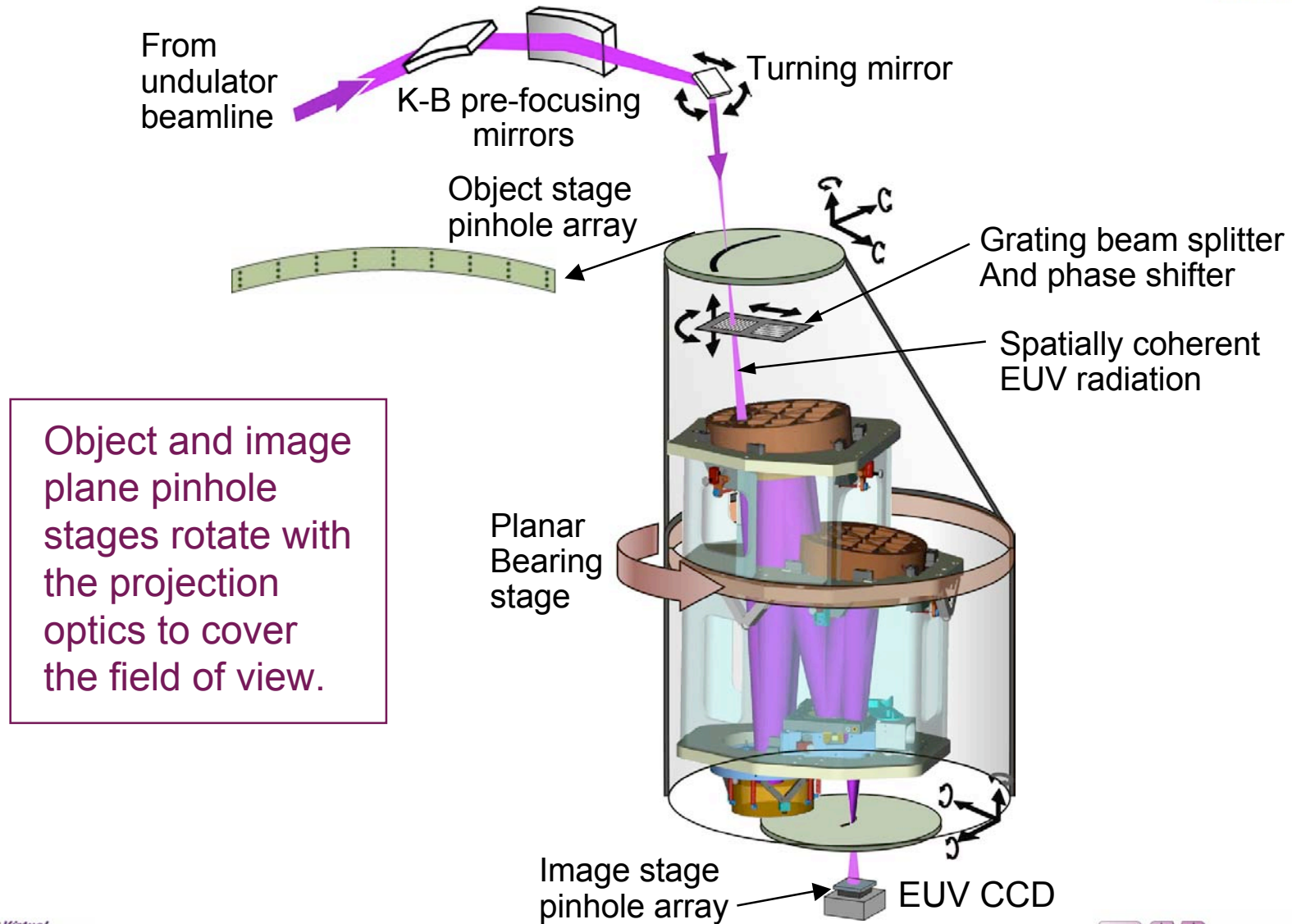


EUV Interferometry of ETS Optics





EUV Interferometry of the ETS Projection Optics

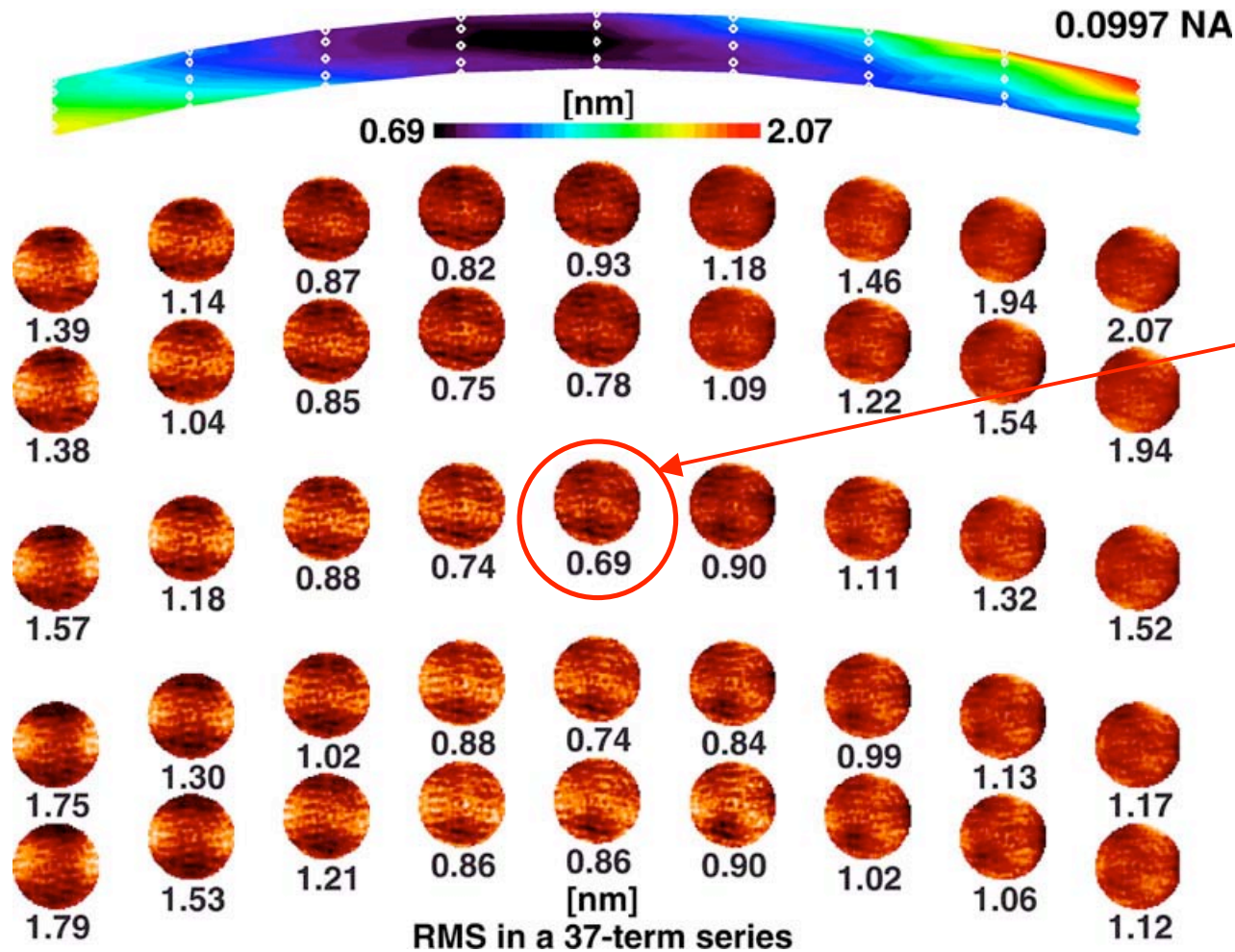


EUV Lithography at the Advanced Light Source in Berkeley





At-Wavelength Interferometry of ETS Set 2 Optics

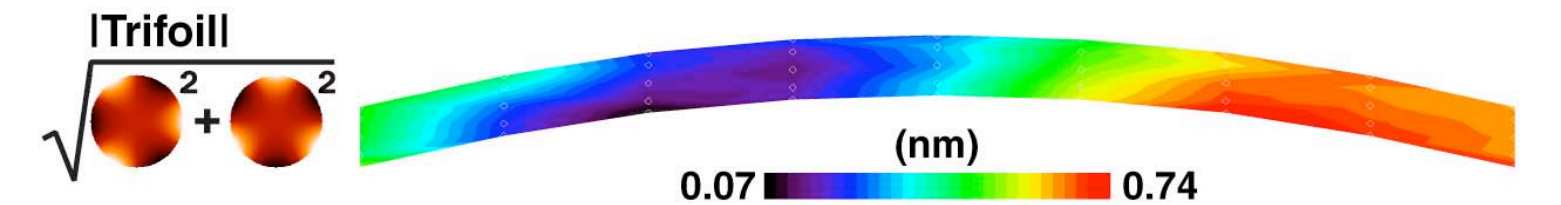
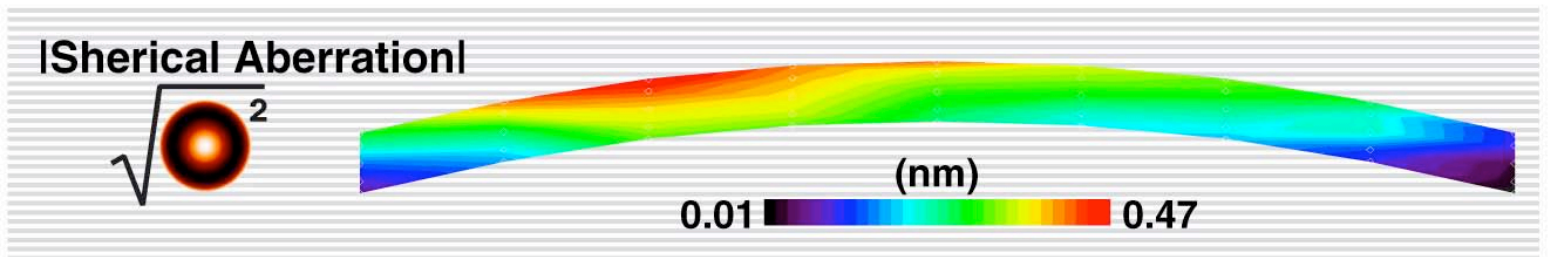
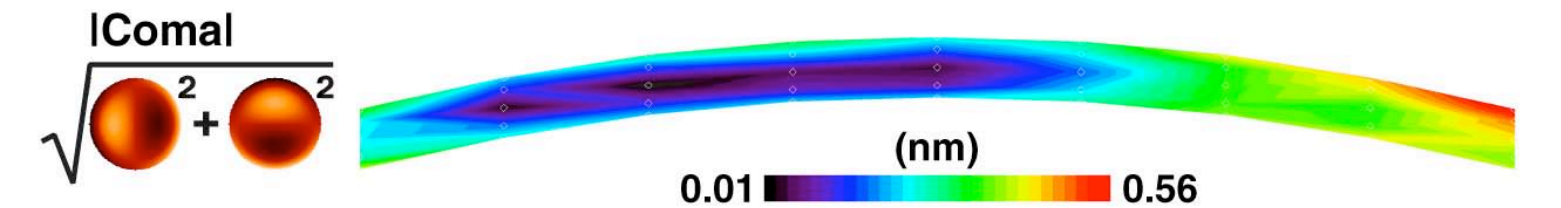
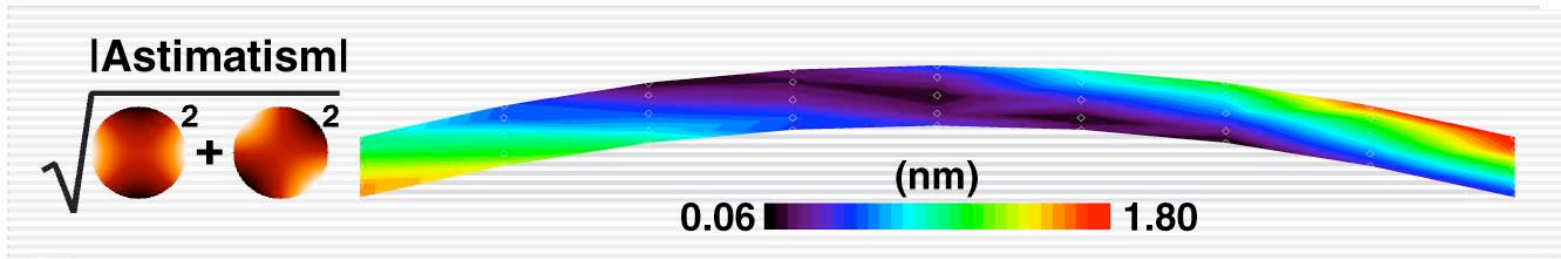


- Quantitative agreement with visible light interferometry to 0.25 nm rms
- Best field points chosen for static imaging

Courtesy of K. Goldberg, P. Naulleau, J. Bokor, et al. (LBNL)

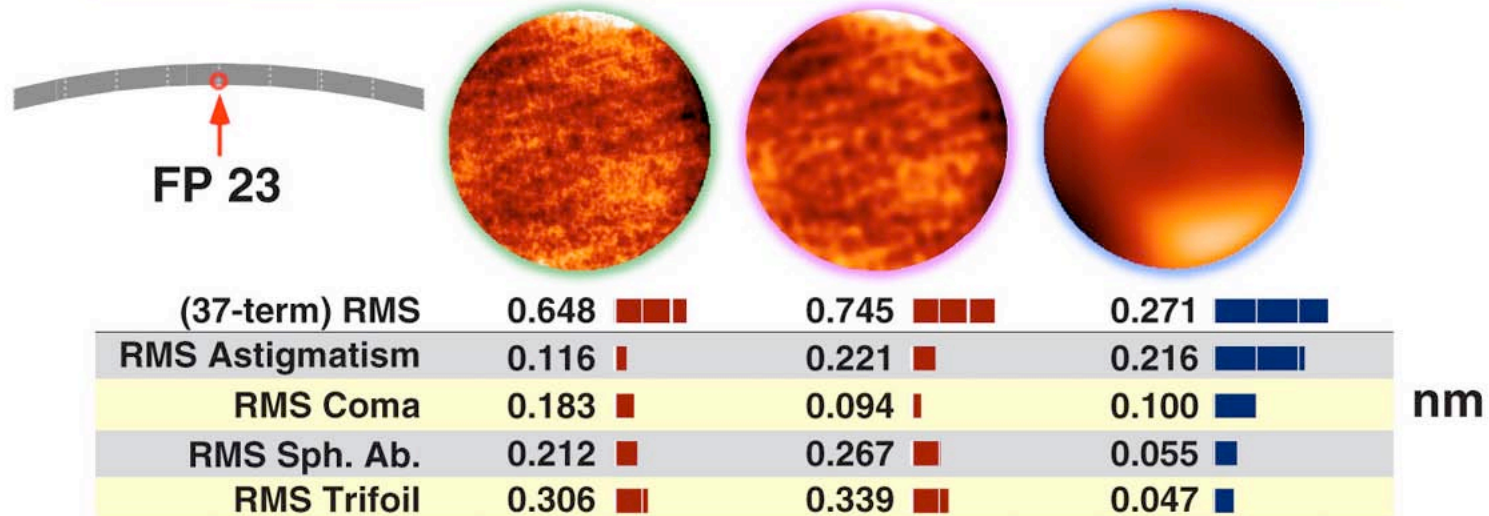
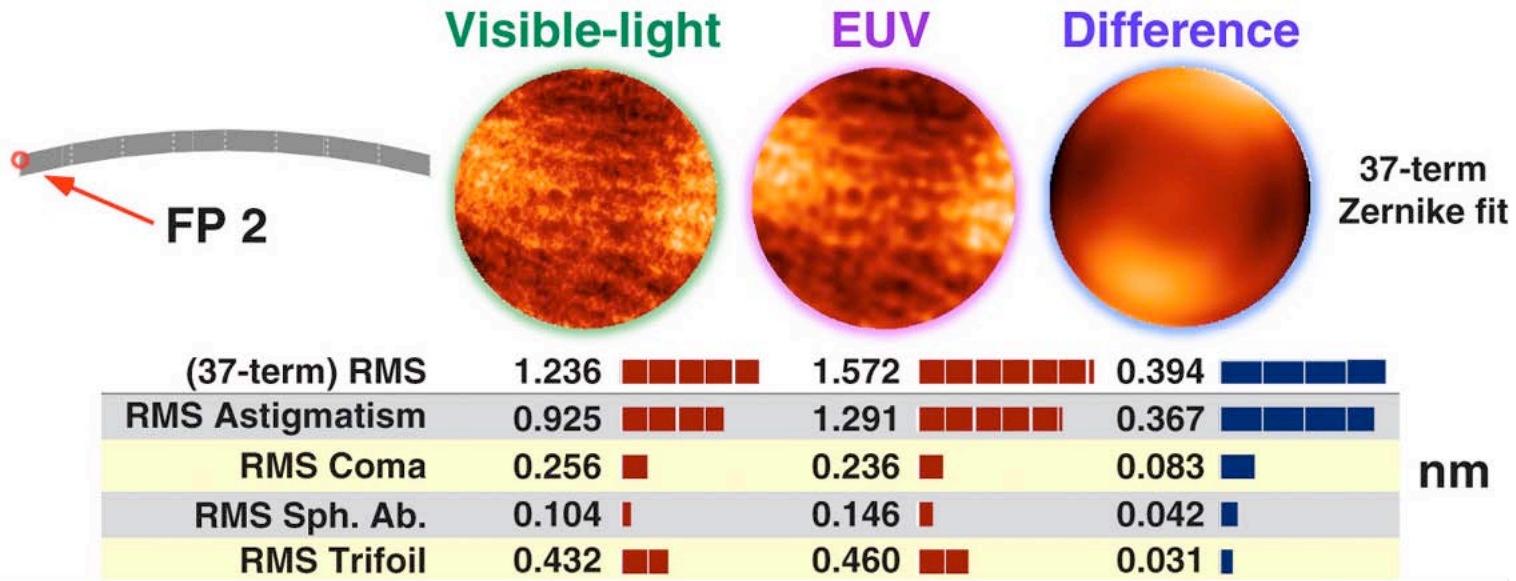


EUV-Wavelength Aberration Breakdown for the ETS Set-2 Optics





Visible and EUV Wavefront Comparison by the Numbers

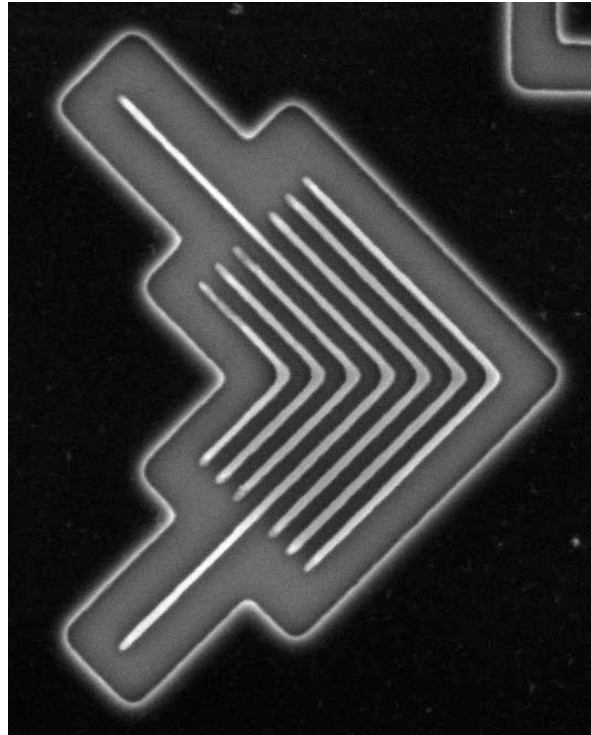




EUV Static Exposures Demonstrated to 39 nm Linewidth



39 nm Isolated Line



Coded as 80 nm (1:1)
narrowed by exposure
bias (x1.4)

ETS Set 2 optics

Static images at ALS

13.5 nm

$\sigma = 0.7$

DOF = $\pm 1/2 \mu\text{m}$

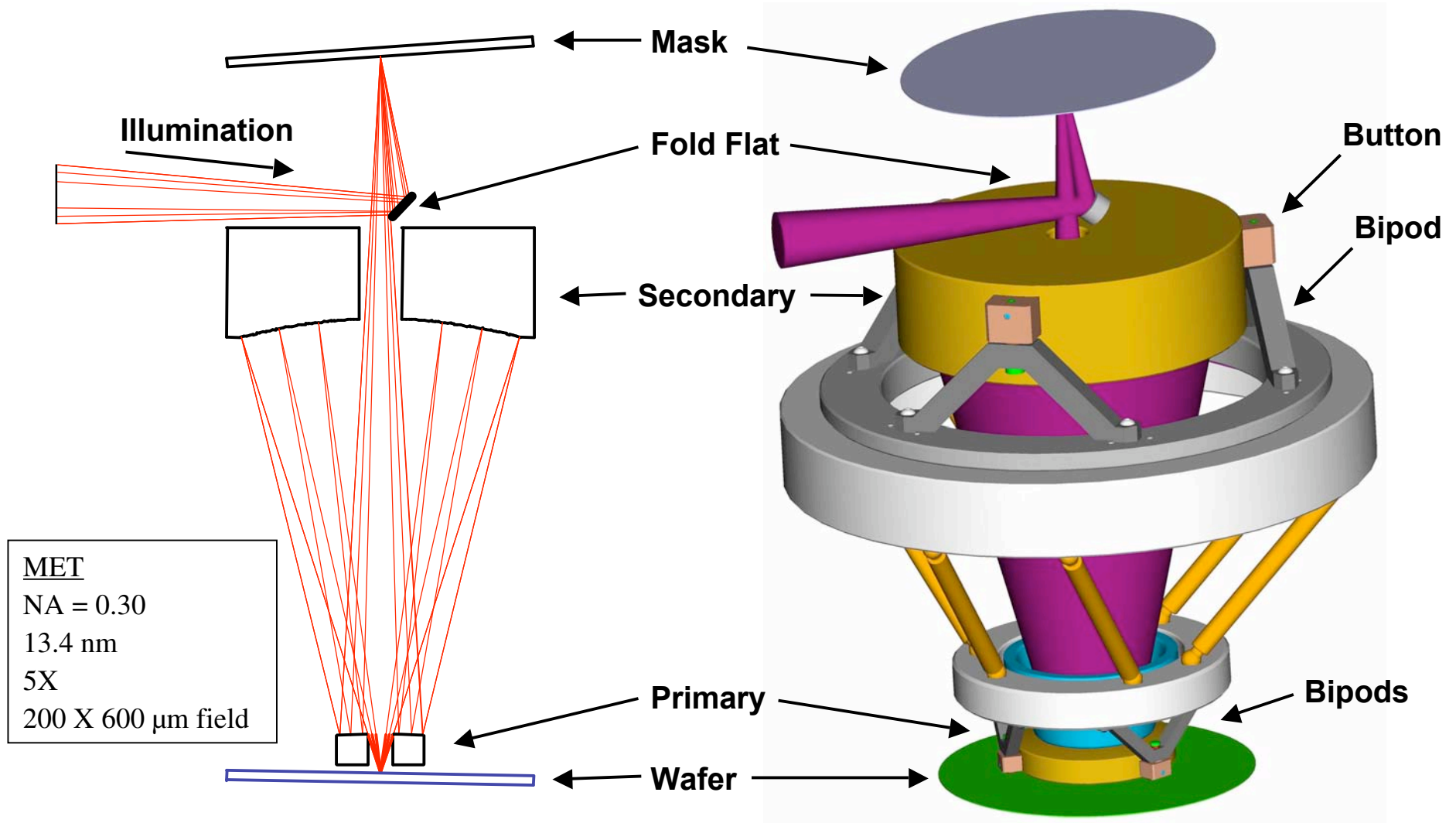
EUV 2D resist, 120 nm
thick

6.2 mj/cm^2 , 4-6 nm LER

Courtesy of P. Naulleau (LBNL)

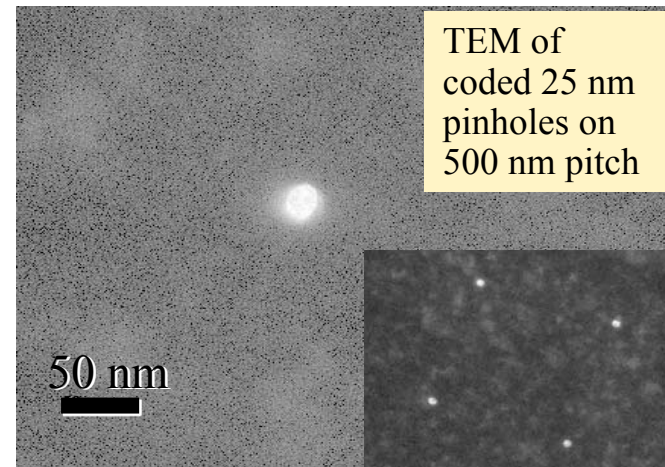
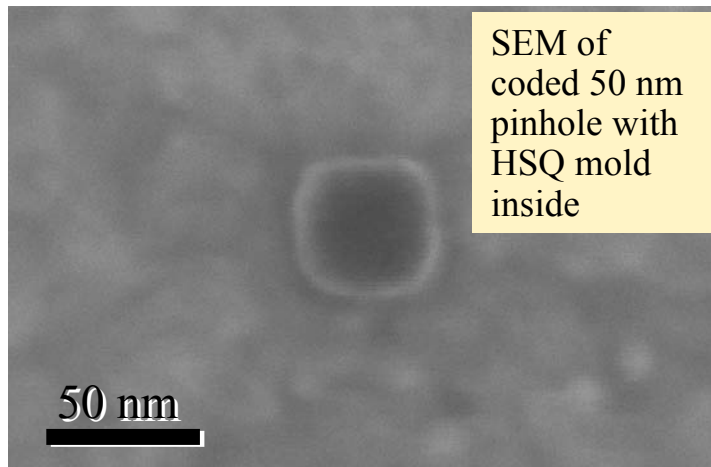
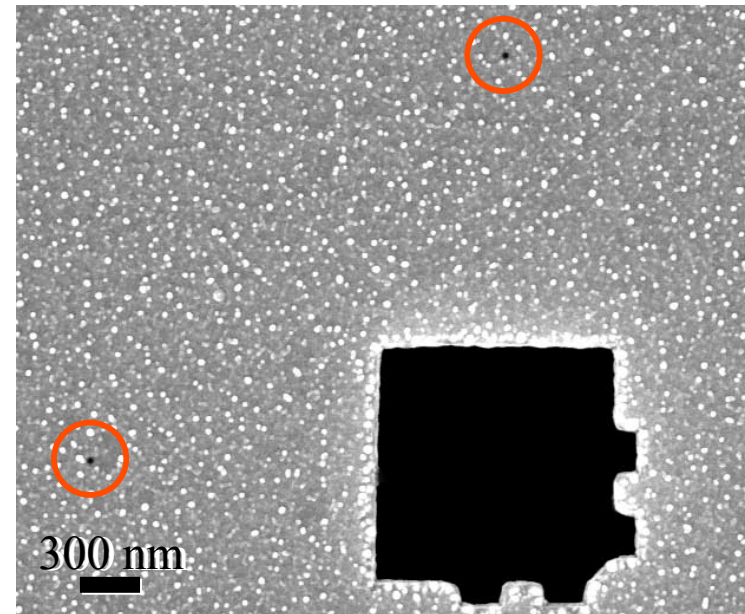
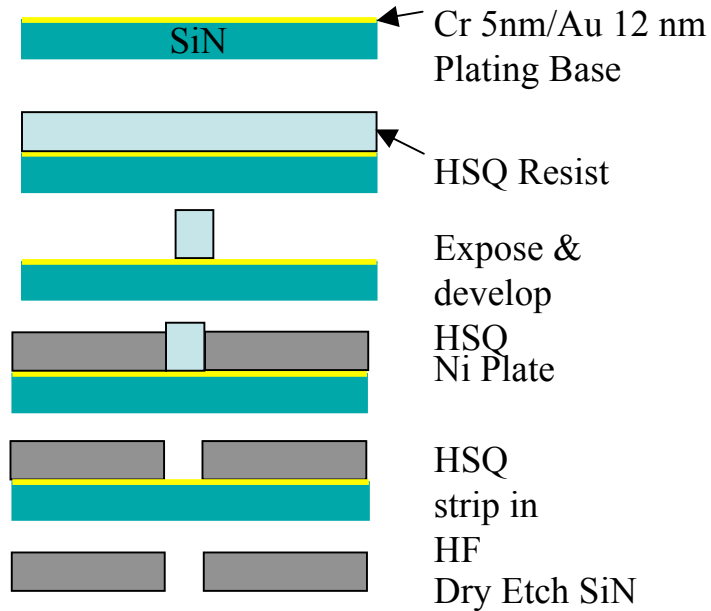


A 0.30 NA Micro-Exposure Tool (MET) has been Fabricated by Zeiss and LLNL





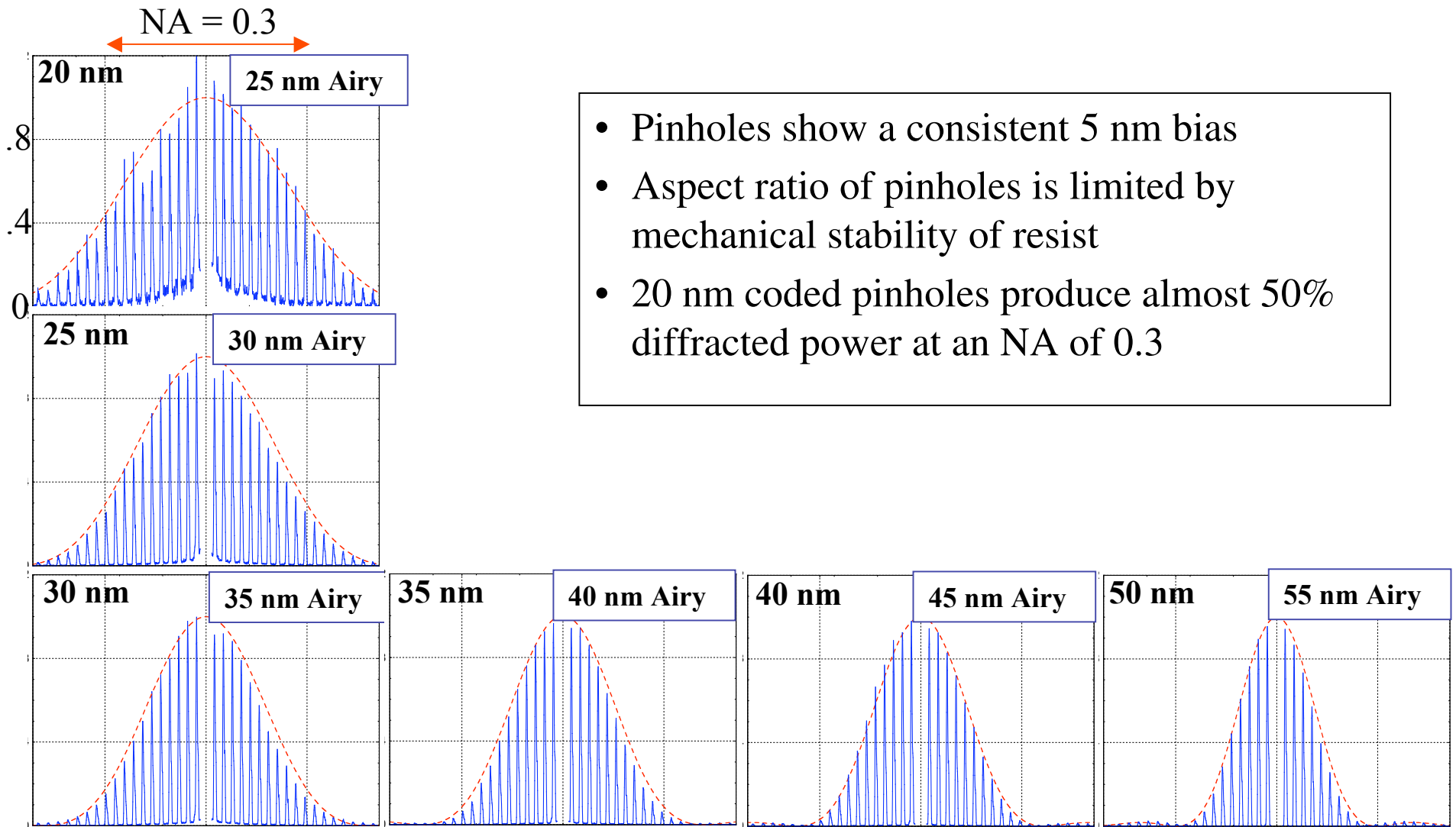
25 nm Pinhole Fabrication



Courtesy of J. Alex Liddle, Deirdre Olynick and Erik Anderson (LBNL)



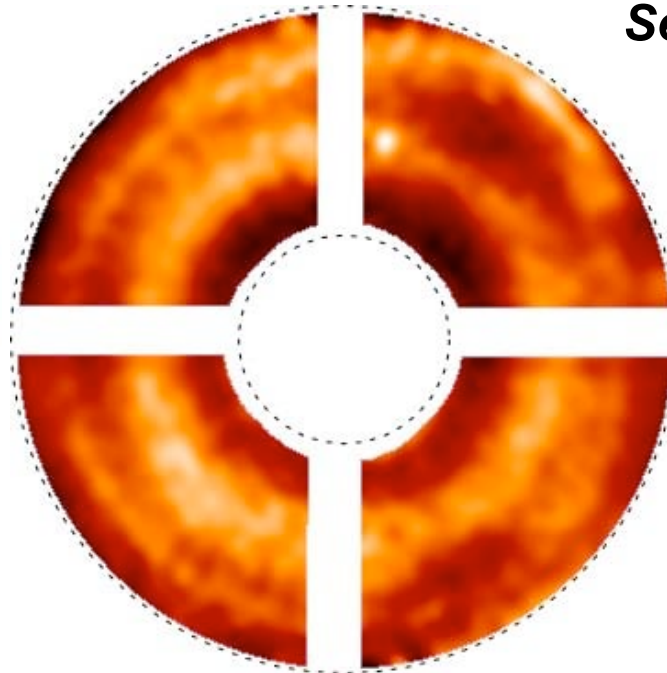
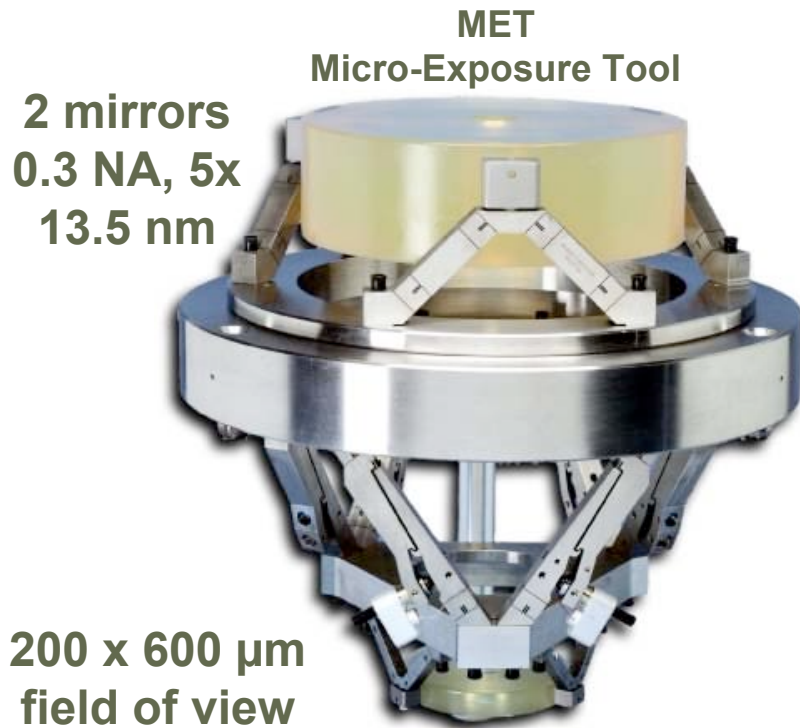
Measured Pinhole Performance



Courtesy of E. Gullikson, K. Goldberg, J.A. Liddle, D. Olynick, E. Anderson, (LBNL)



MET At-Wavelength Interferometry and Alignment Preparation for Static Microfield Imaging



Alignment in progress
September 3, 2003

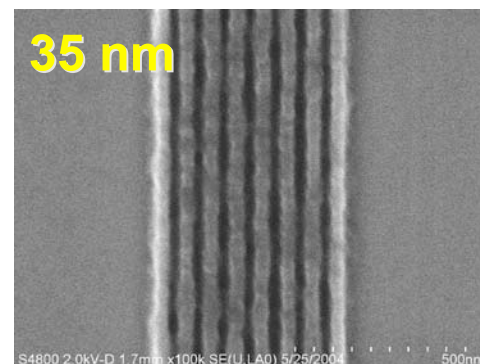
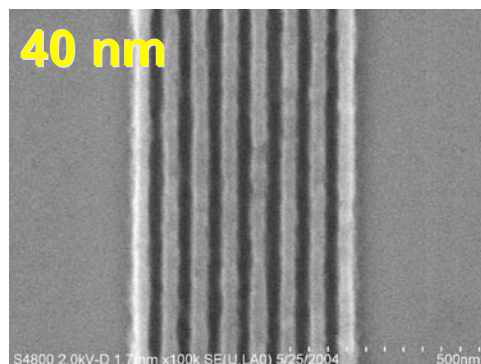
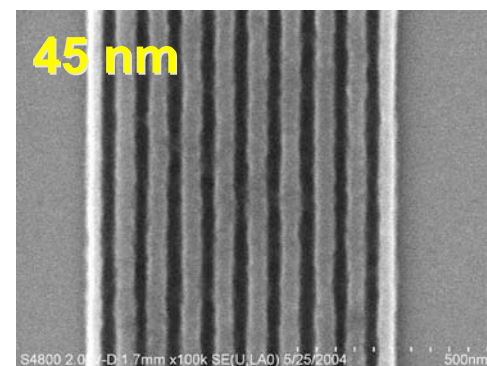
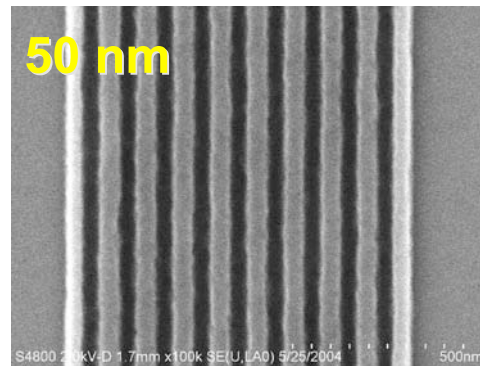
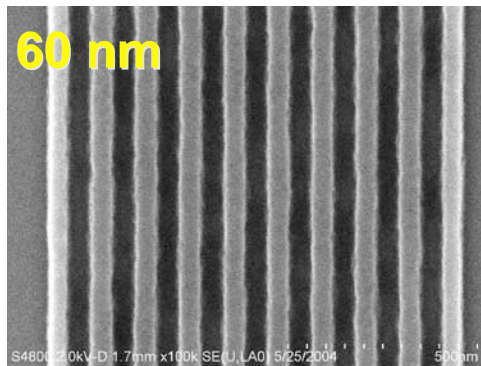
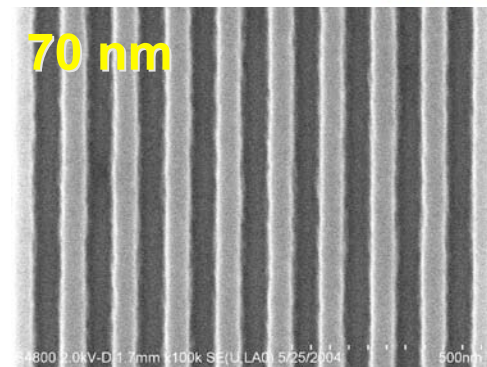
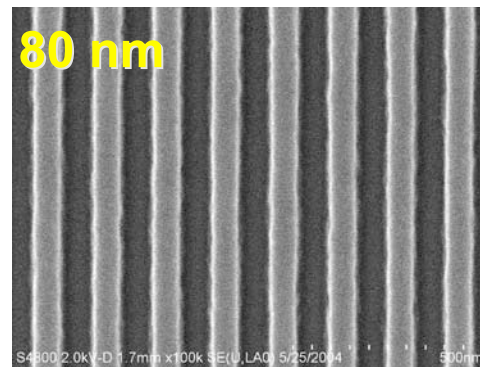
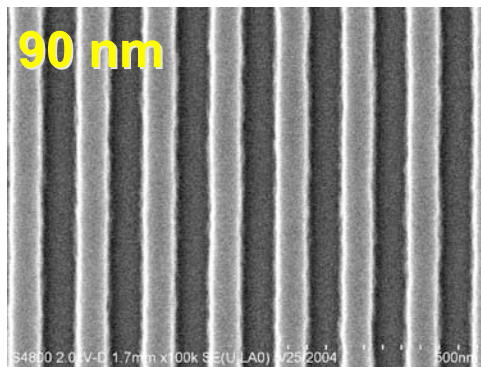
central field point

astig	0.1 nm
coma	0.3 nm
sph ab	0.4 nm
trifoil	0.2 nm
h-o s.	0.4 nm
RMS	0.8 nm
	$\lambda/17$

**aberrations
may be reduced
in final alignment**

- Visible-light alignment at Livermore
- EUV interferometry at Berkeley includes PS/PDI and shearing at 9 points across the field of view and in z.
- Higher-order spherical aberration dominates the wavefront
- A large part of the higher-order spherical is contained in Z35 and Z36. Higher-order spherical magnitude depends strongly on NA.

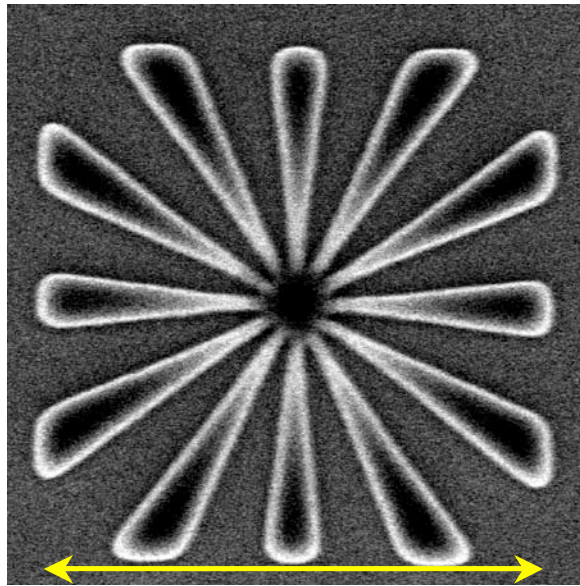
Rohm and Haas MET 1K Resist Shows 10-15 nm Resolution Improvement Over EUV 2D



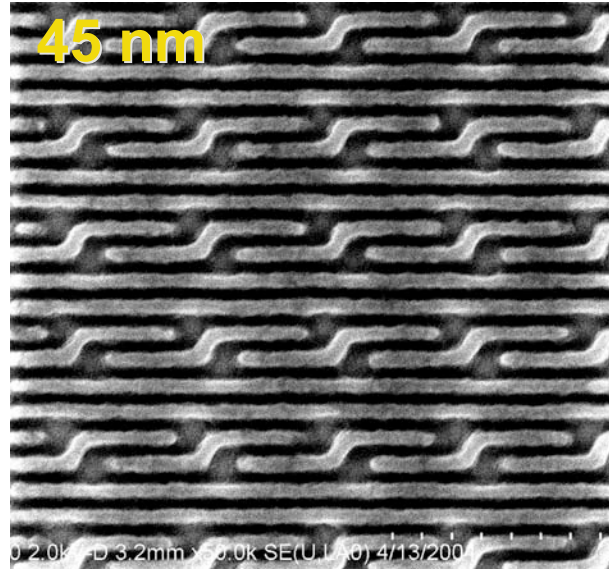
Processing Conditions:

- Thickness 125-nm
- PEB 130 °C 90 Sec
- Develop 45 Sec
- E_{size} 50-nm 21 mJ/cm²

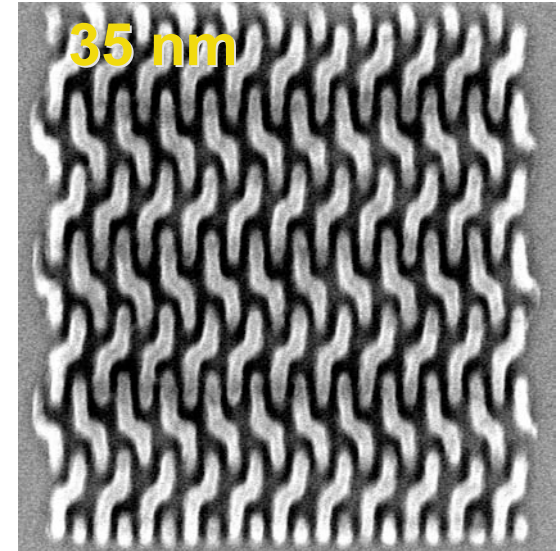
MET 1K Resist Shows Modulation Down to the 25-nm Level



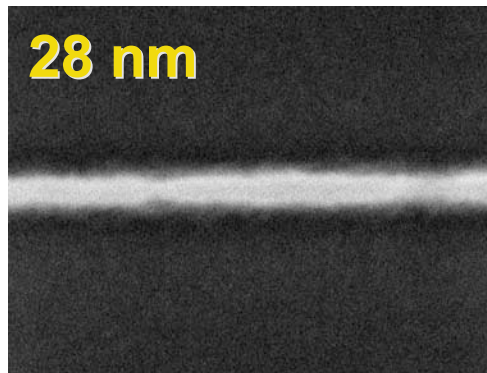
1.8 μm



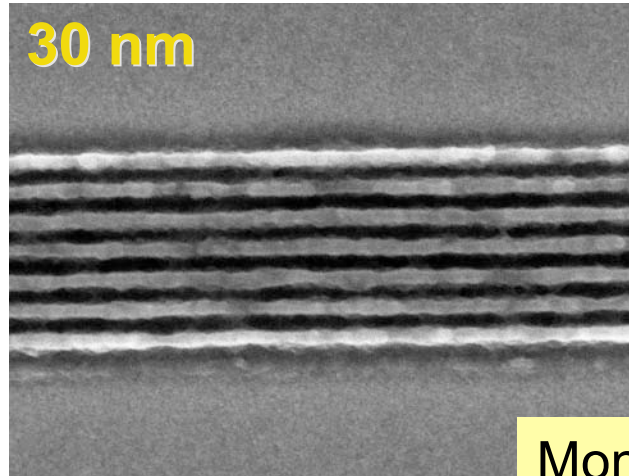
45 nm



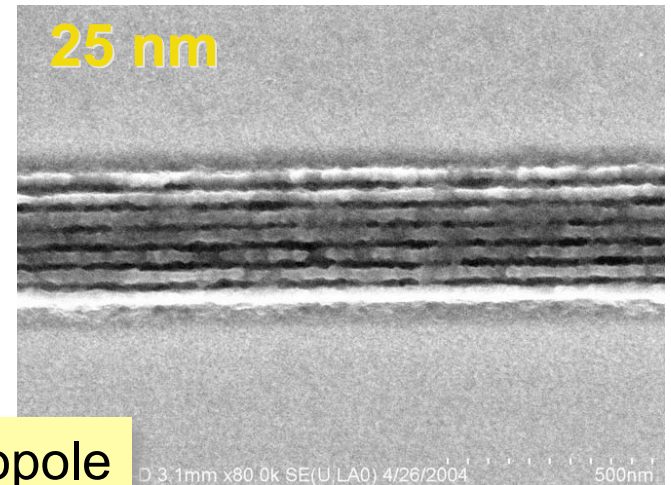
35 nm



28 nm



30 nm

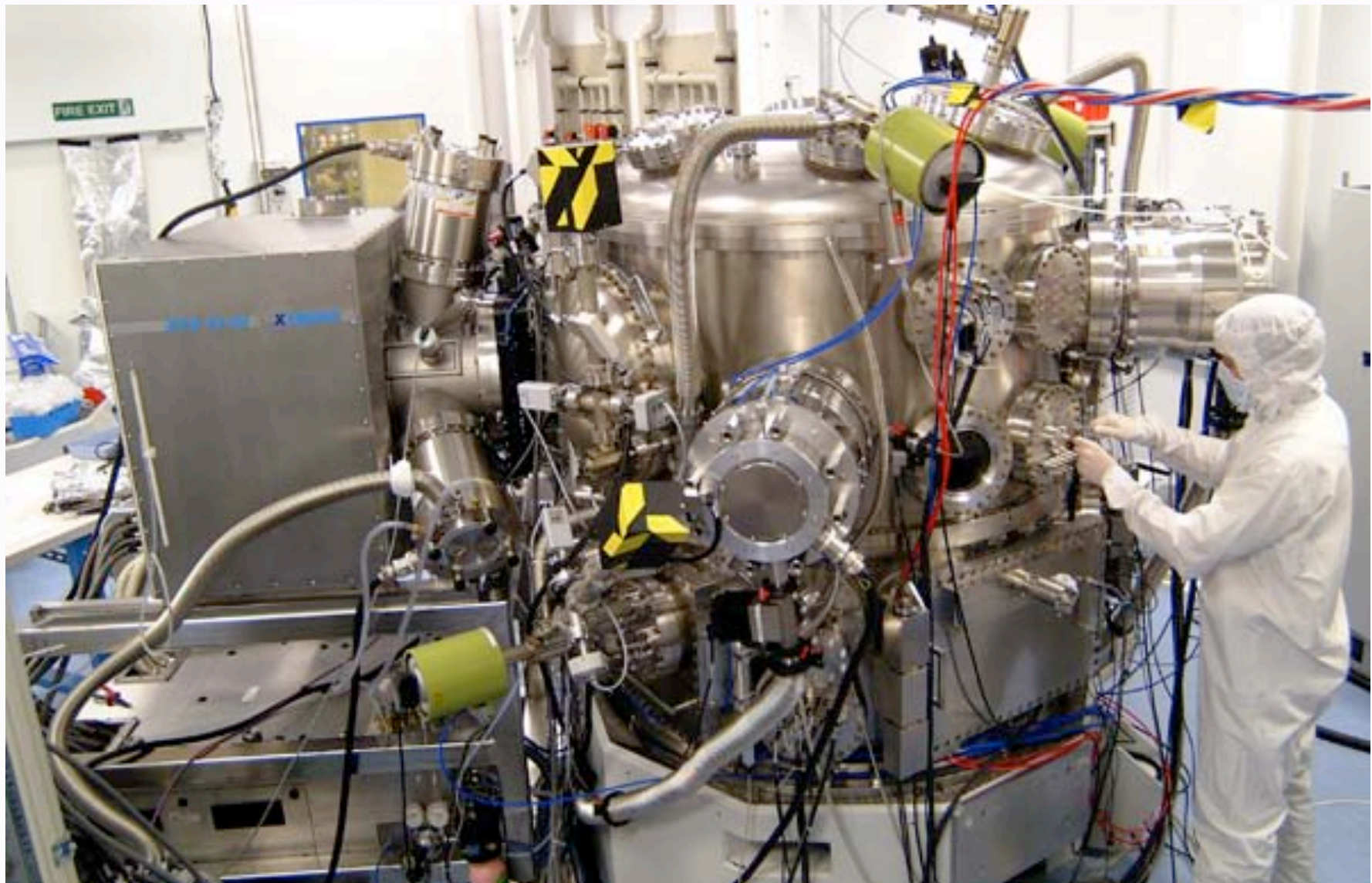


25 nm

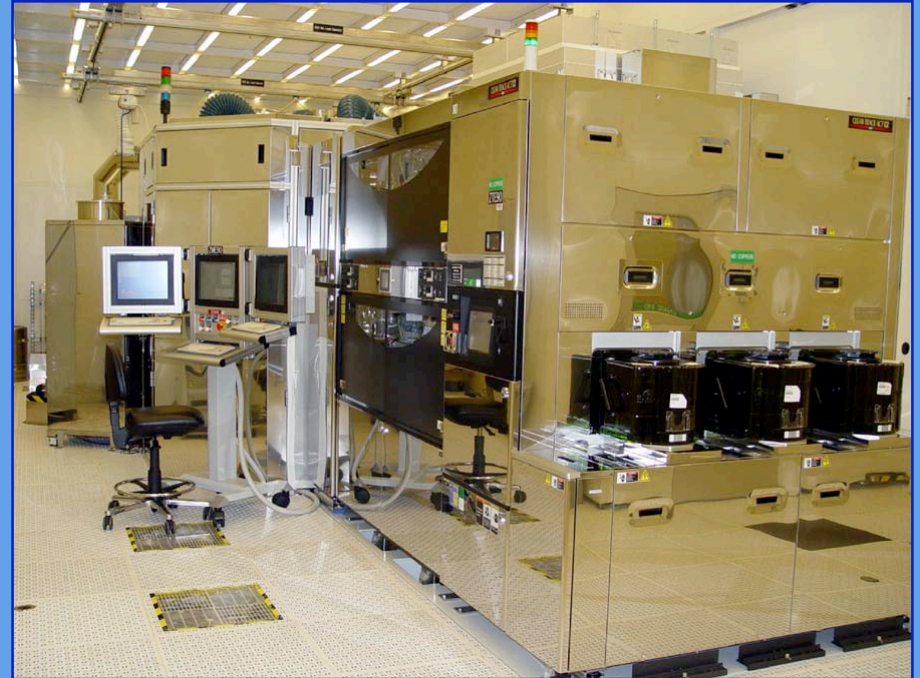
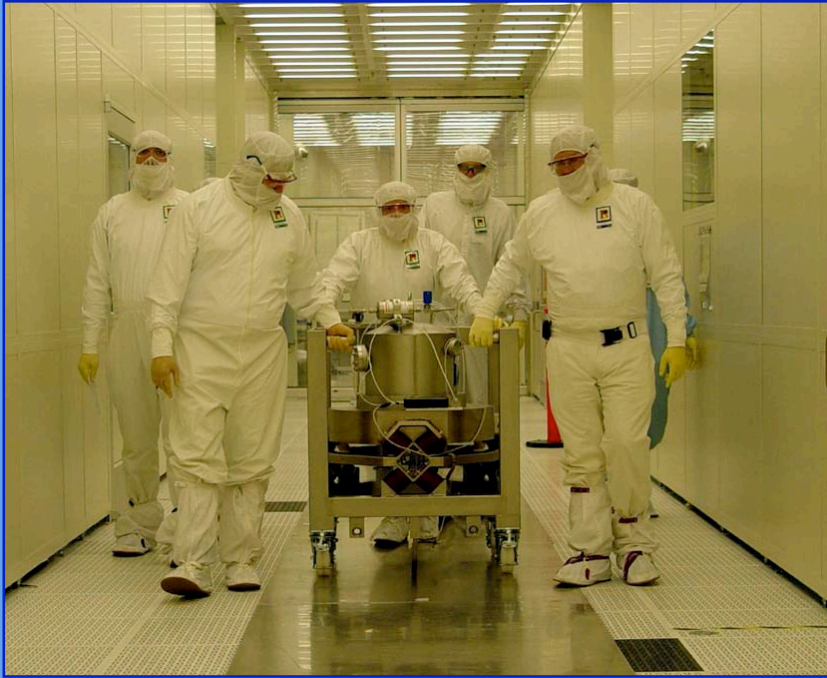
Monopole



MS-13 tool chamber – *subsystem testing*



Intel EUV MET Installation



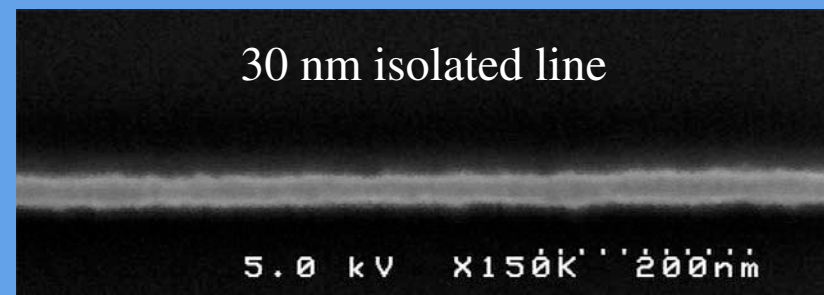
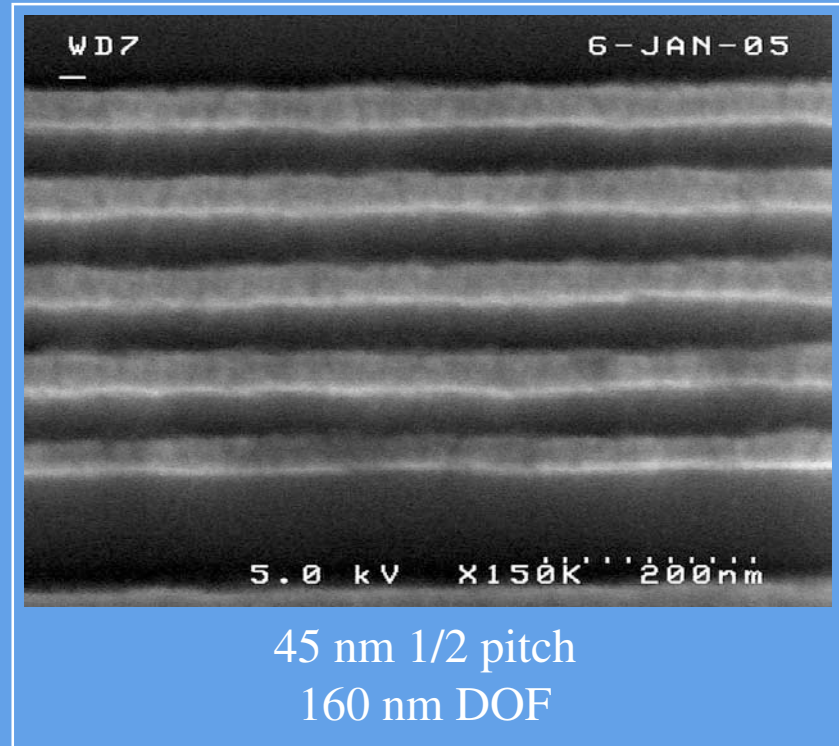
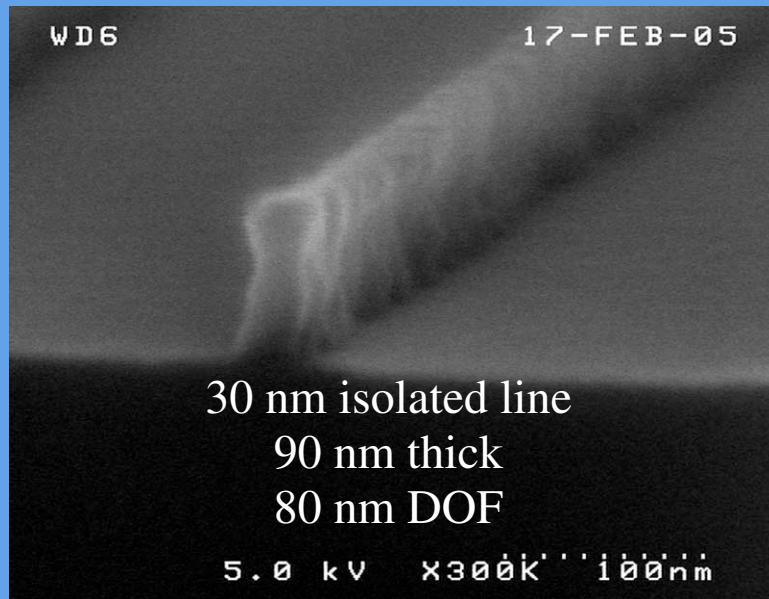
16 crates
17+ tons
15 pumps
All for



intel.

Imaging Performance

0.3 NA
0.55/0.36 σ
8 mJ/cm²



MS-13 EUV Microstepper - at SEMATECH North, Albany, New York, USA



Courtesy of Malcolm Gower, Oxford, UK



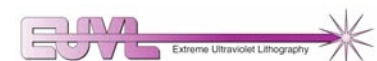
International Technology Roadmap for Semiconductors*



First year of volume production	2001	2003* 2004	2005* 2007	2007* 2010	2009* 2013	2011* 2016
Technology Generation (Dense lines, printed in resist)	130 nm	90 nm	65 nm	45 nm	32 nm	23 nm
Isolated Lines (in resist) [Physical gate, post-etch]	90 nm [65 nm]	53 nm [37 nm]	35 nm [25 nm]	25 nm [18 nm]	18 nm [13 nm]	13 nm [9 nm]
Chip Frequency	1.7 GHz	4.0 GHz	6.8 GHz	12 GHz	19 GHz	29 GHz
Transistors per chip (HV) (3 × for HP ; 5 × for ASICs)	100 M	190 M	390 M	780 M	1.5 B	3.1 B
DRAM Memory (bits)	510 M	1.1 G	4.3 G	8.6 G	34 G	69 G
Gate CD Control (3σ, post-etch)	5 nm	3 nm	2 nm	1.5 nm	1.1 nm	0.7 nm
Field Size (mm × mm)	25 × 32	25 × 32	22 × 26	22 × 26	22 × 26	22 × 26
Chip Size (mm) (2.2 × for HP ; to 4 × for ASIC)	140	140	140	140	140	140
Water Size (diameter)	300 mm	300 mm	300 mm	450 mm	450 mm	450 mm

*Semiconductor Industry Association (SIA), December 2001.

*Possible 2-year cycle.



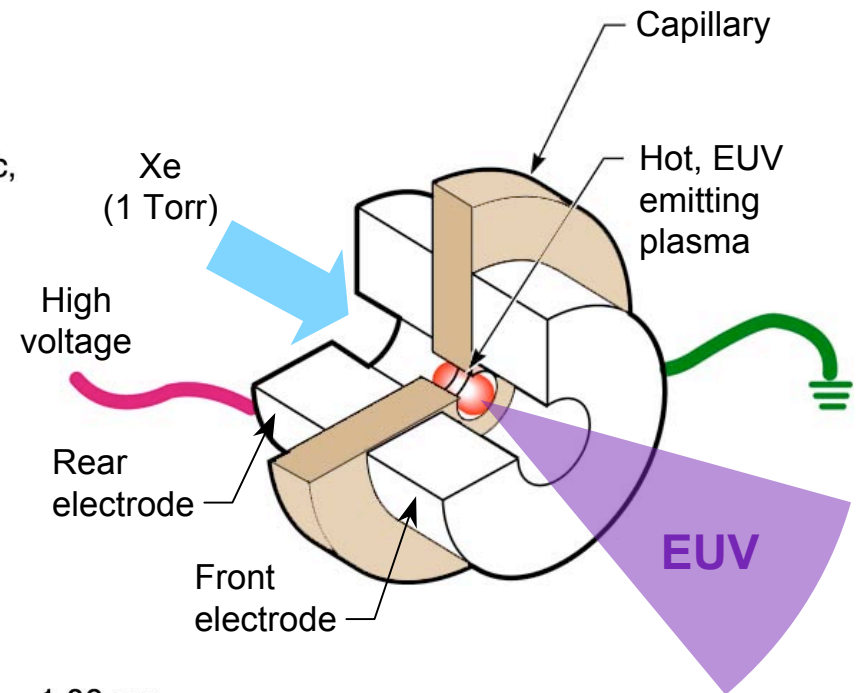
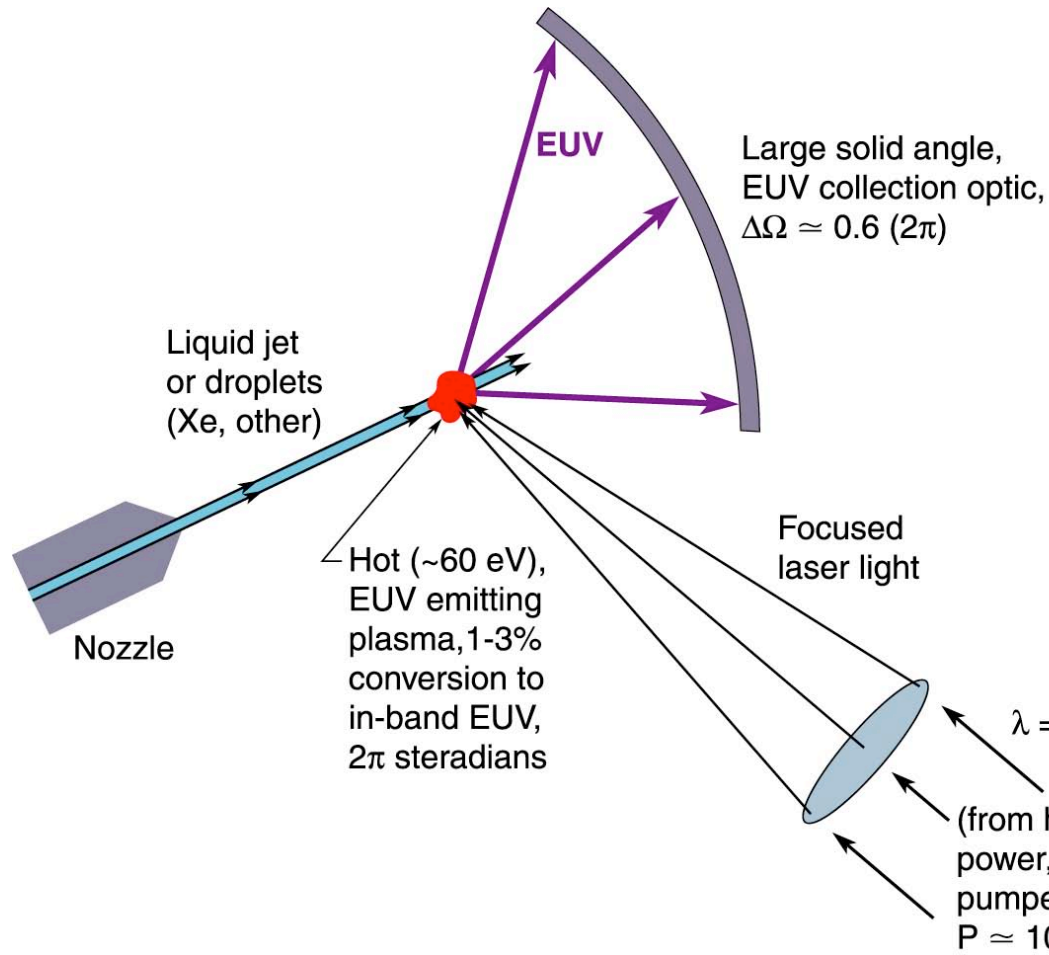


EUV Source Candidates for Clean, Collectable 13-14 nm Wavelength Radiation



Laser Produced Plasma Source

Electrical Discharge Plasma Source





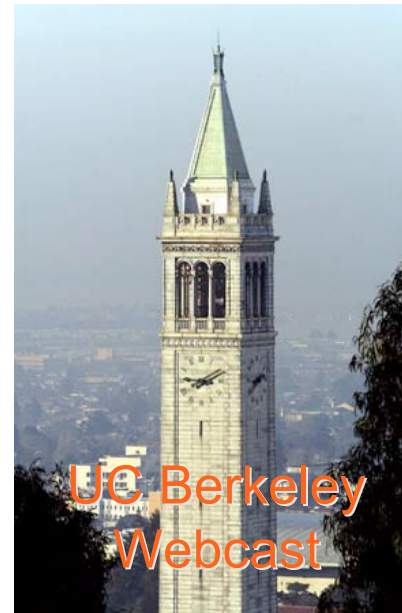
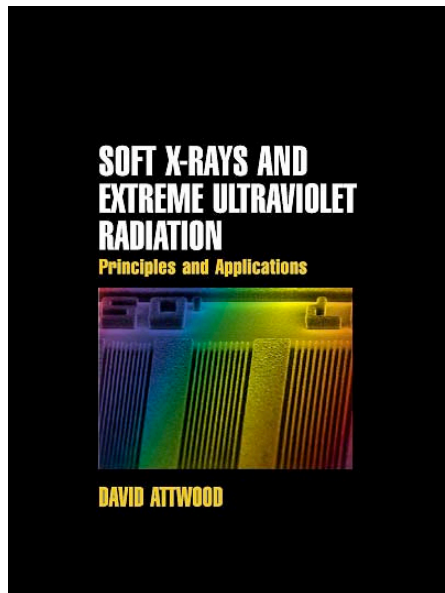
Critical Issues for EUV



- 120W compact EUV Source
- EUV source debris mitigation
- Sensitive ($5\text{m}/\text{cm}^2$) EUV resist with 15 nm resolution and low LER
- Defect free mask
- Environmental controls



Lectures Available Over the Web Free



www.coe.berkeley.edu/AST/sxreu

AST 210 / EECS 213

(offered Fall 2005,
starts Aug. 30, 2 pm PDT,
live over internet plus archived)